

**ISBS 2021 DIGITAL CONGRESS
ON BIOPHYSICS AND IMAGING OF THE SKIN**

Traveling across Borders: Optical Skin Biopsies and Beyond

JUNE 03-05, 2021



Program,
Abstracts and Posters

www.isbs-congress.com





Welcome to the Digital ISBS Congress 2021, June 3-5

This congress is the first digital congress of the International Society of Biophysics and Imaging of the Skin. Three years have passed since the last ISBS Congress in San Diego.

The congress takes place on three days with different time schedules to have also “live” discussions with participants from the Americas as well as from Asia/Australia.

45 talks and 23 posters will be presented as well as contributions from exhibitors on the *Digital Marketplace*.

We start our first congress day *Skin Imaging* with a plenary talk on *Multimodal Optical Imaging* from a leader in OCT development, Professor Wolfgang Drexler from Vienna.

Four invited talks cover the topics *Confocal Reflectance Microscopy*, *Two-Photon Imaging*, *Multiphoton-CARS-FLIM/PLIM-Tomography*, and *Artificial Intelligence in Image Processing* by the Profs. Pellacini (Italy), So (USA/Singapore), König (Germany), and Lee (Canada).

The second congress day focuses on *Skin Biophysics* starting with the plenary talk by Prof. Masayuki Amagai (Japan) on *Skin Barrier Homeostatic Mechanisms*. Four invited talks cover the topics *Skin Transport*, *CARS*, *Raman* and *Skin Hydration* by the experts Prof. Roberts (Australia), Dr. Egawa (Japan), Dr. Bielfeldt and Prof. Fluhr (both Germany).

Our last congress day has the main focus on *Applications of Novel Technologies on Pathological Skin* as well as on *Skin Ageing*. Professor Julia Welzel (Germany) gives the plenary talk on *Optical Biopsies*. The invited speakers Prof. Balu (USA), PD Dr. Kaatz (Germany), Dr. Pena (France) and Prof. Meinke (Germany) speak about *Skin Cancer Detection*, *Skin Ageing Measurement*, and *Skin Damage by UV below 240 nanometers*.

The Congress President, the ISBS Board, and the Scientific Congress Committee are grateful for the “live” participation of all authors in this digital congress and acknowledge the contribution of the sponsors.

We look forward to the next “face-to-face analog” World Congress in Berlin in June 2022 in a relaxed non-pandemic atmosphere.

A handwritten signature in black ink, appearing to read 'König'.

Prof. Dr. Karsten König
Congress President



Welcome!

The International Society for Biophysics and Imaging of the Skin (ISBS) welcomes you to attend and share your research at our upcoming digital congress from 3th-5th June 2021.

After the need to postpone ISBS2020 in Berlin and the persistence of adverse conditions to plan a live conference, the ISBS board members decided to organize this digital event.

Our goal is to have again, the usual friendly, mixed environment, with Dermatologists, Physiologists, Biochemists, Pharmacologists, Toxicologists, Cosmetic scientists, Biomedical engineers, students and industrial partners discussing hot topics on Skin Biophysics and Skin Imaging.

Subtitled Traveling across borders: Optical skin biopsies and beyond, the scientific program includes invited talks of outstanding speakers, oral communications, and posters.

We look forward to meeting you online at our digital Congress.

A handwritten signature in black ink, appearing to read 'B. Querleux', with a long horizontal flourish extending to the right.

Bernard QUERLEUX PhD, Hon. Prof.

ISBS President

Thank you!

138 participants including also sponsors, exhibitors and press from the 23 countries: Australia, Austria, Belgium, Brazil, Bulgaria, Canada, Chile, China, France, Germany, Hungary, Italy, Japan, Korea, Kyrgyzstan, Portugal, Russia, Singapore, Spain, Sweden, Switzerland, UK and USA.

I wish also to thank the players behind the scene: the ISBS board, my secretary Ms. Andrea Kaiser, the registration manager Ms. Denise Mayer, Ms. Cordula Probst from the Remember Management GmbH, and Mr. Heiko Helwig from Röll Media GmbH as manager of the Livestream Video Platform.

The Digital Congress was a great success due to outstanding presentations and live discussions and due to the chairpersons Bernard Querleux (ISBS president, L'Oreal), Joachim Fluhr (Charite Berlin) and Stacy Hawkins (Unilever R&D).

The presentations will be available for three months on the internet:

<https://roellmedia-streams.de/isbs2021>

The International Society of Biophysics and Imaging of the Skin (ISBS) invites you to join “in person” our next ISBS World Congress that will take place in the Langenbeck-Virchow-House in Berlin on June 2-3, 2022. For more details: please visit www.isbs-congress.com

June 6, 2021

Prof. Karsten König
Congress President

Scientific Committee



Joachim Fluhr, Charité – University Hospital Berlin, Germany



Stacy Hawkins, Unilever R&D, USA



Karsten König, Saarland University and JenLab GmbH, Germany



Neelam Muizzuddin, SCR Consultants, USA



Martha Tate, Tate Science, USA

Sponsors



www.dermicolab.com



www.jenlab.de



www.proderm.de



www.uni-saarland.de



www.bl.uni-saarland.de

Exhibitors



www.dermicolab.de



www.eotech.fr



www.jenlab.de

All exhibitor presentations are available online for 3 months
<https://roellmedia-streams.de/isbs2021>



Scientific Program June 3-5, 2021

Thursday, 3.6. SKIN IMAGING 4PM - 8PM Berlin Time
chair: Bernard Querleux, France

- 4.00-4.10 Live Opening (congress president Karsten König, ISBS president B. Querleux)
4.10-4.40 plenary talk (25min + 5min QA live):
Wolfgang Drexler, Austria: Multimodal optical imaging of skin
(prerecorded 25min + 5min QA live)
- 4.40-6.00 4 invited talks (15min + 5min QA live)
- 4.40-5.00 Giovanni Pellacani, Italy: Confocal Microscopy: state of the art
5.00-5.20 Peter So, USA: First two-photon imaging in skin
5.20-5.40 Karsten König, Germany: Multimodal Multiphoton Tomography (MPT)
5.40-6.00 Tim Lee, Canada: Artificial Intelligence in Optical Skin Analysis –
Challenges and Opportunities
- 6.00-07.50 9 presentations (10min + 2min QA live)
- 6.00-6.12 A. Bergheau, France UNDERSKIN®. An exciting new development
in skin elasticity
6.12-6.24 A. Bezugly, Russia Skin Fillers Visualization and Filler Type
Determination with High Frequency Ultrasound.
6.24-6.36 G. Tian, Canada Automated delineation of the Dermal–Epidermal
Junction Zone in Volumetric Multiphoton
Microscopy imaging of Human Skin in vivo
6.36-6.48 M. Pedrazzani, France Line-field optical coherence tomography
for non-invasive skin imaging: Focus on dermal-
epidermal junction and keratinocyte network
6.48-7.00 G. M. D’Angelo Costa, Application of skin imaging techniques
Brazil for the efficacy evaluation of a cosmetic
formulation containing Spirulina sp.
7.00-7.12 P. M. Maia Campos, Brazil In vivo skin penetration of d-panthenol by
Confocal Raman Spectroscopy
7.12-7.24 A. Martin, Brazil Permeation of Nano Encapsulated Vitamin D3
Through Human Skin by in vivo Confocal Raman
Spectroscopy
7.24-7.36 J. Ogien, France Handheld line-field optical coherence
tomography (LC-OCT) device for three-
dimensional skin imaging
7.36-7.48 I. Lange, Germany Feature extraction for classification of lesions and
malignant melanomas in multiphoton tomography
skin images
- 7.50-08.00 Karsten König: Day closing remarks and announcement of World Congress in
Berlin 2022
4PM-8PM Poster Session

Friday, 4.6. SKIN BIOPHYSICS 8AM - 12PM Berlin Time
chair: Joachim Fluhr, Germany

- 08.00-08.30 plenary talk (25min + 5min QA live):
Masayuki Amagai: Corneoptosis, unique cell death process of keratinocytes
- 08.30-09.50 4 invited talks (15min +5min QA)
- 8.30-8.50 Michael Roberts, Australia Using multiphoton microscopy to characterise skin transport determinants and processes
- 8.50-9.10 Mariko Egawa, Japan Potential of coherent Raman scattering microscopy in skin evaluation
- 9.10-9.30 Stephan Bielfeldt, Germany Confocal Raman Spectroscopy: An in vivo technique of many talents
- 9.30-9.50 Joachim Fluhr, Germany Stratum Corneum Hydration: Dry skin – sensitive skin and beyond
- 09.50-12.02 11 presentations (10min + 2min QA)
- 9.50-10.02 J. Choi, Korea Evaluation of perceived skin brightness in Asian women
- 10.02-10.14 S. Wang, China The Skin Phenome Research
- 10.14-10.26 H. Zahouani, France “TOUCHY Finger” an augmented and connected human finger to assess skin and hair feel
- 10.26-10.38 C. Bonnaud-Rosaye, France New Protocol to Evaluate Emotional Experience of Customers
- 10.38-10.50 N. Muizzuddin, USA Balancing skin Microbiome- Fact or fiction
- 10.50-11.02 M. Lee, Korea Pilot study for effects of facial skin colors on facial impressions
- 11.02-11.14 M. Florindo, Portugal Studying the impact of muscular activity and exercise on skin biomechanics
- 11.14-11.26 M. Ayadh, France Quantitative characterization of human skin tension in vivo using a new parameter: Tension index
- 11.26-11.38 C. Ferreira-Pego, Portugal Exploring the impact of vegetarian-vegan and omnivores regimes in human skin physiology
- 11.38-11.50 S. Connetable, France Decoding skin tightness: From a clinical evidence to an instrumental and biological proof of sensorial stimulation perception
- 11.50-12.02 A. König, Germany Optical reprogramming of human dermal fibroblasts
- 12.02-12.10 **Karsten König: Day closing remarks and announcement of World Congress in Berlin 2022**
- 8AM-12PM Poster Session**

Saturday 5.6. PATHOLOGICAL SKIN - SKIN AGEING
4PM - 8PM Berlin Time
chair: Stacy Hawkins, USA

- 4.00-4.30 plenary talk (25min + 5min QA live):
Julia Welzel, Germany: Optical biopsies (25min@200 MB+5min QA)
- 4.30-5.50 4 invited talks (15min + 5min QA)
- 4.30-4.50 Mihaela Balu, USA In vivo multiphoton tomography provides insights into therapeutic response of pigmentary skin disorders
- 4.50-5.10 Martin Kaatz, Germany Multicenter clinical study on melanoma detection
- 5.10-5.30 Ana Maria Pena, France In vivo multiphoton imaging for non-invasive time course assessment over 1 year of melanin modulations and retinoids effects on human skin
- 5.30-5.50 Martina Meinke, Germany Risk assessment of skin damage for far-UVC irradiation below 240 nm which can be used to eradicate multi resistant germs and viruses
- 5.50 - 7.50 10 presentations (10min + 2min QA)
- 5.50-6.02 J. Robic, France Aging of the eye contour and its effect on perceived age
- 6.02-6.14 J. Servant, France 3D imaging: A global approach to aging signs of the skin
- 6.14-6.26 R. Campiche, Austria New methods for digitally transferring visible irradiation-induced pigmentation on the forearm and other treatment sites to the face
- 6.26-6.38 G. Csany, Hungary Comparison of Maximal Lesion Thickness Measurements between two Portable Skin Ultrasound Imaging Devices
- 6.38-6.50 A. Guillermin, France Non - invasive in vivo creep recovery indentation testing for skin modeling
- 6.50-7.02 R. Darlenski, Bulgaria Oxidative stress and anti-oxidant defense in plaque psoriasis
- 7.02-7.14 A. Duev, USA Study of Clinical Efficacy and Microbiome Effects of an Anti-Acne Regimen
- 7.14-7.26 S. Figueiredo, France A fast and reliable tool to self-assess sensitive skin
- 7.26-7.38 Y. Wang, Canada Combining Deep Learning and Polarization Speckle for in vivo Skin Cancer Detection
- 7.50 - 8.00 **Karsten König: Day closing remarks and announcement of World Congress in Berlin 2022**
- 4PM-8PM **Poster Session**

,

Abstracts

Plenary talks

In alphabetical order of the corresponding author

All presentations are available online for 3 months

<https://roellmedia-streams.de/isbs2021>

Corneoptosis, unique cell death process of keratinocytes

Masayuki Amagai^{1,2}

*Department of Dermatology, Keio University School of Medicine, 35 Shinanomach, Shinjuku-ku,
Tokyo, Japan 160-8582*

*Laboratory for Skin Homeostasis, RIKEN Center for Integrative Medical Sciences, 1-7-22 Suehiro-cho,
Tsurumi-ku, Yokohama, Kanagawa, Japan 230-0045*

amagai@keio.jp

KEY WORDS: skin barrier, stratum corneum, keratinocytes

In the skin, uppermost living cells of epidermis (SG1 cells) provide their dead cell bodies to serve barrier function as stratum corneum, rather than are removed by scavengers as found in apoptosis or necrosis. This developmental process harbors a unique form of cell death with dynamic and orchestrated changes in their intracellular structures. However, its precise cell mechanism has not been clarified.

Here, we showed that the SG1 cell death begin with a long-sustained irreversible intracellular Ca^{2+} ($[\text{Ca}^{2+}]_i$) elevation for ~60 min. Then, a rapid drop of an intracellular pH (pH_i) follows within ~15min. These sequential intracellular ionic changes occur *once* in the SG1 cells and their duration and frequency are constant. We mimic these intracellular conditions in primary cultured SG1 cells, and demonstrated that the high $[\text{Ca}^{2+}]_i$ -neutral pH_i condition initiate cell death process with increased cell membrane permeability, whereas the high $[\text{Ca}^{2+}]_i$ -low pH_i condition triggered the elimination of organelles, such as keratohyalin granules, and the DNA degradation without causing unnecessary inflammation. These morphological changes in SG1 cells are essential for corneocyte formation. Finally, we identified TRPV3 cation channel which involved in epidermal barrier function as a time-keeper of ionic changes in SG1 cells.

The Ca^{2+} elevation and acidification in SG1 cells are unique and essential to trigger sequential activation of various Ca^{2+} - and pH-dependent enzymes and chemical reactions under precise time control to execute SG1 cell death and transform them into the corneocytes. This unique cell death cell process is termed corneoptosis. These findings prevail hidden principle on the link between live and dead tissues and contribute to expand the concept of cell death.

Multimodal optical imaging of skin

W. Drexler

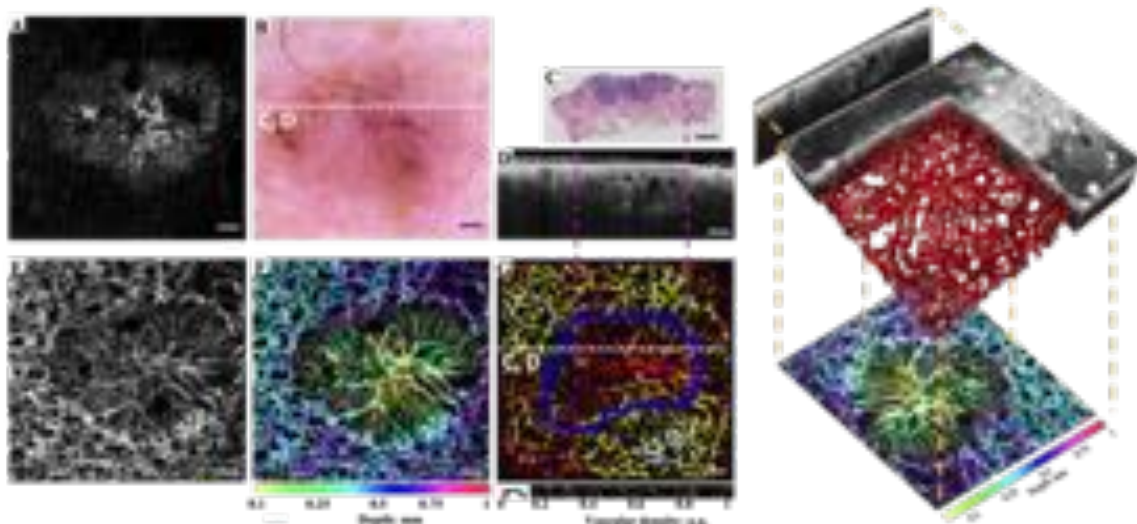
Center for Medical Physics and Biomedical Engineering, Medical University of Vienna, Austria
Wolfgang.Drexler@meduniwien.ac.at; www.meduniwien.ac.at/zbmtp/

KEY WORDS: Optical coherence tomography, photoacoustic imaging, multiphoton microscopy

In the last three decades optical coherence tomography (OCT) has established itself as a unique non-invasive, optical medical diagnostic imaging modality, enabling unprecedented *in vivo* cross-sectional tomographic visualization of internal microstructure in a variety of biological systems. Ophthalmology has been the most successful and commercially most active medical field for OCT so far, but several other OCT applications, e.g., in cardiology, dentistry, gastroenterology or dermatology, are on the verge of expanding their market comparable to or larger than that of ophthalmology.

Especially in the last decade ultrabroad bandwidth light sources as well as spectral/frequency domain OCT detection technology enabled three-dimensional ultrahigh resolution OCT with unprecedented axial resolution, approaching resolution levels of conventional histopathology, enabling optical biopsy of biological tissue. Furthermore, emerging swept source laser technologies and parallel or full-field OCT techniques enabled multiple millions of A-scan rates per second, allowing large area OCT scans with high-definition sampling, investigation of dynamic processes or four-dimensional (3D over time) imaging. In addition, extensions of OCT are under development that should provide enhanced contrast or non-invasive *depth resolved* functional imaging of the investigated tissue, including extraction of birefringent, spectroscopic, blood flow or physiologic tissue information. These extensions of OCT should not only improve image contrast, but should also enable the differentiation and early detection of pathologies via localized functional state.

Recently OCT has also been combined with different complementary imaging technologies (photoacoustics, CARS, multi-photon microscopy, fluorescent imaging) to hybrid/multi-modal approaches to compensate fundamental limits of OCT in order to significantly enhance its performance towards molecular imaging.



Dermatologic multimodal optical imaging of basal cell carcinoma

Optical biopsies

J. Welzel

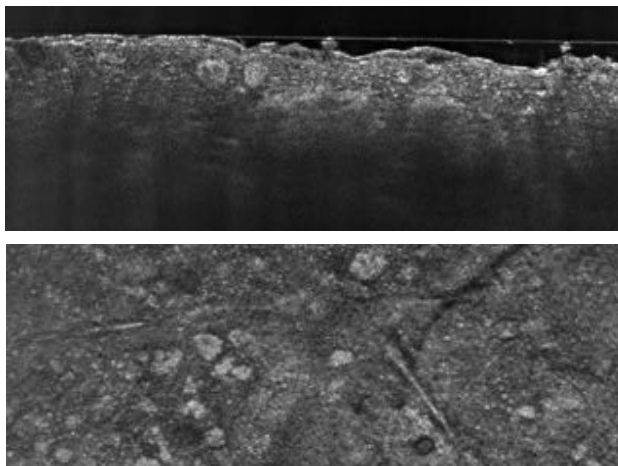
Department of Dermatology, University Hospital Augsburg, Sauerbruchstraße 6, 86179 Augsburg, Germany

KEY WORDS: Optical coherence tomography, reflectance confocal microscopy, line-field confocal microscopy

When do you need an optical biopsy in dermatology? Whenever a diagnosis is unclear clinically and by dermoscopy, functional or dynamic changes are to be visualized, follow-up examinations are pending or a biopsy is to be avoided. Advantages over histology are the non-invasiveness, thus the arbitrary repeatability, the possibility of examining field changes and thus early detection. Requirements for imaging methods are high resolution, good penetration depth, sufficient contrast and, if possible, large field two-dimensional or even three-dimensional imaging.

Optical coherence tomography is established in routine for early detection of basal cell carcinoma including subtyping and determination of tumor thickness¹. Here, the lower resolution is sufficient, and the detection depth is optimal. Confocal laser microscopy has such a high resolution that cytological changes can also be assessed, but at the expense of penetration depth. This method is established for differential diagnosis of pigmented lesions².

Line-field confocal OCT combines the advantages of both methods. It provides real-time three-dimensional images of the skin with cellular resolution. First studies show the potential of this method for the diagnosis of epithelial as well as melanocytic tumors³. This makes optical biopsy at the patient's bedside a reality.



LC-OCT of a compound nevus, vertical (above) and horizontal image (below), both 1.5 mm x 0.5 mm.

¹ Ferrante di Ruffano L et al. Cochrane Database Syst Rev. 4 (2018)12(12):CD013189.

² Dinnes J, et al. Cochrane Database Syst Rev. 4(2018)12(12):CD013190.

³ Ruini C, et al. Skin Res Technol 2020 Oct 21. Epub ahead of print.

Abstracts

Invited Talks

In alphabetical order of the corresponding author

All presentations are available online for 3 months

<https://roellmedia-streams.de/isbs2021>

***In vivo* multiphoton tomography provides insights into therapeutic response of pigmentary skin disorders**

M. Balu¹, G. Lentsch¹, J. Shiu², C. Polleys³, C. Mizzoni³, P. Mobasher², K.König⁴, B. J. Tromberg^{1,5}, I. Georgakoudi³, A. K. Ganesan²

¹ Beckman Laser Institute and Medical Clinic, University of California, Irvine, 1002 Health Sc. Rd., Irvine, CA, USA

²Department of Dermatology, University of California, Irvine, USA

³Department of Biomedical Engineering, Tufts University, Boston, MA, USA

⁴Jenlab, GmbH, Jena, Germany

⁵National Institute of Biomedical Imaging and Bioengineering, Bethesda, MD, USA (current affiliation)

mablu@uci.edu

KEY WORDS: multiphoton tomography, vitiligo, *in vivo* skin imaging, MPTflex

In the past 10 years, our group at the Beckman Laser Institute at UC Irvine, CA has been evaluating the potential of multiphoton tomography (MPT) to diagnose skin cancers^{1,2}, guide therapy of pigmentary skin disorders³ and to understand the biology of skin pigmentation⁴, photodamage and aging. We perform this research by using a clinical multiphoton tomograph (MPTflex, JenLab, Germany) based on two-photon excited fluorescence (TPEF) and second-harmonic generation (SHG). These contrast mechanisms produce images of endogenous biomolecules in the tissue, without using specific fluorescent labels. In multiphoton microscopy of skin, the main sources of fluorescence are NADH, FAD, keratin, melanin and elastin fibers, whereas SHG is used to visualize dermal collagen fibers.

This presentation will focus on a particular application related to monitoring the therapeutic response of vitiligo, a pigmentary skin disorder consisting of white skin patches caused by the destruction of epidermal melanocytes. We performed a clinical pilot study on fifteen vitiligo patients treated by micro-grafting transplantation, a clinical procedure where autologous pigmented skin is transplanted into the affected vitiligo area. We employ *in vivo* MPT to evaluate keratinocyte metabolic state before and during therapy, *in vivo* reflectance confocal microscopy to track the migration of melanocytes during therapy, and single cell transcriptomics, an mRNA-based examination of gene expression level of individual cells, to identify potential unique keratinocyte populations in vitiligo versus adjacent normal skin.

Preliminary data show that before micro-grafting therapy, vitiligo keratinocytes have an altered metabolic state, which may be associated with impaired cell signaling and resistance to prior treatments. The quantitative analysis related to melanocyte migration suggests that the lack of repigmentation correlates with the melanocytes inability to migrate rather than the melanocytes being destroyed during repigmentation. Single cell transcriptomics identified two unique cell populations as being more abundant in stable vitiligo compared to normal skin.

Together, these findings provide insights into the role of certain cell populations in the viability of micro-grafting therapies and motivate further study into the precise factors that affect treatment efficacy.

-
1. Balu M *et al.* Cancer Res., 74 (10) 2688-2697 (2014).
 2. Pouli *et al.* Sci Transl Res., 8 (367) 367rat169 (2016)
 3. Lentsch *et al.* Pigm. Cell and Melanoma Res., 32 (3) 403-411 (2019)
 4. R. Saager *et al.* J Biomed Opt. 20 (6) 066005 (2015)

Confocal Raman Spectroscopy: An in vivo technique of many talents

S. Bielfeldt¹, K-P. Wilhelm¹

¹proDERM GmbH, Kiebitzweg 2, 22869 Schenefeld / Hamburg
sbielfeldt@proderm.de, www.proDERM.de

KEY WORDS: confocal Raman spectroscopy, in vivo skin penetration, skin aging

In vivo Confocal Raman Spectroscopy (CRS) has been widely used to investigate the chemical composition of the stratum corneum (SC). Main components like barrier lipids and natural moisturizing factor (NMF), as well as the content of water at different depth of SC, have been measured without any skin preparation or modification. Due to this advanced technology the knowledge of the outermost barrier of the skin has clearly improved.

Not only the natural content of the SC is available for CRS, also the content of penetrated compounds after external application can be measured quantitatively. As the distribution of such molecules in SC can be followed over at different time points after application, the penetration into SC, as well as from SC into deeper skin layers can be quantified. Results of caffeine penetration in two different topical formulations are presented, showing a clear effect of the formulation on skin penetration.

CRS is also capable to assess the molecule composition of deeper skin layers as the dermis. Strength and elasticity of the dermis is based on the structure and integrity of its main components, collagen and water. Collagen amounts to approx. 90 % of the total protein content of the dermis. However, with 70 %, the most abundant molecule in the dermis is water, that forms a gel with glycosaminoglycans like hyaluronic acid.

In this work we investigated the dermal water content of mild to moderately photoaged human forearm skin by use of CRS.

Our measurements revealed a positive correlation of dermal water with photoaging¹. Figure 1 shows the dermal water content in relation to the photoaging ranks (lowest = 1; highest =23) of the expert grader. A clear positive correlation (Pearson's $r = 0.417$) was found.

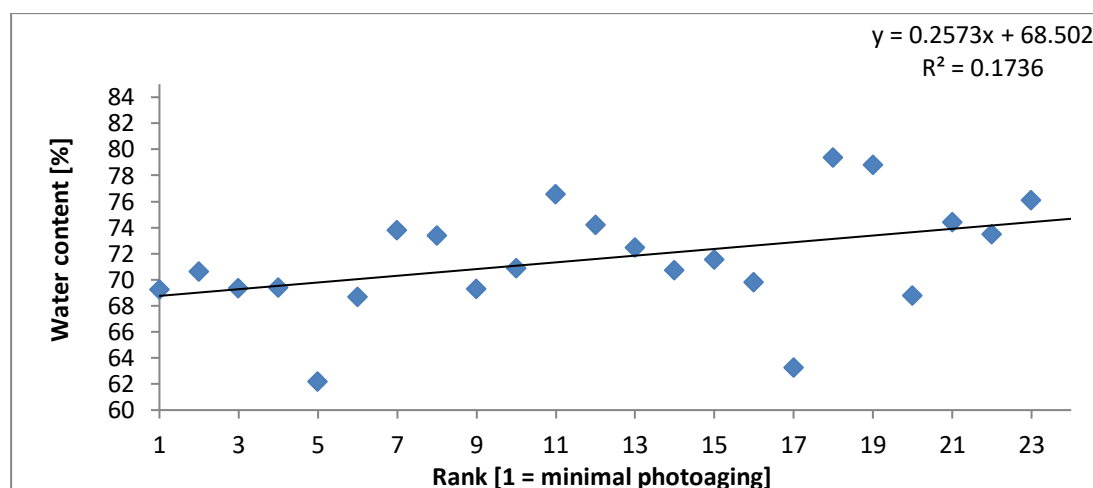


Figure 1: Correlation of water content in the dermis versus photoaging ranks (n = 23)

¹ Kourbaj, G., Bielfeldt, S., Seise, M., & Wilhelm, K. P. (2020). Measurement of dermal water content by confocal RAMAN spectroscopy to investigate intrinsic aging and photoaging of human skin in vivo. *Skin Research and Technology*. DOI: 10.1111/srt.12948.

Potential of coherent Raman scattering microscopy in skin evaluation

M. Egawa¹

*MIRAI Technology Institute, Shiseido Co., Ltd., 1-2-11, Takashima, Nishi-ku, Yokohama 220-0011, Japan
mariko.egawa@shiseido.com*

KEY WORDS: CARS, Epidermis, SRS

The epidermis is of particular importance in dermatology and cosmetology as it is considered to correlate to skin condition. Specifically, smooth epidermal differentiation is thought to result in the generation of a healthy stratum corneum, which maintains the skin's protective barrier function. Many dermatological studies using immunostaining with fluorescent dyes or proteins have had limited success in revealing skin functions as these methods are known to affect the main components of the epidermis, including the water, lipids, and proteins¹.

Recent progress in non-invasive optical imaging—for example confocal microscopy and optical coherence tomography—has enabled us to visualize the structure of each skin layer non-invasively. However, it remains difficult to identify individual skin components using the above optical methods because morphological differences are observed using the refractive index at the cell boundary. Alternatively, molecular vibrational signatures of the skin can be obtained using spectroscopic techniques such as spontaneous Raman scattering microscopy¹. Spontaneous Raman is used to analyze water, lipids, and free-amino acids in the skin. To apply Raman microscopy to the molecular imaging of human skin, coherent Raman scattering microscopy, such as coherent anti-Stokes Raman scattering (CARS) and stimulated Raman scattering (SRS), which enables faster measurement than spontaneous Raman scattering microscopy, is an attractive technique.

In my talk, I will introduce the latest results of intracellular morphologies in the human epidermis during epidermal differentiation using SRS^{2,3} and water and intercellular lipid distribution in the human stratum corneum using CARS^{4,5}. Also I will discuss the potential of coherent Raman microscopy in the fields of skin biology and cosmetology to provide a deep, non-invasive, cellular-level analysis of the skin's functions.

The contents introduced in my talk include some of the results of our joint research with Yasuyuki Ozeki, PhD (Department of Electrical Engineering and Information Systems, Graduate School of Engineering, The University of Tokyo) and Hideaki Kano, PhD (Department of Chemistry, Kyushu University).

¹ M. Egawa, *Analyst*, 146(2021)1142-1150.

² M. Egawa, K. Tokunaga, J. Hosoi, Y. Ozeki, *J. Biomed. Opt.*, 21(8)(2016)086017.

³ M. Egawa, S. Iwanaga, J. Hosoi, M. Goto, H. Yamanishi, M. Miyai, C. Katagiri, K. Tokunaga, T. Asai, Y. Ozeki, *Sci. Rep.*, 9(2019)12601.

⁴ D. Kaneta, G. Makiko, M. Hagihara, P. Leproux, V. Couderc, M. Egawa, H. Kano, *Analyst*, 146(2021)1163-1168.

⁵ D. Kaneta, P. Leproux, V. Couderc, G. Makiko, M. Egawa, H. Kano, *Appl. Phys. Express*, 14(2021)042010.

STRATUM CORNEUM HYDRATION: DRY SKIN – SENSITIVE SKIN AND BEYOND

Joachim W. Fluhr MD

Department of Dermatology, Charité University Clinic, Berlin, Germany

The epidermis and more specifically the stratum corneum represents the outermost part of the human body. This barrier is the interface to potentially harmful exogenous stressors like environmental factors. As an external organ, skin is approachable for non-invasive assessment.

The maintenance of stratum corneum hydration (SCH) homeostasis is of major importance for multiple physiological cutaneous functions: permeability barrier, epidermal differentiation, protection against uncontrolled water and electrolyte loss and defense against exogenous factors.

The formation of skin hydration is a complex and multifactorial process including the natural sources of skin moisturization. In addition, there are at least three known states of water binding in the stratum corneum: partially bound, tightly bound water and unbound water. The water binding state is closely related to hydrogen bonds. Molecular mechanisms and their modulation are classically studied in vitro models (e.g. in cell culture and 3D models) or using invasive biopsy techniques and subsequent immune-and array techniques.

Decreased SCH is a hallmark of a number of diseases such as atopic dermatitis, ichthyosis vulgaris, winter xerosis and sensitive skin. Objectifying SCH is of interest in these dermatoses. Evaluating SCH is used to characterize diseases activity and for claim substantiation of hydro-active compounds and formulations.

New concepts of stratum corneum hydration and the practical impact as well as limitations of non-invasive techniques to evaluate SCH are presented. Assessment of the cutaneous electrical properties (capacitance, resistance, impedance) are the most commonly used principals. Novel techniques such as in vitro and in vivo Raman confocal microspectroscopy, confocal reflectance spectroscopy, atomic force microscopy and others have emerged.

Multicenter clinical study on melanoma detection

M. Kaatz¹

¹SRH Wald-Klinikum Gera GmbH, Gera, Germany
Corresponding Author e-mail address: Martin.Kaatz@srh.de

KEY WORDS: malignant melanoma, optical biopsy, multiphoton tomography

Since malignant melanoma (MM) is a potentially lethal skin cancer with an increasing incidence and advanced MM has a poor prognosis, early detection is of great importance. The gold standard for diagnosing MM is histopathology.

Innovative optical methods have become increasingly important for early, non-invasive diagnostics. Therefore, a multicenter clinical study at the Heidelberg University Hospital and the SRH Wald-Klinikum Gera was conducted in patients with potentially malignant, pigmented skin lesions to investigate the use of a compact multimodal multiphoton tomograph for detection of MM.

Here we present the first preliminary results of this study. Among other things, it was shown that multimodal skin imaging *in vivo* - based on AF, SHG, FLIM, RCM and white light imaging - can be performed in patients with suspicious pigmented lesions in order to obtain imaging data for a further diagnosis.

Multimodal Multiphoton Tomography

K. König

JenLab GmbH, Johann-Hittorf-Strasse 8, 12489 Berlin
info@jenlab.de, www.jenlab.de

KEY WORDS: two-photon imaging, femtosecond laser, autofluorescence, SHG, FLIM, PLIM, CARS, confocal reflection microscopy, dermoscopy

Multiphoton tomography (MPT) based on near infrared femtosecond laser technologies provides label-free optical tissue biopsies with subcellular spatial resolution. Optical metabolic imaging is possible by autofluorescence lifetime imaging. Collagen can be imaged by second harmonic generation. The add-on modules “CARS”, “confocal” and “white light imager” provide additional information on intratissue lipids and water by rapid Raman spectroscopy, on cell membranes and refractive index modifications by confocal reflectance microscopy, and on dermoscopy parameters by wide-field imaging. Furthermore, the phosphorescence lifetime per pixel can be imaged (PLIM) by changing the repetition rate of the excitation pulses using acousto-optic modulators. Multiphoton tomographs can be also combined with high-NA (0.8) two-photon microendoscopes. The latest multimodal MPT system *MPTcompact* consists of a ultracompact 80 MHz femtosecond laser head at 780 nm that is integrated in the measurement head together with a scanning unit and detectors for autofluorescence-, SHG-, confocal reflection-, and white light imaging.

Major MPT applications include the diagnosis of pathological skin, the test of the anti-ageing cosmetic substances, and the study of pharmacokinetics in the skin. Skin modifications of astronauts after long-term space flights has been evaluated.

K. König, D. Pankin, A. Paudel, H. Hänßle, J. Winkler, M. Zieger, M. Kaatz: Invited paper: Skin cancer detection with a compact multimodal fiber laser multiphoton FLIM tomograph. SPIE-Proceed. Vol 116480 (2021) 116480A

K. König. Review: Clinical in vivo multiphoton FLIM tomography. *Methods Appl. Fluoresc.* 8 (2020) 034002.

K. König, H.G. Breunig, A. Batista, A. Schindele, M. Zieger, M. Kaatz. Translation of two-photon microscopy to the clinic: multimodal multiphoton CARS tomography of in vivo human skin. *J. Biomed. Opt.* 25 (2020) 014515.

K. König (Ed.) *Multiphoton Microscopy and Fluorescence Lifetime Imaging*. De Gruyter, Berlin, 2018. ISBN 978-3-11-043898-7, open-access.

Artificial Intelligence in Optical Skin Analysis – Challenges and Opportunities

T.K. Lee

Cancer Control Research Program, BC Cancer, Vancouver, BC, Canada
Department of Dermatology and Skin Science, University of British Columbia, Vancouver, BC, Canada
Photomedicine Institute, Vancouver Coast Health Research Institute, Vancouver, BC, Canada
School of Biomedical Engineering, University of British Columbia, Vancouver, BC, Canada
tle@bccrc.ca

KEY WORDS: Explainable AI, Domain Knowledge, Multimodality

Artificial intelligence has come a long way since its inception in 1956. The technique has been applied to many areas of our daily life, such as self-driving cars, airport security systems, Go games, and mammography screening. In skin imaging, studies have shown that AI techniques achieve a similar level of accuracy as expert dermatologists in skin cancer detection from photographs. However, for AI to be fully accepted in the workflow of skin care practice, there are still hurdles to overcome. One of the criticisms of AI is that it acts as a black box that its results cannot be explained. In addition, although AI achieves impressive results in special tasks of identifying one or two skin disease classes, its performance drops when the number of disease class becomes large. In this talk, I will outline some of the research works in explaining AI results, transferring domain knowledge and combining modalities for handling these challenges.

Risk assessment of skin damage for far-UVC irradiation below 240 nm which can be used to eradicate multi resistant germs and viruses

M. C. Meinke^{1*}, S. B. Lohan¹, L. Busch¹, A. A. Kühl², C. Witzel³, J. Schleusener¹

¹Department of Dermatology, Venerology and Allergology, Charité – Universitätsmedizin Berlin, Charitéplatz 1, 10117, Berlin, Germany; ²iPATH.Berlin-Immunopathology for Experimental Models, Core Facility of the Charité – Universitätsmedizin Berlin, Charitéplatz 1, 10117, Berlin, Germany; ³Division of Plastic and Reconstructive Surgery, Department of Surgery, Charité – Universitätsmedizin Berlin, Charitéplatz 1, 10117, Berlin, Germany
*martina.meinke@charite.de

KEY WORDS: Indicate up to three key words

Surgical site infections (SSIs) represent an important clinical problem resulting in increased levels of surgical morbidity and mortality. UVC irradiation during surgery has been considered to be a possible strategy to prevent the development of SSIs. Germicidal UV lamps, with a broad wavelength spectrum from 200 to 400 nm, are an effective bactericidal option against drug-resistant and drug-sensitive bacteria [1]. So far, however, they are assessed as a health hazard to patients and staff. Recent investigation using a newly developed far-UVC LED source with a peak emission wavelength of 233 nm have shown to reduce Methicillin-sensitive and Methicillin-resistant *Staphylococcus aureus* [2]. We investigated the effect of germicidal radiation doses on skin for human application. Skin cell viability, DNA damage potential and radical production were assessed in comparison to conventional near-UVC irradiation (254 nm) and UVA/B (280–400 nm) irradiation. Far-UVC radiation at 222 nm served as a negative control. At a dose of 40 mJ/cm² the far-UVC LED light source could reduce the bacteria by 5 log₁₀ levels. At 40 mJ/cm², the investigated skin models showed no reduction in immediate viability: The resulting superficial DNA damage was below 0.1 minimal erythema UVB dose which can be regarded as safe. The low damage vanished after 24h, while irradiation with this dose on four consecutive days showed no DNA damage, at all. The radical formation was far below 0.25 minimal erythema UVA dose. This low radical load can be scavenged by the antioxidant defense system [3].

Acknowledgements: The work is funded by the German Federal Ministry of Education and Research BMBF (FKZ 03ZZ0146B) within the program “Zwanzig20 – Partnerschaft für Innovation” and carried out within the consortium Advanced UV for Life

References

- [1] A. Kramer, M. Meinke, A. Patzelt, M.B. Stolpe, J. Lademann, K. Jacobs, Perspektiven physikalischer Verfahren der Antiseptik und Desinfektion, *Hygiene und Medizin*, 45;3/2020 D39
- [2] M. C. Meinke, A Kramer, S Einfeldt, M. Kneissl, Krankenhauskeime mit UVC-Leuchtdioden bekämpfen, *Management und Krankenhaus* 39; 9/2020, S.20
- [3] Lohan SB, Ivanov D, Schüler N, Berger B, Zastrow L, Lademann J, Meinke MC. Switching from healthy to unhealthy oxidative stress - does the radical type can be used as an indicator? *Free Radic Biol Med*. 2020 Nov 1:S0891-5849(20)31593-8. Online ahead of print

Confocal Microscopy: state of the art

Giovanni Pellacani

*Department of Clinical Internal, Anesthesiological and Cardiovascular Sciences, Dermatology
La Sapienza University of Rome*

KEY WORDS: confocal microscopy, melanoma, skin cancer

Reflectance confocal microscopy (RCM) is a non-invasive imaging technique which enables the *in vivo* evaluation of the skin with a near-to-histology resolution up to the depth of 250 μm , which corresponds to the upper dermis. RCM acquisition can be performed with the wide-probe Vivascope 1500 allowing a broad non-invasive examination at cellular-level resolution with a maximum size of 8x8 mm mosaics. The wide-probe device guarantees an overlap of RCM images with dermoscopy. Horizontal images of the skin results in grayscale color which brightness is related to the refractive index of different tissues and cell structures. Melanin, keratin, melanocytes and pigmented keratinocytes are examples of structures and cells that present high reflective index appearing bright. Therefore, RCM is employed for the evaluation of both melanocytic and non-melanocytic skin lesions.

To date, histopathology represents the gold standard for the diagnosis of skin cancers. However, the advent of this advanced non-invasive technology is increasingly inserting RCM in daily practice in order to increase diagnostic accuracy of cutaneous suspicious lesions as it has been shown that RCM is able to improve the early recognition of these lesions.

RCM in clinical practice is used for diagnosis of melanoma and non-melanoma skin cancers. Concerning Basal cell carcinoma, pon RCM, tumor islands (with peripheral palisading and cords showing bright outline and clearly defined shape) can be seen at the dermal layer, especially in pigmented/hypopigmented lesions. Whereas, keratinizing tumors are characterized by keratinocyte disorder and pleomorphism. Early diagnosis of melanoma and differential diagnosis with nevi results in the most common application, focusing on the identification of two melanoma-specific key-features: “atypical cells” and “dermal-epidermal junction disarray”, which may improve diagnostic accuracy, saving over the 50% of unnecessary excisions.

***In vivo* multiphoton imaging for non-invasive time course assessment over 1 year of melanin modulations and retinoids effects on human skin**

A.-M. Pena¹, T. Baldeweck¹, S. Brizion¹, E. Decenci re², S. Victorin¹, B. Ngo¹, E. Raynaud¹, L. Souverain¹, M. Bagot^{3,4}, E. Tancrede-Bohin^{4,5}

¹L'Or al Research and Innovation, Aulnay-sous-Bois, France; ²Center for Mathematical Morphology, MINES ParisTech – PSL Research University, Fontainebleau, France. ³Inserm U976, H pital Saint-Louis, Universit  de Paris, Paris, France ; ⁴Service de Dermatologie, H pital Saint Louis, Paris, France ; ⁵L'Or al Research and Innovation, Clichy, France.

ana-maria.pena@rd.loreal.com; <https://orcid.org/0000-0001-9943-2513>;
<https://www.loreal.com/en/beauty-science-and-technology>

KEY WORDS: Indicate up to three key words

In vivo multiphoton imaging and automatic 3D image processing tools provide quantitative information on human skin constituents¹. These multiphoton based tools allowed evidencing retinoids epidermal effects in the occlusive patch test protocol developed for antiaging products screening. This study aimed at investigating their relevance for non-invasive, time course assessment of retinoids cutaneous effects under real-life conditions for one year². Thirty women, 55-65 y, applied either retinol (RO 0.3%) or retinoic acid (RA 0.025%) on one forearm dorsal side versus a control product on the other forearm once a day for 1 year. *In vivo* multiphoton imaging was performed every three months, and biopsies were taken after 1 year. Epidermal thickness and dermal-epidermal junction (DEJ) undulation were estimated in 3D with multiphoton and in 2D with histology, whereas global melanin density and its z-epidermal distribution were estimated using 3D multiphoton image processing tools. We evidenced i) epidermal thickening with RO (+30%); ii) slight increase in DEJ undulation with RO; iii) slight decrease in 3D melanin density with RA; iv) limitation of the melanin ascent observed with seasonality and time within supra-basal layers with both retinoids. With a novel 3D descriptor of melanin z-epidermal distribution, *in vivo* multiphoton imaging allows demonstrating that daily usage of retinoids counteracts aging by acting not only on epidermal morphology, but also on melanin that is shown to accumulate in the supra-basal layers with time.

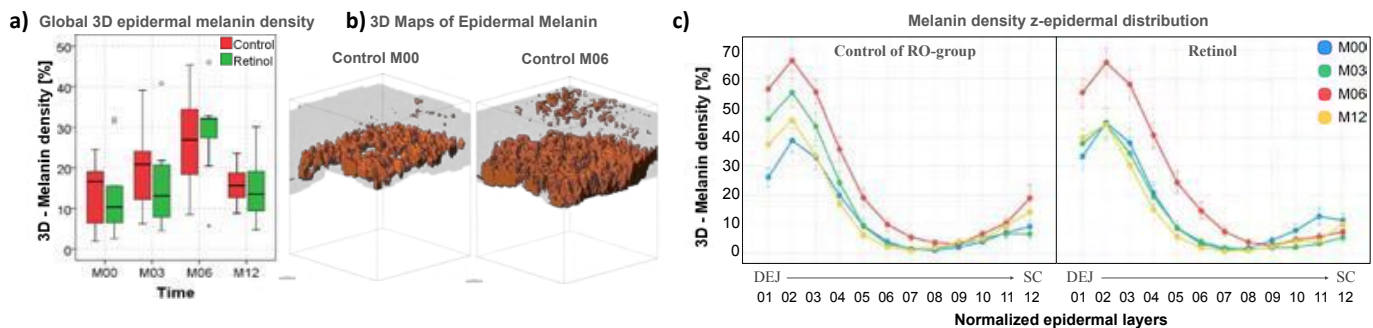


Fig. Modulation of global 3D epidermal melanin density and z-epidermal distribution with seasonality and retinol.

¹ A.-M. Pena *et al.* "Multiphoton FLIM in cosmetic clinical research" in: K. K nig (ed.) *Multiphoton Microscopy and Fluorescence Lifetime Imaging. Applications in Biology and Medecine*, (De Gruyter, Berlin, Boston, 2018, pp. 369-393).

² E. Tancrede-Bohin *et al.* *In vivo* multiphoton imaging for non-invasive time course assessment of retinoids effects on human skin, *Skin Res. Technol.*, 26 (2020) 794-803.

Using multiphoton microscopy to characterise skin transport determinants and processes

Michael Roberts, Sean Mangion, Lydia Sandiford and Amy Holmes

Clinical & Health Sciences, University of South Australia, Adelaide and Diamantina Institute, University of Queensland, Brisbane, Australia m.roberts@uq.edu.au

KEY WORDS: multiphoton microscopy, fluorescent emission, fluorescent lifetime imaging, phasor analysis, human skin, retinoids, zinc pyrithione

Retinoids are a widely used in dermatology and one of the few classes of drugs with optical properties suitable for multiphoton imaging. They are especially used in acne, solar photodamage, psoriasis and for cosmetic purposes. In this work, we describe the multiphoton and fluorescent lifetime imaging microscopy of a series of retinoids applied to human skin. These retinoids include several generations of retinoids: Retinyl palmitate, Retinal, Retinol, Tretinoin, Adapalene and Tazarotene. We measured their fluorescence intensity for a number of two photon excitation wavelengths, together with the fluorescence lifetime and phasor plots. We then characterised these in a range of formulations, in the human stratum corneum and in immortalised human keratinocytes. We will show specific examples of how the retinoids distribute in different regions of the skin over time after topical application.

In work, related to our previous studies on the topical safety of nanoparticulate zinc oxide, we also explored the optical properties and distribution in the skin of the common medicated dandruff ingredient, zinc pyrithione. These studies including characterising the optical properties of the zinc pyrithione and the quantifying the relative uptake of this agent into the various human skin structures.

First Two-Photon Imaging in Skin

Peter T. C. So, Barry R. Masters, Karsten Koenig, Enrico Gratton

Shortly after the developing of two-photon fluorescence microscopy by Drs. Winfred Denk, Watt Webb, and co-workers in Cornell University in early 1990s, Dr. Barry Masters worked with Dr. David Piston to demonstrate the potential of this approach for deep tissue imaging by studying ocular structure *ex vivo*. With the kind assistance of the Webb lab, especially, Dr. Piston, we developed our own two-photon system in Dr. Enrico Gratton's laboratory in University of Illinois. Dr. Masters has a long standing interest also in dermatology and has been a pioneer in using confocal reflectance approach for studying skin structures *in vivo*. In a very fruitful collaboration, Dr. Masters visited University of Illinois many times and worked with me and Dr. Gratton in establishing the utility of multiphoton microscopy for skin imaging. We demonstrated the first *in vivo* imaging of skin structures down to the dermis in the first human subject. We have further demonstrated a combination of multiphoton fluorescence and confocal reflected light imaging. By resolving fluorescence spectral and lifetime information, we attributed metabolically important fluorescence signal to NAD(P)H signal in keratinocyte mitochondria. We also observed strong narrow band emission in the dermis but did not realize the signal being second harmonic generation from collagen structures. With the addition of Dr. Karsten Koenig, we started to investigate potential two-photon photodamage mechanisms in tissue including pathways related reactive oxygen generation and pathways related to thermal damage in the presence of strong absorber such as melanin.

Abstracts

Oral Presentations

In alphabetical order of the corresponding author

All presentations are available online for 3 months

<https://roellmedia-streams.de/isbs2021>

Quantitative characterization of human skin tension in vivo using a new parameter: Tension index

M. Ayadh^{1,2}, A. Guillermin¹, M-A. Abellan¹, C. Didier¹, A. Bigouret², H. Zahouani¹

1. Université de Lyon, ECL-ENISE, LTDS, 36, avenue Guy de Collongue, 69134 Ecully, France.

2. Laboratoires Clarins, 5 Rue Ampère, 95300 Pontoise, France

Corresponding Author e-mail address and URL: meriem.ayadh@ec-lyon.fr

KEY WORDS: natural skin tension, non-contact impact tests in vivo, tension index

Natural skin tension was discovered by Dupeyren¹ in 1834 and demonstrated by Langer^{2,3} in 1861. This tension plays an important role in the phenomenon of cicatrization and during surgical procedures⁴. The existing studies are performed ex vivo and give a qualitative mapping of the skin tension. They show the preferred direction of the skin tension.

In this study we propose a quantitative characterization of the skin tension in vivo by two methods. The first method is based on non-contact impact tests performed with the WaveSkin device⁵. This device applies an air flow onto the outer surface of the skin in vivo which generates the propagation of Rayleigh waves. The speed of the propagation of the Rayleigh waves are measured in 7 directions. From the measured speed it is possible to calculate the tension forces and to identify the main directions of skin tension. The second method consists of calculating the tension index from images of skin relief. This tension index, developed at the LTDS by Pr Hassan Zahouani, gives a quantification to characterize the skin tension forces. The method is based on the equilibrium equation of the tension in the Fourier spectrum after a decomposition of the spatial frequencies according to the two directions x and y of the relief of the analyzed zone. The result of the analysis makes it possible to quantify the tension index of skin.

The study was carried out on 42 volunteers with two age groups: the young group [20 - 30] years-old and the older group [45 - 65] years-old. Non-contact impact test measurements are performed on the skin of the forearm and thigh. The skin relief analysis is performed on seven areas of the body: the forearm, thigh, cheek, belly, upper chest, and arm (front and back face). The results show that the skin tension depends on the area of the body in terms of main directions and state of tension. The skin loses its tension and suppleness with age which creates an imbalance of tension forces between the family of tension lines and the family of suppleness lines.

¹ Langer, K. ON THE ANATOMY AND PHYSIOLOGY OF THE SKIN I. The cleavability of the cutis. Br. J. Plast. Surg. 31, 277–278 (1978).

² Langer, K. ON THE ANATOMY AND PHYSIOLOGY OF THE SKIN II. Skin Tension. Br. J. Plast. Surg. 31, 93–106 (1978).

³ Langer, K. ON THE ANATOMY AND PHYSIOLOGY OF THE SKIN III. The elasticity of the cutis. Br. J. Plast. Surg. 31, 185–199 (1978).

⁴ Cerda, E. Mechanics of scars. J. Biomech. 38, 1598–1603 (2005).

⁵ M. Ayadh, M. Abellan, A. Bigouret, and H. Zahouani, “Methods for characterizing the anisotropic behavior of the human skin ’ s relief and its mechanical properties in vivo linked to age effects,” *Surf. Topogr. Metrol. Prop.*, vol. 8, no. 1, p. 14002, 2020.

Subcutaneous Skin Elasticity Imaging: UNDERSKIN®

A. Bergheau¹, R. Vargiolu², L. Ouillon³, H. Zahouani⁴

University of Lyon - Ecole Centrale de Lyon - Laboratory of Tribology and System Dynamics (LTDS) - UMR 5513
CNRS, ECL-ENISE, 36 avenue Guy de Collongue, 69134, ECULLY
Corresponding Author e-mail address and URL: alexandre.bergheau@ec-lyon.fr

KEY WORDS: Skin Sublayers, Elastography, Surface Waves

The study of the mechanical behavior of human skin is a very rich topic due to the multiple applications in plastic surgery, dermatology, and cosmetics. The focus of this work is the development of UNDERSKIN®¹; which studies and measures the mechanical behavior of skin in vivo and reconstructed skin subcutaneously. This includes a detailed dimensional look at the effects of a diverse range of applications overtime at the surface and beneath it. To see the elastic properties of the skin beneath the surface, we use the principles of the propagation of surface waves. UNDERSKIN® records and measures these ripples with an optical displacement sensor which is composed of 400 receivers spaced of 17.5µm with a total length of 7mm. This, going from the skin ripple to the subcutaneous skin elasticity via the dispersion analysis of the Rayleigh speed, is the whole process of UNDERSKIN®'s signal processing. Indeed, one of the key steps is the dispersion analysis in which the ratio of the phase velocity and the frequency will result in the corresponding wavelength, hence the penetration depth of the shear wave. Consequently, for a given phase velocity and wavelength, we have access to the shear velocity with its penetration depth and so the Elastic Modulus. We then produce a detailed visual of what's happening in the elastic behavior across the epidermis, the dermis, and the hypodermis.

UNDERSKIN® is a device comprised of a multi-jointed robotic arm (to reach any zones of the human body you want to measure. It extends and swivels), an airflow source of the surface waves (no contact indenter), and an optical displacement sensor to record the displacement of the surface waves. Therefore, not only will it provide essential skin information such as the anisotropy of the skin tension lines, tension forces, and the density of the collagen fibers but it will also tell you about the effectiveness of a cosmetic product, the healing of a wound, the reading of cellulite and have the potential of early foreign body detection. The result is a 1D-3D internal visual shown in figure 1 and 2.

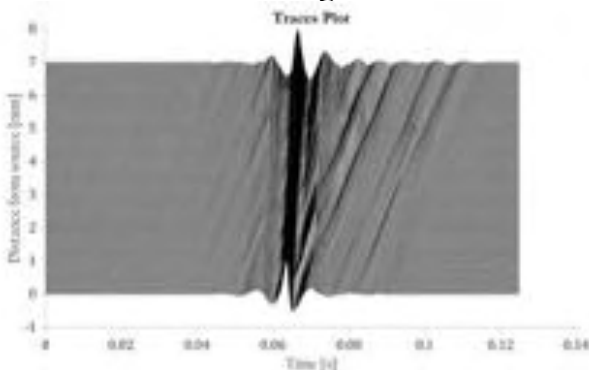


Figure 1: Surface wave recorded at the skin's surface with UNDERSKIN®: displacement image at each receiver location

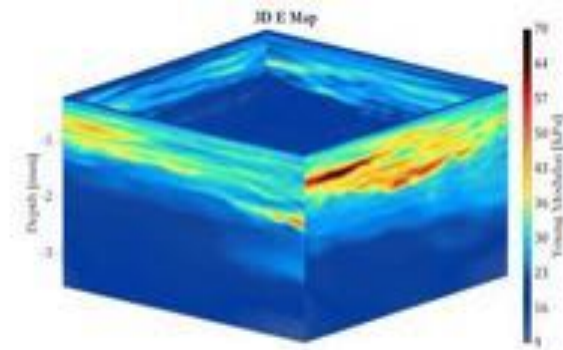


Figure 2: 3D Elastic Modulus map resulted from UNDERSKIN®'s signal processing

¹ Patent filed in November 2020 with PULSALYS

Skin Fillers Visualization and Filler Type Determination with High Frequency Ultrasound.

A. Bezugly¹, P. Belkov², T. Sedova³.

1- Academy of Postgraduate Education of the Russian Federal Medical Biological Agency.

2- ANTA-Med clinic, Moscow, Russia.

3- E.A. Vagner Perm State Medical University, Moscow, Russia.

KEY WORDS: skin filler; high frequency ultrasound skin imaging.

Introduction:

Filler injections are one of the most popular procedures in aesthetic medicine. There is a significant increase in fillers production, their composition complexity, and injections methods variety, which may contribute to potential risks grows. Also, still, no "ideal" safe, biodegradable fillers, which are easy for use, and provide a long-lasting effect with the side effects absence. It is especially important to take into account the large patients group with an unclear anamnesis. Unfortunately, often, they cannot provide information about the previously injected fillers. Therefore, the preliminary examination for previously injected filler detection and its type identification is necessary. The high frequency ultrasound skin (HFUS) imaging was reported as the instrument for skin fillers visualization. The information about filler resorption degrees and the surrounding tissue condition also critical and helpful for the next injection possibility decision.

Aim:

Study of the different fillers HFUS patterns features, and the filler type differentiation possibilities at 22, and 75 MHz frequencies.

Materials and methods:

Skin and soft tissues 22 and 75 MHz HFUS examination was performed in 78 patients who previously had various fillers injections. Filler type was confirmed by anamnesis and clinical documentation records. Patients with unclear anamnesis were excluded from the study. Acoustic density was evaluated on a scale of 0 to 255 units. The HFUS patterns of the hyaluronic acid (HA), polymethylmethacrylate (PMMA), polyacrylic gel (PAAG), calcium hydroxyapatite (CaHA), and silicone were studied.

Results:

High frequency ultrasonic patterns and features for HA, PMMA, PAAG, CaHA and silicone were described. An algorithm for filler type differentiation, based on the high frequency ultrasound examination results was proposed.

Conclusion:

High frequency ultrasound examination useful for determining of the filler presence and location in the skin and soft tissues. The HFUS fillers patterns differences and features of the filler volume and acoustic density dynamic changes useful for the filler type differentiation. A preliminary patient's skin examination before filler injections significantly increases the safety and effectiveness of these procedures.

New Protocol to Evaluate Emotional Experience of Customers

C Bonnaud-Rosaye¹, I Bonnet¹, A Courtois¹

1-BASF Beauty Care Solutions France, 32, rue Saint Jean de Dieu, Lyon, France
catherine.bonnaud-rosaye@basf.com

KEY WORDS: non verbal evaluation method, emotion evaluation, holistic evaluation

Setting up in the food industry, emotional claims are now spreading to related sectors such as the cosmetics industry. In order to prove these benefits in relation to well-being, clinical protocols from neuroscience have been adapted for the cosmetic industry. In this study, we used an original clinical protocol to measure sensitive skin benefits not only by measuring roughness or redness of the skin but with volunteer feelings after a single application of a cream.

We run a specifically designed emotional test, on 87 Asian female volunteers (30-50 years old) with sensitive skin. Just after the application of a cream containing 2% of a molecular patch blend or a placebo, the volunteers were asked to correlate their perceived emotions to visual stimuli (emotion boards test).

This method is a non-verbal tool based on boards of pictures built to convey emotions (9 boards of several pictures expressing one specific emotion: surprise, tenderness, curiosity, disgust, desire, anger, ill at ease, happiness or sadness) and to measure projected emotions related to a product or its use. The name of the emotion is never cited, allowing to go beyond declared feelings. Emotional content of boards was previously validated with more than 1200 naive consumers from 8 countries from Europe, America and Asia. Volunteers indicated how the emotion expressed by each board matched the emotion they felt while using this product on a scale from 1 to 7 (positive answer corresponded to the sum 5 to 7).

As a result, we demonstrated that the method allows to discriminate perceived emotions. molecular patch formulation matches the tenderness, happiness and tenderness emotion boards by 93, 90% and 61% respectively (better results than placebo), whereas the other emotions were not significantly selected by panelists.

Thanks to this original method using emotion boards, we demonstrated that a specific molecular patch formulation is able to deliver emotional benefits immediately after application.

Using this method, on the top of classical methods, contributes to a better holistic evaluation of product effectiveness.

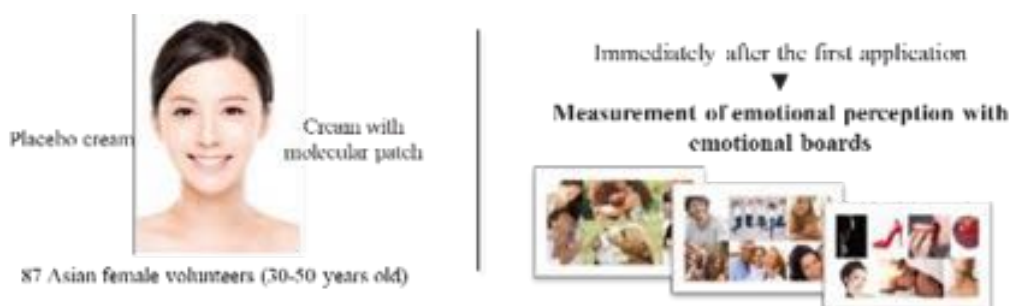


Fig 1: New protocol using emotional boards to evaluate emotional benefits of a cream

New Methods for Digital Transfer of Visible Pigmentation from Forearm Irradiation and other Treatment Sites to the Face.

Remo Campiche¹, Sarah Gougeon², Marie Chere², Magalie Roche², Mathias Gempeler¹, Dominik Imfeld¹

1 DSM Nutritional Products, Personal Care & Aroma, Kaiseraugst, Switzerland

2 Newtone Technologies, Lyon, France

KEY WORDS: imaging, digital transfer, pigmentation

The study of cutaneous pigmentation and the development of means to modulate this pigmentation is common place in both academia and industry. In order to evoke a pigmentation reaction in skin, one needs to irradiate the skin with ultraviolet radiation (UVR) or high energy visible light (HEV, or blue light). Wavelengths, doses, and fluencies used are usually so that irradiation in the face is not feasible due to ethical concerns. Therefore, irradiation must be done on surrogate body sites such as the inner forearm or the back. Nevertheless, particularly the cosmetic industry is interested how pigmentation reactions and their modulation would look like in the face. Thus, we set out to develop a method to digitally transfer pigmentation of the inner forearm of volunteers to their faces. Figure 1 summarizes this method. We used two different approaches. 1) We irradiated inner forearms with a specific blue light irradiation protocol inducing visible pigmentation which we modulated with a cosmetic active ingredient. We measured skin pigmentation using a chromameter device and took photographs. We also took photographs of the volunteer's faces. We then transferred the pigmentation of the inner forearm to the face of the same volunteer. Using a dedicated and newly developed algorithm, we adjusted facial pigmentation to match forearm pigmentation. As such, we were able to show how a pigmentation reaction evoked on the forearm would look like in the face. 2) We induced pigmentation of forearms using a combination of ultraviolet irradiation and a pro-pigmenting peptide. As no real faces of the volunteers were available in this case, we transferred the pigmentation reaction to artificial mean faces. Using these methods, we can predict facial pigmentation reactions on surrogate body sites like e.g. forearm or back without irradiating individuals directly in the face.

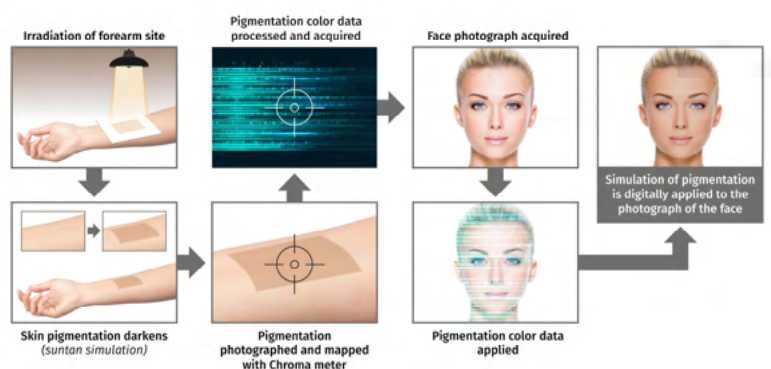


Figure 1: Flow chart illustrating the method. A pigmentation reaction is induced on the forearm. It is then digitally applied on face images to simulate facial tanning as if the face had been irradiated instead of the forearm.

Evaluation of perceived skin brightness in Asian women

Jiyei Choi¹, Ji Yeon Han¹, Myeong ryeol Lee¹, Eun Joo Kim¹

AMOREPACIFIC Research and Development Center
1920, Yonggu-daero, Giheung-gu, Yongin-si, Gyeonggi-do, Republic of Korea
eon827@amorepacific.com

KEY WORDS: skin color, reflectance spectrum, perceived skin tone

Asian women tend to prefer bright and transparent skin. Generally, a high L^* value is considered a bright skin tone. However, the L^* value is often difficult to explain visual perception of skin tone because the perceived skin tone reflects the interaction of various factors that affect skin surface reflections¹. In this study, the perception about skin tone was investigated in Korean women, and based on the result, new evaluation method correlated with perceived skin tone was developed. Facial images of the woman (38 ± 8.9 years old, $n=61$) were photographed using VISIA-CR and their skin tone was evaluated using spectrophotometer CM-2600d (Minolta, Japan). Images of the women were presented on monitor to 8 clinical experts. They assessed the perceived skin tone and scored the level of brightness as five-grade (1; very dark, 5; very light). The perceived skin tone was compared with L^* value and VB ratio (%), new developed method using reflected skin spectrum. Visually assessed skin brightness and L^* value was positively correlated in grade 1 to 4, however, the L^* value of grade 5 ($L^* = 63.3$) was significantly lower than grade 4 ($L^* = 65.1$). As we compared the skin spectrum between the visually dark group and bright group, the light reflection amount in short wavelength spectrum zone (400~490nm) was significantly different by perceived skin tone. Therefore, VB ratio (%) which is ratio of the short spectrum zone in total zone was developed. As a result, perceived skin brightness and the VB ratio (%) was positively correlated in overall grade (Figure 1), and the correlation coefficient was higher ($r=0.598$, $p<0.001$) than previous method ($r=0.383$, $p=0.002$). The L^* value is an indicator of skin brightness, however, the correlation is lowered in very bright skin tone. In the case of bright skin tone, the effect of a^* and b^* value is considered to be larger than that of dark skin tone. Newly developed VB ratio might be an alternative to this problem, and also can be used to develop products improving perceived skin tone.

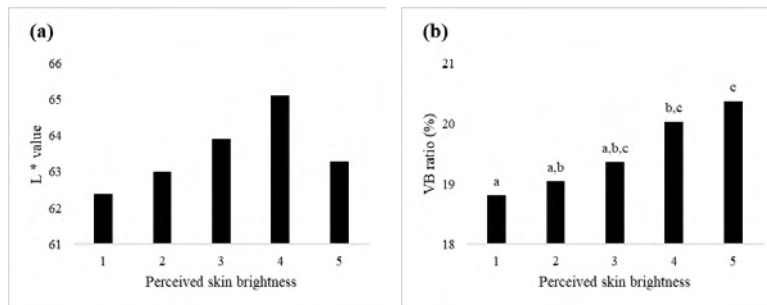


Figure 1. Comparison between perceived skin brightness score (1; very dark, 5; very light) and parameters; (a) L^* value, (b) VB ratio(%).a-c; values with different alphabets are significantly different ($p<0.05$).

¹ Citation of a journal article: Wang L, Wan X, Xiao G. Skin Res Technol., 25(5)693-700. 2019

Decoding skin tightness: From a clinical evidence to an instrumental and biological proof of sensorial stimulation perception

S. Connétable¹, O. Dufour¹, A. Tazé¹, A. Foucher¹, E. Arbey¹, N. Misra¹, B. Lynch¹, R. Abdayem¹, D. Bernard¹, Y. Domanov¹, and A. Potter¹

¹L'Oréal Research and Innovation, 1 avenue Eugène Schueller, 93600 Aulnay-sous-Bois, France
Sophie.Connetable@rd.loreal.com

KEY WORDS: Tightness, stratum corneum, proteomics, metabolomics, sensitive skin

The sensation of comfort perceived by consumers after using a cosmetic treatment is expressed in subjective terms, such as feelings of “tightness”, “softness” or “moisturization”. Our challenge was to better understand the triggers for tightness and the typology of tight skin, in particular the contribution of skin surface biomechanics to tightness perception.

For this purpose, we performed a consumer survey to identify the triggers for tightness and then conducted two clinical studies. The facial skin of women prone to feeling tightness and of women not prone to feeling tightness was characterized using instrumental, biological and clinical methods as well as subjective questionnaires.

The consumer survey that included 3046 adult women, representative of the French population, showed that 71% of them declare feeling skin tightness, usually on the cheeks. These women tend to be wealthier, to use more cosmetic products and to live more often in cities and/or in areas where the water is hard than those that declared to never feel any tightness. Contact with water (shower/bath/swimming pool/beach) or cleansers, as well as some climate conditions (wind, cold, overheated area, UV/sun exposure) are the main triggers of skin tightness sensations.

A harsh cleanser was therefore used to induce skin tightness sensation in a standardized manner during two consecutive clinical studies. Clinical scores of dryness, as well as instrumental measurements of hydration, barrier function, sebum level, superficial skin and corneocytes mechanical properties were performed on the face. A wide range of biomarkers was analyzed: lipids, NMFs, proteins and other metabolites.

Results show that *stratum corneum* (SC) from women who are prone to tightness is more rigid at baseline and, in addition, that using a cleanser increases SC rigidity in all women. This difference in rigidity between tightness-prone and non-tightness-prone skin could be caused by differences in the composition of the lipids and keratin matrix. Volunteers perceive a strong association between tightness and dryness but differences in hydration could not be objectified. Tightness sensation is strongly associated with sensitive skin but the barrier function does not appear to play a major role.

Perception of comfort / discomfort is partly driven by activation of multiple mechanoreceptors inside the skin and recent computational studies have shown a direct correlation between modifications of skin biomechanics by formulas and consumer perception of comfort¹. This demonstrates that the stiffness of *stratum corneum* is a major factor in order to explain skin tightness perception, but not sufficient. Several other biomarkers gave us new clues about the origins of tightness and consequently new research avenues and products opportunities.

¹ Decoding the sensorial perception of our skin: biomechanics & the role of mechanotransduction, R. Bennett-Kennett, J. Pace, B. Lynch, G. Luengo, Y. Domanov, D. Batisse, K. Sun, A. Potter, R. Dauskardt, IFSCC 2020

Comparison of Maximal Lesion Thickness Measurements between two Portable Skin Ultrasound Imaging Devices

G. Csány¹, L. H. Gergely³, Klára Szalai³, Domonkos Csabai¹, Péter Marosán-Vilimszky^{1,2}, Krisztián Füzési¹, Miklós Sárdy³, Miklós Gyöngy^{1,2}

¹*Dermus Kft, Sopron út 64., H-1116, Budapest, , Hungary*

²*Faculty of Information Technology and Bionics, Pázmány Péter Catholic University, Práter utca 50/A, H-1083, Budapest, Hungary*

³*Department of Dermatology, Venereology and Dermatocology, Semmelweis University, Mária utca 41., H-1085, Budapest, Hungary*

Corresponding Author e-mail address and URL: gergely.csany@dermusvision.com, <https://www.dermusvision.com>

KEY WORDS: dermatological ultrasound, portable ultrasound, skin lesion thickness

Measurement of the maximal lesion thickness is an essential part of the ultrasound examination of skin cancer¹. The aim of the current work is to compare maximal lesion thickness measurements with two portable devices, the Dermus SkinScanner (which also provides colocalized optical imaging), and the Damiński DermaMed; with nominal centre frequencies of 33 and 48 MHz, respectively. As part of an ongoing clinical study², melanocytic and non-melanocytic lesions (N=49) and skin inflammatory lesions (N=8) had been recorded with both devices. In the current study, the lesion thicknesses were measured by 3 observers, and images of a wire phantom with 5-mm depth spacing were recorded as reference. On average, the SkinScanner returned higher thickness measurements, namely 37.9±41.5%, 40.4±54.5% higher for melanocytic and non-melanocytic lesions, inflammatory lesions, respectively; the interobserver variability was always below 25%. In comparison, the wire depths were both correctly measured within an average 5% error. The results suggest that the SkinScanner consistently provides higher measures of lesion thickness, without evidence of a major measurement bias in either imager for the wire phantom measurements. In a previous study comparing sub-mm lesion thickness measurements between a 20 MHz and 100 MHz ultrasound transducer³, the lower frequency was found to provide approximately 5% higher estimates of tumour thickness, while the current results show a much larger difference at closer operating frequencies. The results highlight the potential for measurement variability between devices. The variability is hypothesized to originate from depth-variability of resolution and contrast, which is especially present in single-element-imagers such as in the present case. In addition to the potential role of optical guidance for better transducer placement, the results highlight the importance of focal plane design choices in single element imaging systems to better approximate the performance of more expensive, linear-array-based ultrasound machines.

¹ F. Alfageme, X. Wortsman, O. Catalano, G. Roustan, M. Crisan, D. Crisan, D. E. Gaitini, E. Cerezo, R. Badea. "European Federation of Societies for Ultrasound in Medicine and Biology (EFSUMB) position statement on dermatologic ultrasound." *Ultraschall in der Medizin-European J. Ultrasound* (2020).

² G. Csány, L. H. Gergely, K. Szalai, K. K. Lőrincz, L. Strobel, D. Csabai, I. Hegedüs, P. Marosán, K. Füzési, M. Sárdy, M. Gyöngy, "First clinical experience with a novel optical-ultrasound imaging device on various skin pathologies" (manuscript in preparation)

³ T. Gambichler, G. Moussa, K. Bahrenberg, M. Vogt, H. Ermert, D. Weyhe, P. Altmeyer, K. Hoffmann.

"Preoperative ultrasonic assessment of thin melanocytic skin lesions using a 100-MHz ultrasound transducer: a comparative study." *Dermatologic surgery* 33.7 (2007): 818-824.

Application of skin imaging techniques for the efficacy evaluation of a cosmetic formulation containing *Spirulina* sp.

Gabriela Maria D'Angelo Costa¹, Patrícia Maria Berardo Gonçalves Maia Campos¹

¹ Center of Advanced Studies in Cosmetic Technology - School of Pharmaceutical Sciences of Ribeirao Preto - University of Sao Paulo, Brazil
Av do Café, s/nº, Monte Alegre, Ribeirão Preto, SP, Brazil 14040-903.
gmdcosta@usp.br and pmcampos@usp.br

KEY WORDS: Skin hydration, Reflectance Confocal Microscopy, Skin uniformity

The use of active substances with hydration and film-forming properties in the development of cosmetic formulations is very important to obtain more effective skin care formulations.¹ *Spirulina* sp., a blue-green microalgae, due to its a complex composition, such as proteins, polysaccharides, vitamins, lipids and pigments, has potential for application in cosmetic formulations for the improvement of mature skin conditions.² In this context, the instrumental measurements, such as Reflectance Confocal Microscopy (RCM), are important tools for evaluation of the clinical benefits of *Spirulina* sp. Thus, the aim of this study was to evaluate the clinical efficacy of a cosmetic formulation containing *Spirulina* sp. in the improvement of skin hydration and uniformity. For this, after approval by Ethnics Committee of Faculty of Pharmaceutical Sciences of Ribeirão Preto – University of Sao Paulo, 16 health female subjects, aged 39 to 55 years, skin Fitzpatrick Phototypes II and III were enrolled. The subjects were divided in two groups: G1- applied the formulation with 0,1% of *Spirulina* sp. (FS) and G2 – applied the formulation without *Spirulina* sp. (vehicle) on the face once a day at night for 42-day period. RCM analyses were performed before and after 42-day period of application of the studied formulations in terms of stratum corneum thickness, granular layer thickness, viable epidermis thickness, dermal papillae depth, interkeratinocytes brightness in the granular layer, furrows morphology and skin surface homogeneity. Skin luminosity was also evaluated by high resolution images. In addition, perceived efficacy of skin hydration and uniformity were evaluated at the end of the study by subjects. The obtained results showed a significant increase in the granular layer thickness and interkeratinocytes brightness after the treatment period of the formulation added with *Spirulina* sp. when compared to baseline values and vehicle formulation. These results suggest an increase of skin hydration in the epidermis deeper layers.³ In addition, a significant improvement of the furrows morphology and the homogeneity of the skin surface were observed.⁴ The skin luminosity significant reduced after 42-day period of treatment with FS, which suggests an improvement of skin uniformity. Finally, study participants perceived these effects once they reported an improvement of skin hydration and uniformity after the treatment with FS. In conclusion, the proposed formulation was effective in the improvement of skin hydration and morphological characteristics, as well as improved the skin uniformity. Finally, *Spirulina* sp. can be suggested as an effective multifunctional active ingredient obtained from biotechnological process for the development of moisturizing cosmetic products for mature skin care.

¹M.O. de Melo, P.M.B.G. Maia Campos. Int. J. Cosmet. Sci., 41(2019)579–584. ²F.B.Jr. Camargo, P.M.B.G. Maia Campos inventors. WO2012135928A1(2012)1-19. ³D.G. Mercurio, R. Jdid, F. Morizot et al. Br. J. Dermatol.,174(2016)553–561. ⁴M. Manfredini, G. Mazzaglia, S. Ciardo, S. et al. Skin Res. Technol., 19(2013)299–307.

Oxidative stress and anti-oxidant defense in plaque psoriasis

Razvigor Darlenski*, Evgeniya Hristakieva*, Joachim Fluhr**

* Department of dermatovenereology, Trakia University-Stara Zagora

** Department of Dermatology and Allergy, Charité Univerätsmedizin, Berlin, Germany

KEY WORDS: carotenoid, oxidative stress, psoriasis

Background: Psoriasis as a multifactorial systemic disease presents with systemic inflammation that primarily affects the skin. An imbalance between pro-oxidative stress and antioxidant defense mechanisms are known in psoriasis patients.

Aim: The aim of this talk is to summarize the current knowledge on oxidative stress and antioxidant defense of the skin in psoriasis.

Material and methods: Patients with mild-to-moderate plaque psoriasis were enrolled in the study. All underwent 12 sessions of narrow band UVB (NB-UVB) phototherapy. Serum levels of the end product of lipid peroxidation - malondialdehyde (MDA), Reactive oxygen species (ROS), ascorbyl radicals (Asc) and detoxifying activity of catalase (CAT) were measured in the peripheral blood with spectrophotometric and EPR spectroscopy methods. Carotenoid levels of the skin in vivo were assessed by spectroscopic method.

Results: Disease activity improved in all patients compared to baseline witnessed by significant decrease in PASI and DLQI. ROS and Asc declined during therapy in parallel to a decrease in MDA. A mild decrease in the antioxidative enzyme CAT activity which did not reach the significance was observed. Psoriasis patients show decreased levels of carotenoids in the skin at baseline, however, no significant dynamics was observed during NB-UVB.

Conclusion: Psoriasis displays hindered antioxidant defense and the disease activity is accompanied by increased oxidative systemic stress. NB-UVB is effective in modifying the antioxidant defense in psoriatic patients

Study of Clinical Efficacy and Microbiome Effects of an Anti-Acne Regimen

A. Duev¹, H. Cao¹, S. Schwartz², E. L. Salvador Junior³, A. Denes¹, R. Frumento²

1) JAFRA Cosmetics International Inc, 2451 Townsgate Rd, Westlake Village, CA, USA, 91361

2) International Research Services Inc, 222 Grace Church St, Port Chester, NY, USA, 10573

3) Allergisa pesquisa Dermato-Cosmetica LTDA, Avenida Dr Romeu Tortima, 452 – Barão Geraldo, Campinas, SP, Brazil, 13084-791

KEY WORDS: acne, microbiome, clinical testing

There is a growing understanding of the role of microbiome in skin health and disorders. Progress in tools and methods of microbiome study has advanced the understanding of acne vulgaris from “overgrowth of *P. acnes*” to importance of skin microbe diversity, pathogenicity of specific *P. acnes* strains and genes¹, and ability of other skin flora to suppress *P. acnes*².

A novel anti-acne regimen was designed to target multiple mechanisms of acne, with goals of rapid efficacy, mildness, and clear effect on skin microbiome. Design included salicylic acid as monograph ingredient, succinic acid, honey ferment, lactobacillus ferment and extract from meadowsweet for targeting the microbiome, as well as other ingredients for anti-sebum, anti-microbial, anti-inflammatory, and skin moisturization benefits. Regimen was evaluated in an 8-week clinical study of 32 subjects with acne and oily skin. Evaluation included lesion counts, expert grading of lesions, erythema and appearance, measurements of moisture, TEWL and sebum. Swabs taken at baseline and 2 and 8 weeks were analyzed by shallow shotgun metagenomic sequencing³ at 2 million reads per sample.

Statistically significant findings for cosmetics claim substantiation included: regimen was well tolerated, decreased acne and non-acne lesions in 2 weeks, decreased erythema, desquamation and sebum, and improved skin moisture. Regimen decreased *P. acnes* and *S. aureus* in 2 weeks and *P. granulosum* in 8 weeks, while preserving microbiome diversity.

There were also observations helpful for future studies. Sample collection and DNA quality is challenging with skin swabs. Sequencing at 2 million reads did not resolve all species, but genus identification was more reliable. Microbiome changed in two phases – initial suppression showing opportunistic flora from other body areas and gut, then returning to a state more like baseline. Mean Shannon index first slightly increased then slightly decreased, but ranked-sum test showed these changes as not statistically significant. Spearman correlation analysis at family level found significant inverse correlations: *Lactobacillaceae* and erythema, *Staphylococcaceae* and blackheads, *Bifidobacteriaceae* and pimples. Presumably, these reflect altered skin conditions more than causation. Sequencing also found pathogenicity factors – a tight adhesion protein and a pore-forming toxin – in samples from 5 panelists. Of these, 3 showed worse than median decrease of inflammatory lesions, while in 1, lesion count increased. This suggests importance of not just species, but strains and genes, for clinical outcomes.

These observations show how shallow shotgun metagenomic sequencing with more time points adds insight to a clinical study, and efficacy of a microbiome-inspired skin care product design.

¹ “Acne Pathogenesis” in G. Plewig, B. Melnik, W. Chen. “Plewig and Kligman's Acne and Rosacea, 4th ed.”, (Springer Nature Switzerland AG, Switzerland, 2019)

² Y. Wang, S. Kuo, M. Shu, *et al*, Appl. Microbiol. Biotechnol., 98(2014)411–424.

³ B. Hillmann, G. Al-Ghalith, R. Shields-Cutler, *et al*, MSystems., 3.6(2018).

Exploring the impact of vegetarian-vegan and omnivores regimes in human skin physiology

Cíntia Ferreira-Pêgo^{1*}, Rejane Giacomelli Tavares¹, Sofia Lopes², Tatiana Fontes², Catarina Rosado², Luís Monteiro Rodrigues¹

¹*CBIOS – Universidade Lusófona’s Research Center for Biosciences & Health Technologies, Campo Grande 376, 1749-024 Lisboa, Portugal.*

²*School of Sciences and Health Technologies, Universidade Lusófona de Humanidades e Tecnologias, Lisboa, Portugal*

Corresponding Author: cintia.pego@ulusofona.pt

* Cíntia Ferreira Pêgo is funded by Foundation for Science and Technology (FCT) Scientific Employment Stimulus contract with the reference number CEEC/CBIOS/NUT/2018. This work is funded by national funds through FCT - Foundation for Science and Technology, I.P., under the UIDB/04567/2020 and UIDP/04567/2020 projects.

Key-words: vegetarian diet; vegan diet; visceral adipose tissue; subcutaneous adipose tissue; skin

The subcutaneous adipose tissue (SAT) is regarded as a crucial connective tissue with unique specifications involving skin support and insulation of the whole body. Its distribution together with the visceral adipose tissue (VAT) changes from childhood to puberty and adulthood and differs in man and woman due to specific neuro-endocrine regulators. Total body fat, involving SAT and VAT are both associated to cardiometabolic risk factors, which includes hypertension, insulin resistance, steatosis, and metabolic syndrome. In this study we aimed to examine the total body composition and the distribution of visceral and subcutaneous fat tissue among vegetarians-vegans and omnivores individuals. At the same time a preliminary assessment of skin biomechanics was conducted, having in mind the importance of SAT to body contour and the “envelope” function. A cross-sectional study involving 12 participants of both sexes (27.0±7.17years old) was conducted, in compliance with good clinical practices. Body composition was assessed using a dual-energy x-ray absorptiometry (DXA Lunar Prodigy Advance - General Electric Healthcare®) while skin characterization was achieved by noninvasive measurements of hydration, cutaneous barrier, sebum secretion, as well as elastic and viscoelastic parameters (CK Electronics GmbH). Other descriptive variables were also collected such as dietary habits, weight, height, physical activity practice and abdominal perimeter. We found no significant differences between these two groups for weight, height, BMI, smoking status, and physical activity. The same regarding total bone mass, fat mass, lean mass, tissue mass, and fat-free mass. Nevertheless vegetarian-vegan individuals consistently showed higher values of VAT and SAT (p-value>0.05) compared to the omnivores group. Concerning the cutaneous condition of the different dietary groups, no statistically significant differences were established in the skin properties assessed.

1 Spoto B, Di Betta E, Mattace-Raso F, et al. (2014). doi: 10.1016/j.numecd.2014.04.017.

2 Mittal B. (2019). doi.org/10.4103/ijmr.IJMR_1910_18

3 Fischer K, Pick JA, Moewes D, Nöthlings U. (2015). doi: 10.1093/nutrit/nuu006.

4. Ronquillo MD, Mellnyk A, Cárdenas-Rodríguez N, et al. (2019) doi: 10.4103/ijmr.IJMR_1165_17.

A fast and reliable tool to self-assess sensitive skin

S. Figueiredo¹, A. Nkengne¹, A. Bigouret¹

¹Laboratoires Clarins, 5 rue ampère, Pontoise, France
Corresponding Author: Sara Figueiredo sara.figueiredo@clarins.com

KEY WORDS: sensitive skin, diagnostic, prediction

Background: Sensitive skin is a syndrome affecting 60% of women and 40% of men¹. Many methods can be used to diagnose sensitive skin, including the Sensitive Scale, a long and complex questionnaire published and validated by Dr Misery². This study aimed to develop and validate a faster and easier method than the SS, assessing skin sensitivity by self-diagnosis.

Method: Five binary questions (Yes/Non) were identified, corresponding to thermal, chemical, and emotional factors which can cause unpleasant sensations linked to sensitive skin. To validate the questionnaire, 84 women (20-70 yo) were recruited and divided into three groups depending on their sensitive score (SS), from the sensitive scale: 48 vol. with sensitive skin (SS > 20) and 36 with non-sensitive skin (SS=0). These women were asked to answer the five skin sensitivity assessment questions. Their answers to the questions were then combined, using a neural network (NN), to determine a unique skin sensitivity index, predictive of the SS. The built prediction model was validated using a Leave-one-out approach on the entire panel.

Results: The simplified questionnaire's responses showed a good agreement with the SS. More than 80% of the volunteers who answered "yes" to more than two out of the five questions end up being sensitive. Moreover, the NN model constructed showed a sensitivity of 97.9%, a specificity of 94.6%, and a classification rate of 96.4%. (cf. table 1)

Conclusion: The five questions determined for creating the simplified questionnaire are relevant to discriminate sensitive skin groups. Therefore, this survey is a fast, easy, and inexpensive new method for self-diagnosing skin sensitivity.

Simplified Questionnaire			
		Sensitive Skin	Non-sensitive skin
Sensitive Scale	Sensitive Skin	46	2
	Non-sensitive skin	1	35

Table 1. Confusion matrix between the sensitive skin determined by the sensitive scale and those determined by the simplified questionnaire

¹ Misery L, Myon E, Martin N, Verriere F, Nocera T, Taieb C. Peaux sensibles en France: approche épidémiologique. Ann Dermatol Venereol 2005; 132: 425-429

² Misery L., Jean-decoster C., Mery S., Georgescu V., Sibaud V. (2014). A new ten-item Questionnaire for Assessing Sensitive skin : The Sensitive Scale-10. 94.

Studying the impact of dynamical movement on skin physiology

M. Florindo^{1,2}, S. Nuno^{1,3,4}, S. Andrade¹, C. Rocha¹, C. Rosado¹, L. Monteiro Rodrigues¹

¹ Universidade Lusófona CBIOS - Research Center for Biosciences and Health Technologies, Av Campo Grande, 376, 1749- 024, Lisboa, Portugal

² ESSCVP the Portuguese Red Cross Health School. Dep. Physiotherapy | Lisboa, Portugal

³ Clínica S João de Deus – CTD | Lisboa Portugal

⁴ Escola Superior de Tecnologia da Saúde de Lisboa –ESTeSL Lisboa' Polytechnic Institute | Lisboa, Portugal

Corresponding Author e-mail address: mflorindo@esscvp.eu

KEYWORDS: Skin anisotropy, perfusion, and exercise OR walking, blood flow

Discussion regarding the benefits of exercise to skin health still evokes some controversy. Previous studies have indicated that prolonged or strenuous exercise may not be beneficial for skin health, causing not only significant cardiovascular-respiratory changes, but also impacting exocrine glands, skin microcirculation, and epidermal “barrier” function, among other effects. In the present study, we aim to better understand how moderate dynamical movements such as walking impact basic skin functional indicators.

Ten healthy volunteers (39.3 ± 16.4 y.o.) previously selected, both sexes, performed a regular gait exercise on a treadmill (4 Km/h). All procedures complied with principles of good clinical practice. The applied protocol included a 5 min sitting phase (Phase 1, baseline), 5 min walking on the treadmill (Phase 2), and a 5 min seated post-walk (Phase 3, recovery) while sitting. During Phases 1 and 3, blood flow-related measurements included perfusion by laser Doppler flowmetry (LDF) and Polarized Spectroscopy (PS) on the dorsal aspect of the foot (close to the 3rd and 4th toes). Skin physiological variables included transepidermal water loss (TEWL) (Tewameter TM300) and biomechanics (CutiScan). Non-parametric tests (Wilcoxon) were used, adopting a 5% significance level.

Walking evoked significant perfusion increases (LDF and PS) still present 3 min after finishing the exercise ($p=0.028$ and $p=0.046$, respectively). Regarding skin indicators, no changes were detected for TEWL - a direct indicator of the epidermal “barrier” - while a consistent decrease in skin elasticity and viscoelasticity was detected ($p=0.028$). Perfusion and skin variables returned to baseline levels by the end of Phase 3. Therefore, according to the results obtained in this study, a direct impact of gait on skin parameters can be established, although further studies are needed to better understand its mechanisms and significance.

1 Rosado C, Antunes F, Barbosa R, et al. (2016) doi: 10.1111/srt.12353

2 Di Nardo, V., Conte, A., Finelli, F. and Lotti, T. (2019). doi.org/10.1002/9781119476009.ch23

3 Ben Williamson (2015) doi: 10.1080/13573322.2014.962494

Non - invasive in vivo creep recovery indentation testing for skin modeling.

A. Guillermin¹, M. Ayadh¹, R. Chatelin¹ E. Feulvarch¹, H. Zahouani¹

I. University of Lyon, Laboratory of Tribology and Dynamic of Systems, UMR-CNRS 5513, ENISE - ECL, 36 Avenue Guy de Collongue, 69134, Ecully, France

Corresponding Author: A. Guillermin (amaury.guillermin@ec-lyon.fr)

KEY WORDS: in vivo test, skin rheology, viscoelasticity

For more than a couple decades, skin rheological properties evaluation is a cross – cutting issue studied by many researchers; but as a living tissue, *in vivo* protocols and measurements are quite complex. In the late 90’s, a device, named cutometer¹, was used to measure the skin elasticity. However, from those measurements, only phenomenological metrics were extracted. With the WaveSkin device², we conducted a study to establish elastic and viscous phenomenological and rheological properties of the skin, as well as anisotropic behavior.

This device is an air flow system, blowing, out of pipe, a downstream jet with a controlled force. This device enables contact free indentation tests. Skin displacements, generated by the air blast, are measured along a laser line, in Langer’s lines direction and an orthogonal direction to assess anisotropy. This device is suitable for non - invasive measures or/and *in vivo* characterization.

The testing protocol uses this device to submit, in vivo, human skin to quick creep – recovery test in multiple directions. Measurements are, then, processed to retrieve creep recovery curves of the underlying material. To analyze this curve, a viscoelastic model is manipulated to link deformations and stresses, based on Prony serie. Least – square optimization is, finally, operated to determine viscoelastic parameters.

A finite element numerical model is exploiting the computed viscoelastic parameters to create the *in vivo* relevant model, based on the measurement. The model is, then, simulating the global response to different types of load testing. It is also delivering new insights on skin tension or skin reaction in depth.

¹ A.O. Barel, W.Courage, P. Clarys, (1995) Suction method for measurement of skin mechanical properties: The Cutometer. In: Serup, J. and Jemec, G.B.E. Eds., *Handbook of Noninvasive Methods and the Skin*, CRC Press, Boca Raton, 335-340., J. Microsc., 200(2000)83-104.

² G. Boyer, C. Pailler Mattei, J. Molimard, M. Pericoi, S. Laquizez, H. Zahouania, (2012). Non contact method for in vivo assessment of skin mechanical properties for assessing effect of ageing. *Medical Engineering & Physics*, Volume 34, Issue 2., pp. 172-178., 2012

Optical reprogramming of human dermal fibroblast

Aisada Koenig

Department of Biophotonics and Laser Technology, Saarland University

Corresponding Author e-mail address and URL: a.koenig@blt.uni-saarland.de and www.blt.uni-saarland.de

KEY WORDS: dermal fibroblasts, reprogramming, induced pluripotent stem cells, femtosecond laser pulses, nanosurgery

Dermal fibroblasts are the first¹ and currently the most frequently used cells for the generation of patient-specific induced pluripotent stem cells (iPS cells)².

The forced expression of the defined transcription factors *KLF4*, *OCT3/4*, *SOX2*, and *C-MYC* converts human fibroblast into induced pluripotent cells that can be used to generate various cells or tissues. Typically, Retro- or lentiviruses are applied for efficient intracellular gene/transcription factors delivery but are hindered by issues that might prevent them from being used clinically³⁻⁴.

Here we demonstrate a virus-free optical approach to human cell reprogramming into iPS cells with spatially shaped extreme ultrashort laser pulses of sub-20 femtoseconds which enables contamination-free transfection of cells in a microfluidic tube with multiple genes at the individual cell level in order to achieve optical reprogramming of large cell populations⁴⁻⁵. We found that the ultrashort femtosecond laser-microfluidic cell transfection platform enhanced the efficacy of iPS-like colony-forming following merely a single transfection.

In contrast to conventional approaches which utilize retro- or lentiviruses to deliver genes or transcription factors into the host genome, the laser method is virus-free; hence, avoid the risk of virus-induced cancer generation limiting clinical application.

¹Takahashi et al., *Cell*. 131(5) (2007) 861-872

²Sacco et al., *J Cell Mol Med*. 23 (2019) 4256–4268

³Okita, K., Ichisaka, T and Yamanaka, S., *Nature* 448(7151)(2007) 313–317

⁴Miyazaki et al., *Jpn. J.Clin. Oncol*. 42(9) (2012) 773–779

⁵Uchugonova et. al., *J. Biomed. Opt.* 20(11) (2015) 115008

⁶Uchugonova et. al., *J Biophotonics* 9(9) (2016) 942-7

Feature Extraction for Classification of Lesions and Malignant Melanomas in Multiphoton Tomography Skin Images

I. Lange¹, P. Prinke¹, Ł. Piątek², M. Warzecha³, K. König^{3,4}, J. Hauelsen¹

¹*Institute of Biomedical Engineering and Informatics, Technische Universität Ilmenau, 98639 Ilmenau, Germany
Corresponding Author e-mail address: Irene.Lange@tu-ilmenau.de*

²*Faculty of Applied Information Technology, University of Information Technology and Management,
Suchbarskiego 2, 35-225 Rzeszów, Poland*

³*JenLab GmbH, Johann-Hittorf- Straße 8, 12489 Berlin, Germany*

⁴*Department of Biophotonics and Laser Technology, Saarland University, Campus A5.1, 66123
Saarbrücken, Germany*

KEY WORDS: two-photon-excited fluorescence (TPEF), skin cancer diagnosis, biomedical analysis

Skin diseases impair the quality of life of those affected and, in the case of skin cancer, can even lead to death. Early detection allows the initiation of appropriate therapy with the aim of alleviating or even completely curing the disease. Such early detection at the subcellular level can be realized without the use of exogenous markers and completely non-invasively using multiphoton tomography¹.

Interpretation of multiphoton data is performed by medical professionals with many years of experience. Depending on the extent of the tomograph's depth scans, extensive data must be viewed, evaluated, and documented. At this point, we provide an automated evaluation to support the medical personnel. In addition, our novel evaluation option is intended to strengthen the acceptance and prevalence of multiphoton tomography in the clinical environment.

For the classification of healthy skin, lesions, and malignant melanoma, physicians use features such as architectural disorder², separability of cells and nuclei, and aspects of pleomorphism³. We modelled the architectural disorder by using the variance in cell shape (cell symmetry by principal component analysis), cell spacing by Delaunay triangulation, and cell density. The local contrast provided information on the separability of cells to the intercellular matrix. Possible pleomorphisms were approximated by the variance of cell shape and the ratio of cell nuclei to cytoplasm. The semantic cell and nuclei regions originate from pre-segmented multiphoton images.

As a result, we obtained the features for each individual cell for the different classes. These were transferred into a feature space as training data for a subsequent classification. The evaluation of the separated features showed a difference in cell shape for malignant melanoma and healthy skin, particularly due to the presence of melanocytes. The evaluation of the separability of all three classes considering further features will be investigated in future.

We acknowledge financial support from the Federal Ministry of Education and Research under the DigiSkinDia-project (Grant# 01DS19012A) and from the Thüringer Aufbaubank commissioned by the Freistaat Thüringen (Grant# TAB 2018 IZN 0004).

¹ K. König, "Multiphoton Tomography (MPT)", in *Multiphoton Microscopy and Fluorescence Lifetime Imaging*, De Gruyter, 2018.

² W.F. Lever, G. Schaumburg-Lever, "Histopathology of the skin: melanocytic nevi and malignant melanoma", 6th ed. Philadelphia: Lippincott Williams and Wilkins, 1983.

³ S. Seidenari, F. Arginelli, S. Bassoli, et al., "Multiphoton laser microscopy and fluorescence lifetime imaging for the evaluation of the skin" in *Dermatol Res Pract.*, 2012.

Pilot study for effects of facial skin colors on facial impressions

Myreongryeol Lee^{1,2}, Sue Im Jang^{1,2}, Yochul Jung¹, Eunjoo Kim¹

1. AMOREPACIFIC R&D Center, 1920 Yonggu-daero, Giheung-gu, Yongin-si, Gyeonggi-do, Republic of Korea, 17074

2. Department of Medicine, Graduate School, Chung-Ang University, 84, Heukseok-ro, Dongjak-gu, Seoul, Republic of Korea, 06974
eon827@amorepacific.com

KEY WORDS: Facial impressions, skin facial color, Korean female color

The skin is not only the organ that covers the entire body, but also the organ that expresses abnormalities of the internal organs. Skin color is a factor that affects subjective impressions such as beauty and attractiveness^{1,2}, but there are few studies of the effects of these factors on impressions, preference and attractiveness of Korean female. In this study, we tried to find out how skin color affects impression and attractiveness, and a preliminary test was conducted before a large-scale experiment. The stimuli images were prepared as follows. After selecting a model of a female in her 30s, facial makeup was applied on her face, and a facial image was taken with VISIA-CR. A standard 2 mode image was converted to 125 color case images (L* 5 levels, a* 5 levels, and b* 5 levels) using a computer program. Questionnaire assessments of each facial image displayed on computer screen were performed by normal adult men and women (n = 15), and they subjectively assessed the impressions they receive from the images including “transparency”, “healthy”, “dullness”, “vitality”, “tiredness”, and “brightness” (9 points scale). Statistical analysis was performed using SPSS (Statistical Package for the Social Science) 23 software. When skin brightness (L*) increased, skin redness (a*) decreased, skin yellowness (b*) decreased, “brightness” score and “transparent” response score increased. When L* increased, b* decreased, “dullness” and “tiredness” response scores decreased. Skin redness shows a convex down relationship with the impression items. There was no significant correlation with the level of skin brightness, and the levels of skin redness and yellowness showed a convex up relationship with “healthy” and “vitality”. Modified Individual typology angle (ITA) value ($ITA_M^\circ = \text{ArcTan}((L^*-50)/\sqrt{(a^{*2}+b^{*2})})^3$) and ITA value were corelated with skin L* value (r = 0.573, 0.475, respectivley) and modified ITA value showed higher correlation coefficient (p < 0.05)

These results indicate that skin color affects facial impressions of Korean female. Especially, modified ITA value is a better parameter for skin brightness in Korean female.

¹ Kang NG et al, J Soc Cosmet Sci Korea, 2014;40(4):373-382.

² Minami K et al., IFSCC Mag. 2007;10(2):111-117.

³ Wang L, et al., Skin Res Technol. 2019; 25(5): 693-700

***In vivo* skin penetration of d-panthenol by Confocal Raman Spectroscopy**

P.M.B.G. Maia Campos^{1*}, V.T.P. Ferreira¹, G.C. Silva², A.A. Martin^{2,3}.

¹*School of Pharmaceutical Sciences of Ribeirao Preto, University of Sao Paulo, Av. do Cafe, Ribeirao Preto, SP, Brazil;* ²*Science and Technology Institute, University of Brazil, 235 R. Carolina Fonseca, Sao Paulo, SP, Brazil;*

³*Dermo PROBES – Skin and Hair Technology, Av. Cassiano Ricardo, 601, Sao Paulo, SP, Brazil.*

**pmcampos@usp.br.*

KEY WORDS: Skin penetration; Confocal Raman Spectroscopy; skin hydration

Introduction. Topical d-panthenol has been very used as a moisturizer with barrier-enhancing properties, exerting healing and penetration effects¹. Despite its extensive and consolidated application, the exact action mechanism and other biochemical processes underlying its main moisturizing action have not been fully elucidated¹. In this context, the *in vivo* characterization of the skin permeation of the d-panthenol allows determination of the extent of permeation with semi-quantitative analysis per skin layer, under actual use conditions. Thus, the aim of the present study was to evaluate the skin penetration and changes provoked in epidermis after application of a gel cream formulation added to d-panthenol. **Methods.** A total of 10 healthy women, aged between 20 and 35 years, participated in the study. Informed consent was obtained from the subjects prior to entering the study. The permeation evaluation was performed using a 3510 Confocal Raman Spectrometer Skin Analyzer (RiverD International BV) and measurements were taken randomly on the skin of the volar forearm region before (T0) and after 120 min (T120) of application of the studied formulation containing or not (vehicle) 5% of d-pantenol. Spectral data was acquired in the fingerprint region (400-1800 cm⁻¹) for the stratum corneum and epidermis from surface up to 48 µm. Extent of permeation and semi-quantitative analysis at different depths were calculated with respect to the intensity of the 2nd derivative of a d-panthenol peak at 808 cm⁻¹ and by the classical least square (CLS) fit by Skintools (RiverD International BV). Descriptive statistics (mean, standard deviation, 95% confidence interval) were calculated for these parameters. **Results.** Alterations in the biochemical composition of different skin layers were observed after topical application of the cosmetic formulation. The permeation profile derived with respect to the intensity of the 2nd derivative of the d-panthenol peak at 808 cm⁻¹ confirmed the profile outlined by the CLS fit. Semi-quantitative analysis revealed that the active substance was found in greater relative amounts in the stratum corneum (SC), accounting for 60.3% of the permeate, while in the epidermis it accounted for 39.7%. The maximum depth permeated by d-panthenol was 45 µm. **Discussion and Conclusion.** The close correlation of d-panthenol permeation profiles obtained by different methods points to the consistency and reliability of the results obtained. D-panthenol permeability and its accumulation in the skin's outer layers were verified. Its greater relative amount at the SC favours superficial moisture retention, needed to maintain and restore the skin's barrier function². Increased inter-personal variability observed at greater depths is probably due to loss of resolution and nonspecific melanin incidence. Thus, protocols comprising larger cohorts are indicated in order to verify permeation beyond the dermal-epidermal junction and the permeation extinction. In conclusion, evidence on skin permeability and retention of d-panthenol in different layers contributes to elucidate the main hydration mechanisms of formulations based on d-panthenol for skin care.

¹ Citation of a journal article: E.Prokscha, R.Bonyb, S.Trappb, S.Boudonb, *J. Dermatol. Treat.*, 2018,28(8):766-773.

² Citation of a journal article: Z.D.Draelos, *J. Cosmet. Dermatol.*, 2018,17(2):138-144.

Permeation of Nano Encapsulated Vitamin D3 Through Human Skin by *in vivo* Confocal Raman Spectroscopy

A.A. Martin^{1,2*}, F.R. Lemos², G.C. Silva¹, L.P. M. Neto², N.B. Moreira², D. Monteiro², E. Carità³

¹Science and Technology Institute, University of Brazil, 235, R. Carolina Fonseca, Sao Paulo, SP, Brazil; ²Dermo PROBES – Skin and Hair Technology, Av. Cassiano Ricardo, 601, São José dos Campos, Sao Paulo, SP, Brazil; ³Funcional Mikron Indústria e Comercio Ltda, Al. Itajubá, 1564 - Joapiranga Valinhos, SP, Brazil.

*airton.a.martin@gmail.com; probes.com.br/dermoprobes

KEY WORDS: Vitamin D3; skin permeation; Confocal Raman Spectroscopy.

Introduction: It has been shown that the continuous use of sunscreen interferes the cutaneous production of Vitamin D3¹, which is photosynthesized by UV-B radiation, and its deficiency is related to the increase on risk of cardiovascular disease, diabetes, cancer, bone problems and other comorbidities². The increased use of sunscreen by the population, aiming to prevent skin problems, leads to D3 deficiency, which could result in an increase of those diseases. In this context, it is evident the need to combine both protection against UV radiation and topical delivery of Vitamin D3 to the body. The present study aims to verify - *in vivo* - the permeation of a product containing Nano Encapsulated Vitamin D3 through the human skin layers in different times after topical application. **Methods:** A total of 14 healthy volunteers (men and women), aged between 20 and 30 years and which signed an informed consent form, participated in a permeation analysis of a solution containing nano Vitamin D3. The permeation evaluation was performed *in vivo* using Confocal Raman Spectroscopy (Rivers Diagnostics® - Model 3510 Skin Composition Analyzer) and measurements were taken on the skin's anterior forearm region before application (T0) and 2h (T2), 4h (T4) and 6h (T6) after solution application. Raman spectral data was acquired in the fingerprint region (400 – 1800 cm⁻¹) from the skin's surface up to 110 microns (dermis). **Results:** Data acquired after treatment was compared to basal measurements. It has been found that the maximum content of vitamin D3 occurs in the stratum corneum (SC) at T2. A further content decrease of about 41.7% occurs, for SC, between T2 and T6, indicating the product permeation to deeper skin layers. The maximum amount of Vitamin D3 for the epidermis and the dermis is found at T4 and T6, respectively. Nano Vitamin D3 permeability and accumulation in the skin's layers were verified, as shown in Figure 1. **Conclusion:** It has been demonstrated by *in vivo* Confocal Raman Spectroscopy that topical Nano Encapsulated Vitamin D3 permeated through the skin layers up to dermis.

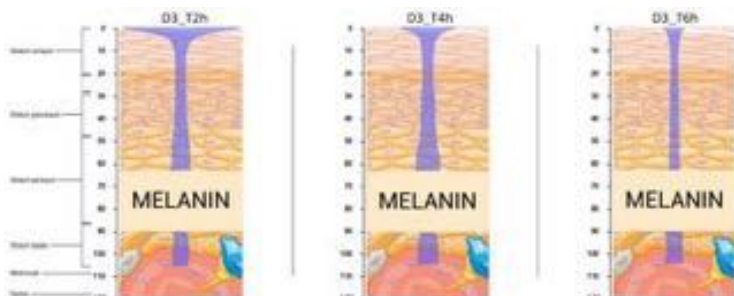


Figure 1: Schematic Permeation profile of Vitamin D3 after different times of application.

¹ Lois Y. Matsuoka, Lorraine Ide, Jacobo Wortsman, Julia A. Maclaughlin, Michael F. Holick, Sunscreens Suppress Cutaneous Vitamin D₃ Synthesis, *The Journal of Clinical Endocrinology & Metabolism*, Volume 64, Issue 6, 1 June 1987, Pages 1165–1168.

² Bandeira, Francisco, Griz, Luiz, Dreyer, Patricia, Eufrazino, Catia, Bandeira, Cristina, & Freese, Eduardo. (2006). Vitamin D deficiency: a global perspective. *Arquivos Brasileiros de Endocrinologia & Metabologia*, 50(4), 640-646.

Balancing skin Microbiome- Fact or fiction

N Muizzuddin

*Skin Clinical Research Consultants LL, 405 Boundary Ave, Bethpage. NY 11714. USA
neelam@skinclinicalresearch.com*

KEY WORDS: microbiome, skin, balance

The skin is the human body's largest organ, colonized by a diverse environment of microorganisms, most of which are harmless or even beneficial to their host. "Microbiome" describes a biodiverse ecosystem composed of living biological and physical components that create a balance between host and microorganism. Symbiotic microorganisms occupy a wide range of skin niches and protect against invasion by more pathogenic or harmful organisms. Studies have shown that skin microbiota play an integral role in the maturation and homeostatic regulation of keratinocytes and host immune networks with systemic implications. Disruptions in the balance on either side of the equation can result in skin disorders or infections.

An enhanced understanding of the skin microbiome would gain insight into microbial involvement in human skin disorders and to enable novel promicrobial and antimicrobial therapeutic approaches for their treatment. However, the human skin microbiome varies considerably over time, thus study of the effect of topical agents on skin microbiome is wrought with inconsistencies. There is a deluge of skin care products claiming to "balance" skin microbiome, however, the description of this "balance" is rather nebulous. This talk will provide an overview of skin microbiome, discuss testing methods and whether some claims in this field are fact or fiction.

Handheld line-field optical coherence tomography (LC-OCT) device for three-dimensional skin imaging

J. Ogien¹, M. Cazalas¹, O. Levecq¹, and A. Dubois²

1. DAMAE Medical, 14 rue Sthrau, 75013 Paris, France

2. Université Paris-Saclay, Institut d'Optique Graduate School, CNRS, Laboratoire Charles Fabry, 91127 Palaiseau, France

Corresponding Author e-mail address and URL: jonas@damae-medical.com

KEY WORDS: OCT, confocal microscopy, skin

Line-field confocal optical coherence tomography (LC-OCT) is a recently introduced optical imaging technique, based on a combination of reflectance confocal microscopy and optical coherence tomography. LC-OCT allows vertical and horizontal sectional imaging of skin tissues, *in vivo*, with an isotropic resolution of $\sim 1 \mu\text{m}$, offering the possibility of three-dimensional (3D) visualization of skin morphology at the cellular level.

This presentation introduces a compact LC-OCT device designed to fit into a handheld probe, allowing easy access to any region of the skin by the practitioner. The LC-OCT device has three acquisition modes: real-time acquisition of vertical section images, real-time acquisition of horizontal section images, and full volume (3D) acquisition obtained either from a concatenation of vertical section images or from a concatenation of horizontal section images. The user can switch from one acquisition mode to the other, as well as record images and videos, using buttons on the probe handle.

The device is also equipped with a video camera that allows to obtain color images of the skin surface, similar to dermoscopy images, with a field of view of $\sim 3 \text{ mm}$ in diameter. These images are obtained in real time simultaneously with the LC-OCT images, which facilitates precise targeting and placement of the LC-OCT probe.

Images of healthy human skin and skin affected by various pathologies, including basal cell carcinoma and melanoma, are presented to demonstrate the potential of the latest LC-OCT technology in daily dermatological practice.

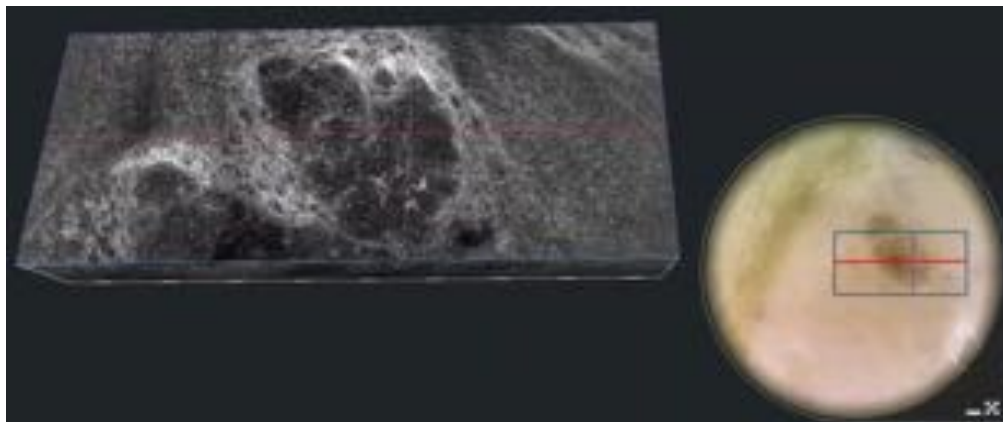


Figure: Three-dimensional LC-OCT image of a basal cell carcinoma and corresponding image of the skin surface.

Line-field optical coherence tomography (LC-OCT) for non-invasive skin imaging: Focus on dermal-epidermal junction and keratinocyte network

J. Chauvel Picard¹, V. Berot², M. Suppa^{3,4}, L. Tognetti⁵, M. Fontaine³, C. Lenoir³, J. Perez^{6,7}, C. Orte Cano³, S. Puig^{6,7}, A. Dubois⁸, S. Forestier⁹, J. Monnier¹⁰, R. Jdid⁹, G. Cazorla⁹, M. Pedrazzani¹¹, A. Sanchez¹¹, S. Fischman¹¹, P. Rubegni⁵, V. Del Marmol³, J. Malvehy^{6,7}, E. Cinotti⁵, J.L. Perrot²

1 Department of Craniomaxillofacial surgery, University Hospital of Saint-Etienne, Saint-Etienne, France

2 Department of Dermatology, University Hospital of Saint-Etienne, Saint-Etienne, France

3 Department of Dermatology, Hôpital Erasme, Université Libre de Bruxelles, Brussels, Belgium.

4 Institut Jules Bordet, Université Libre de Bruxelles, Brussels, Belgium.

5 Dermatology Unit, Department of Medical, Surgical and Neurological Sciences, University of Siena, Siena, Italy.

6 Melanoma Unit, Hospital Clinic Barcelona, University of Barcelona, Spain.

7 CIBER de enfermedades raras, Instituto de Salud Carlos III, Barcelona, Spain.

8 Université Paris-Saclay, Institut d'Optique Graduate School, Laboratoire Charles Fabry, Palaiseau, France

9 Chanel Parfums Beauté, innovation Research and Development, Pantin, France

10 Department of Dermatology and skin cancer, la Timone hospital, Aix-Marseille University, Marseille, France.

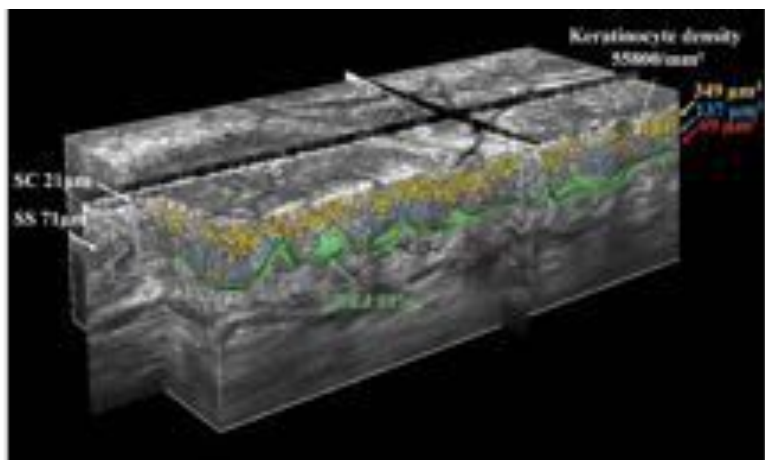
11 DAMAE Medical, Paris, France

Corresponding Author e-mail address and URL: melanie.pedrazzani@damaemedical.fr

KEY WORDS: LC-OCT, skin, 3D quantification

A precise description of the morphology of healthy skin *in vivo* and its variability between different body areas is critical to better understand the skin changes leading to aging or some pathologies. To visualize the inner structure of the skin in a non-invasive way, we worked with a microscopic imaging device based on Line-field Confocal Optical Coherence Tomography (LC-OCT) technology. The LC-OCT combines the technological advantages of both confocal microscopy and OCT allowing a three-dimensional (3D) imaging of the skin with an isotropic spatial resolution of about 1.3 micron up to 400 microns in depth. We focused our study on the quantification of the epidermal layer and more precisely on the thickness of the Stratum Corneum, the keratinocyte network and the morphology of dermal-epidermal junction (DEJ). By analyzing 3D LC-OCT images with algorithms based on artificial intelligence, we were able to fully describe and quantify the epidermis on a panel of eight volunteers on seven body areas including the head (cheek, forehead and tip of the nose), the upper limbs (dorsal forearm and hand) and the trunk (pre-sternal chest and mid-back). The process of keratinocyte maturation was evidenced *in vivo* with small and relatively spherical keratinocytes near the DEJ becoming flatter as they get closer to the skin surface. These 3D *in vivo* quantifications open the door in clinical practice to diagnose and monitor pathologies for which the keratinocyte maturation process is impaired leading to cellular atypia in the epidermis.

Figure: 3D LC-OCT skin image of the dorsal hand describing epidermis parameters such as Stratum Corneum (SC) and Stratum Spinosum (SS) thicknesses, DEJ undulation index and keratinocyte network. The average volumes of keratinocyte nuclei at different depths are specified.



Impact of aging of the eye contour on perceived age

J. Robic¹, A. Nkengne¹

¹Laboratoires Clarins, 5 rue ampère, Pontoise, France
Corresponding Author: Julie Robic julie.robic@clarins.com

KEY WORDS: eye contour, aging, prediction

Objective: Aging of the clinical signs of the face is well documented. Perceived age is mostly affected by the eye contour. The objective of this paper is to study the aging of the eye contour of women from different ethnicity and to propose specific models to predict their perceived age.

Method: 240 volunteers are recruited from 4 different ethnicities (Caucasian, Hispanic, Afro-American, and Asian) and divided into three different age groups: 30 vol. from 20-35yo., 30 vol. from 35-45yo. and 30 vol. from 45-60yo. Standardized photographs are acquired using the Colorface® (Newtone Technologies, Lyon, France) and cropped around the eye contour area. The following clinical signs are scored^{1,2,3}: crow's feet wrinkles, underneath eyes wrinkles, glabellar wrinkles, inter ocular wrinkles, sagging of the upper eyelid, eye bags, intensity of dark circles, and perceived age. Where data are parametric, mean and standard deviation are analyzed using Student's unpaired t-test; non-parametric data are subjected to a Mann-Whitney. Partial Least Squares models (PLS) are used to predict the perceived age from the clinical annotations.

Results: The effect of age is statistically significant for the four populations on wrinkles and sagging. Caucasian and Asian women wrinkles are generally more severe and the rates of increase are higher than those of Hispanic and African-American women. Eye bags and dark circles seem to be a transversal problem between age groups. The PLS models show R² superior to 0.65 for all populations except for Afro-American women after cross-validation. The importance of each clinical annotation in the perception of age is presented in descending order in Table 1.

Conclusion: The eye contour of all the population is affected by age with different rates and severity. The perceived age is affected by different clinical signs between populations. Hence, treatment of the eye contour should be specific to each population.

Importance	Caucasian	Asian	Hispanic
1	Glabellar wrinkles	Underneath eye wrinkles	Underneath eye wrinkles
2	Crow's feet wrinkles	Crow's feet wrinkles	Glabellar wrinkles
3	Underneath eye wrinkles		Inter ocular wrinkles
4	Eyelid sagging		
5	Eye bags		

Table 1. Importance of clinical annotation in the age perception

¹ Atlas du vieillissement cutané, Vol.1. Population européenne (R. Bazin & E. Doublet)

² Atlas du vieillissement cutané, Vol.2 Population asiatique (R. Bazin & F. Flament)

³ Atlas du vieillissement cutané, Vol.3 Population afro-américaine (R. Bazin, F. Flament & F. Giron)

3D imaging for a global approach to aging signs of the face

J.J. Servant¹, G. Koeller¹, C. Lille¹

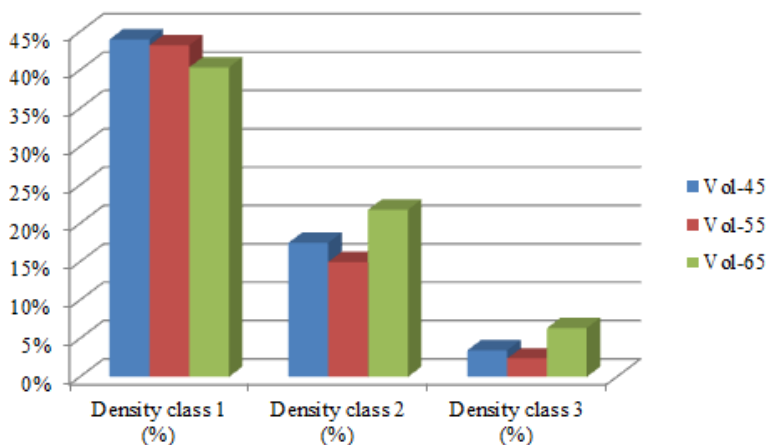
1-Eotech 1 ZI du Fond des Près 91460 Marcoussis France

jj.servant@eotech.fr, www.eotech-sa.com

KEY WORDS: Antiaging, Skin lines, volumes

So far and still for some time, topological measurement of the aging signs focuses on control areas where the first aging signs such as fine lines, wrinkles and folds appear. These areas such as crow's feet, cheekbones, cheek, puffiness, nasal fold serve as a benchmark for the claim of anti-aging efficacy testing.

Technical advances in three-dimensional measurement nowadays, make it possible to measure the entire face with sufficient resolution to resolve all these aging signs, from the formation of fine lines, wrinkles and folds to the sagging of the tissues in these control areas. Acquiring measurements on the entire face effectively requires a lot of rigorous control, but once this mastery of the measurement has been acquired, the data processing and analysis algorithms make it possible to characterize with finesse and objectivity the overall state of the skin on the face depending on age and/or following dermo-cosmetic treatment to measure their efficacy. These analyzes are carried out on these areas, which are extracted automatically from the 3D face data in order to quantify these signs by their numbers, their surfaces, their depths and their volumes. However, dermo-cosmetic treatments are applied on the entire face, so we were interested in developing new tools for a global approach and close to perception effect and not only just by these reference areas. The new analysis functions integrated in the coming version 4 of the AEVA software make it possible to establish by class the changes in facial lines on one hand, and on the other hand, by a global geometric identification of the effects due to slackening. We propose to present and explain in detail these new analysis tools, their performances and limitations with illustrations of first results obtained.



***In Vivo* Assessment of the Human Dermal–Epidermal Junction Zone by Volumetric Multiphoton Microscopy**

Yunxian (Giselle) Tian^{1,2,3}, Zhenguo Wu^{1,2,3}, Harvey Lui^{1,2,3}, Jianhua Zhao^{1,2,3}, Sunil Kalia^{1,2,4,5},
Haishan Zeng^{1,2,3}

¹*Department of Dermatology and Skin Science, University of British Columbia, Vancouver, Canada.*

²*Photomedicine Institute, Vancouver Coastal Health Research Institute, Vancouver, Canada.*

³*Imaging Unit – Integrative Oncology Department, BC Cancer Research Centre, Vancouver, Canada.*

⁴*Department of Cancer Control Research, BC Cancer, Vancouver, Canada*

⁵*BC Children's Hospital Research Institute, Vancouver, Canada*

hzeng@bccrc.ca

KEY WORDS: Skin Imaging, Multiphoton, Skin Aging

Background and Objectives: The dermal-epidermal junction (DEJ) zone can be studied to assess physiologic changes and characterize features to aid in the diagnosis of skin disease. Under conventional histopathology microscopy, this region is visualized and assessed two-dimensionally from sections of biopsied skin. Here we propose a novel optical method to automatically delineate and quantify DEJ zone morphometrics in human skin *in vivo* on a three dimensional (3D) basis.

Method: 3D volumetric imaging under dual wavelength multiphoton excitation was carried out on the upper inner arm of 16 volunteers. An automatic segmentation algorithm was developed to delineate the DEJ using two-photon excited fluorescence cellular imaging and second harmonic collagen imaging, thereby separating the epidermis from the superficial dermis. Quantitative characterization of the DEJ in terms of 3D interdigitation (I), arithmetic mean roughness (Sa), and root mean square roughness (Sq) were calculated and analyzed as a function of age.

Results: The age range of the participants was between 24 to 65. The average and standard deviation value of the interdigitation index (I), arithmetic mean roughness (Sa) and root mean square roughness (Sq) were 1.22 ± 0.07 , 12.34 ± 4.89 , 16.77 ± 5.47 respectively. Linear regression shows that all three parameters are negatively correlated to age ($p < 0.05$, Spearman). These parameters suggest that the overall DEJ surface becomes flatter with chronological aging.

Conclusion: *In vivo* DEJ surfaces show age-dependent morphological differences. Three dimensional volumetric multiphoton microscopy imaging of the skin can be analyzed by automated segmentation algorithms to yield quantitative and objective assessments of DEJ morphology.

The Skin Phenome Research

Sijia Wang

*Chinese Academy of Sciences – Max Planck Partner Institute for Computational Biology
320 Yueyang Road, Shanghai 200031, China
wangsijia@picb.ac.cn*

KEY WORDS: Skin, Phenome, Omics

Genetics has led the biomedical research over the past decades. Particularly in the genomic era, the discovery of genes associated with phenotypes (traits/diseases) has provided important clues for revealing the relevant biological mechanisms. However, this genetic paradigm has recently been challenged. When strong associations between genotypes and phenotypes have mostly been discovered, weak associations – often found in the cases of complex traits/diseases – were not practically useful. This poses a severe challenge for precision medicine. Here we propose a new paradigm focusing on the phenotypic end. We show proof-of-principle examples based on better dissection of phenotypes, effective modeling of latent phenotypes, and direct prediction from strongly linked phenotypes. Ideally, such phenotype-focused approaches shall work on large scale cohorts, where standardized ultra-deep phenotyping could be performed among the same samples. Recently the Human Phenome Project has been initiated in China to achieve this goal.

In the Human Phenome Project, standardized platforms have been built to perform ultra-deep phenotyping at the molecular, cellular, and organ levels (including both imaging and functional assessment platforms). Skin, as the largest organ of human body, has its specific phenotyping platform in the project. This skin phenotyping platform would measure a large number of phenotypes including skin characteristics (color, oiliness, water content, barrier function, elasticity, etc.), dermatoglyph and skin appendages (hair, nails, sweat glands, etc.). The platform also includes a solar simulator in order to measure MED and MPPD, as well as high resolution 2D and 3D cameras to take images of skin. The platform is still expanding, and we are calling for fast, accurate, reproducible, non-invasive, and inexpensive phenotyping technologies to help measure the skin phenome.

Using the whole spectrum of data generated from the Human Phenome Project, we shall be able to greatly expand our knowledge about the skin phenotypes in the following perspectives: 1) the heritable genetic basis underlying the variation of skin phenotypes; 2) the environmental factors (also including DNA methylation and skin microbiome) affecting skin phenotypes; 3) the relationship between skin phenotypes and other disease and health conditions. This comprehensive project would build the basis of skin phenome research and provide a rich resource for the relevant research communities.

Combining Deep Learning and Polarization Speckle for in vivo Skin Cancer Detection

Yuheng Wang^{1,2,3,4}, Daniel Louie^{1,2,3,4}, Jiayue Cai^{5,6}, Lioudmila Tchvialeva^{2,3}, Harvey Lui^{2,3,4}, Z. Jane Wang^{1,5}
Tim K. Lee^{1,2,3,4,*}

¹. School of Biomedical Engineering, University of British Columbia, Vancouver, BC, Canada

². Department of Dermatology and Skin Science, University of British Columbia, Vancouver, BC, Canada

³. Photomedicine Institute, Vancouver Coast Health Research Institute, Vancouver, BC, Canada

⁴. Departments of Cancer Control Research and Integrative Oncology, BC Cancer, Vancouver, BC, Canada

⁵. Department of Electrical and Computer Engineering, University of British Columbia, Vancouver, BC, Canada

⁶. School of Biomedical Engineering, Health Science Center, Shenzhen University, Shenzhen, China

* Corresponding Author e-mail address and URL: tlee@bccrc.ca

KEY WORDS: Deep learning, Polarization speckle, Skin cancer detection

Polarization speckle is a novel imaging technique that captures rich information of the imaged object; however, the interference pattern of speckles is difficult to be interpreted. Previously, we proposed to analyze the pattern using statistical moments and achieved excellent results in differentiating melanoma and seborrheic keratosis, a benign lookalike skin lesion.¹ However, the performance degraded when the same method was applied to a more general classification problem of skin cancer and a group of benign lesions. In this project,² we hypothesized that deep learning approach could unlock the diagnostic information hidden in speckles and distinguish skin cancers and benign lesions. In a study of 318 skin lesions of cancerous and pre-cancerous (melanoma, squamous cell carcinoma, basal cell carcinoma, actinic keratosis) and benign (nevus and seborrheic keratosis) lesions, we classified their speckle patterns using deep learning, traditional machine learning (support vector machine, K nearest neighbor, and random forests) and statistical moments. The results of the machine learning and statistical moments were less than 65%, despite the fact that these analytical methods achieved a high 90% and 80% accuracy, respectively, when they were applied to a simpler classification problem of melanoma vs. seborrheic keratosis. On the other hand, the deep learning network, ResNet, along with patch cropping augmentation achieved 82% accuracy for the same classification task. These experiment results demonstrate that polarization speckle imaging capture diagnostic information for detecting skin cancer, and deep learning could extract the hidden information. Combining deep learning with polarization speckle, the technique could be further developed to an automated real-time system for skin cancer detection.

¹ Tchvialeva L., et al., Polarization speckle imaging as a potential technique for in vivo skin cancer detection, J. Biomed. Opt., 2012. 18 (6) : p. 061211.

² Wang, Y., et al., Deep learning enhances polarization speckle for in vivo skin cancer detection. Optics & Laser Technology, 2021. 140: p. 107006.

“TOUCHY Finger” an augmented and connected human finger to assess skin and hair feel

H. Zahouani , R. Vargiolu , L. Ouillon

*Laboratory of Tribology and System Dynamics (LTDS) Ecole Centrale de Lyon -ENISE
UMR CNRS 5513 – University of Lyon
36, Avenue Gut de Collongue – 69134 Ecully – France
roberto.vargiolu@ec-lyon.fr*

KEY WORDS: Human finger, Touch, Softness.

Gaining knowledge and understanding the sense of touch allows us to gain insight into the consumer's personal experience and becomes an essential asset for cosmetic marketing.

Today, to assess the tactile sensation of their products, cosmetics manufacturers call on groups of experts. Their objective is to subjectively note the sensory quality perceived on the skin or hair. While this method provides a sensory indication, it does not objectively measure the softness of the skin or hair. To respond to this technological challenge, the LTDS has developed an innovative augmented and connected human finger device capable of assessing touch. (Figure 1)

During touch, the mechanoreceptors located in the fingertip will be subjected to mechanical stress. These biosensors will then transmit vibratory signals to the brain to classify the touch¹. Like the human finger, the developed device is equipped with vibration sensors² and a sensor for measuring the contact force³. It comes in the form of a half-ring which slides over the tip of the index finger. During the measurement, the fingertip is in direct contact with the surface. Softness and contact force parameters are calculated and transmitted via a tablet application. The results obtained showed a correlation with the sensory classification of expert groups.

Up to now, there is no connected device on the cosmetics industry market that can be used to measure the softness of skin or hair with an instrumented human finger. For the first time, consumers will be able to assess the sensory quality of a cosmetic product applied to their skin or hair simply by using their finger equipped with sensor technology. They will be able to track the progress of their treatment and receive personalised advice tailored to the condition of their skin or hair. The ring data will be remotely analysed by an AI algorithm, which will draw up a sensory profile. Ultra-personalised cosmetic treatments may then be offered by brands in order to offer their customers a new sensory experience.



Figure (1) “Touchy Finger” device

¹ C. Thieulin and al “Study of the tactile perception of bathroom tissues: Comparison between the sensory evaluation by a handfeel panel and a tribo-acoustic artificial finger” <https://doi.org/10.1016/j.colsurfb.2016.11.006>

² Patent R. Vargiolu, H. Zahouani n° WO2011089370 A1

³ Patent H. Zahouani, R. Vargiolu n° FR3099359 A1

Abstracts

Poster Presentations

In alphabetical order of the corresponding author

All presentations are available online for 3 months

<https://roellmedia-streams.de/isbs2021>

Use of the Novel Finger Temperature Device for Assessment of the Efficacy of New Warming Gel in Patients with Primary Raynaud's Phenomenon

T. Aleksiev, Z. Ivanova, H. Dobrev

Department of Dermatology and Venereology, Medical University, Plovdiv, Bulgaria

Corresponding Author: t_aleksiev91@abv.bg

KEY WORDS: Skin temperature, cold-water provocation test

Introduction: Raynaud's phenomenon (RP) represents recurrent vasospasm of the fingers and toes in response to cold exposure or stress. Various local warming products can be used to relieve the RP symptoms. This study was aimed to evaluate the efficacy of a new warming gel in patients with primary RP.

Methodology : A total of 20 patients with primary RP (3 male, 17 female, mean age 44.9 ± 19.1) were studied. Cold-water provocation test was performed before and after a single application of a new warming gel containing plant oils derived from *Cannabis sativa*, *Aesculus hippocastanum*, *Eucalyptus globulus*, *Abies sibirica*, and *Helianthus annuus*, Camphor, and Capsicum). Changes in skin temperature of both wrists and 2-5 fingers were measured using a novel Finger temperature device (Courage & Khazaka).

Results and conclusions: Before treatment, all patients showed a vasospastic type of cold-water provocation test with a recovery time of skin temperature over 15 min. After the application of warming gel, 14 of 20 (70%) patients showed a normal type of cold-water provocation test with a recovery time of skin temperature below 15 min. The second test also showed statistically significantly shorter mean times of complete recovery of baseline temperature with respect to the first finger, the average value of 2-4 fingers, and for all fingers.

Conclusion: The single application of the new rewarming gel improves skin microcirculation determined by cold stimulation test. The method used is appropriate for objective and quantitative assessment of the effects of a single application of warming and other products.

Use of a Novel Finger Temperature Device for Assessment of the Efficacy of New Warming Gel in Patients with Primary Raynaud's Phenomenon



T. ALEKSIEV, ZL. IVANOVA, H. DOBREV

DEPARTMENT OF DERMATOLOGY AND VENEREOLOGY, FACULTY OF MEDICINE, MEDICAL UNIVERSITY, PLOVDIV, BULGARIA



Introduction

Raynaud's phenomenon (RP) represents recurrent vasospasm of the fingers and toes in response to cold exposure or stress. Various local warming products can be used to relieve the RP symptoms.

Objectives

To evaluate the efficacy of a new warming gel in patients with primary RP.

Methodology

A total of 20 patients with primary RP (3 male, 17 female, mean age 44.9 ± 19.1) were studied.

Standardised cold-water provocation test consisting of exposure of both hands to a temperature of 10°C for 5 min, was performed before and after single application of a warming gel.

Test product was a new warming gel Thermolka (Kanaderm, Asenovgrad, Bulgaria) containing Cannabis Sativa seed oil, Aesculus Hippocastanum seed extract, Eucalyptus Globulus Leaf Oil, Abies Sibirica Oil, Helianthus Annuus Seed Oil, Camphor, and Capsicum Frutescens Resin.

The gel was applied to the patient's dorsal and palmar side of both hands and fingers, moving from carpe to finger tips.

Changes in skin temperature were measured by means of prototype of a new Finger temperature device (Courage+Khazaka, Cologne, Germa-ny). The device measures simultane-ously the temperature of dorsal fingertip of 2-5 fingers and wrist. Skin temperature of both hands was measured at baseline and at 5, 10, 15, 10, 25 and 30 min after the cold challenge, to determine the time required for a return to baseline skin temperature.

Results

Before treatment, all patients showed a vasospastic type of cold-water provocation test with a recovery time of skin temperature over 15 min. After the application of warming gel, 14 of 20 (70%) patients showed a normal type of cold-water provocation test with a recovery time of skin temperature below 15 min. The second test also showed statistically significantly shorter mean times of complete recovery of baseline temperature with respect to the first finger and for all fingers.

	BEFORE TREATMENT			AFTER TREATMENT		
	% of cooling ($^{\circ}\text{C}$)	Time of skin temperature full recovery of the first finger (min)	Time of skin temperature full recovery of all 2-5 fingers (min)	% of cooling ($^{\circ}\text{C}$)	Time of skin temperature full recovery of the first finger (min)	Time of skin temperature full recovery of all 2-5 fingers (min)
Right hand	67,2	26,0	31,0	70,8	16,5	23,0
Left hand	65,7	26,3	30,8	69,0	15,0	21,0

Discussion

We considered that the camphor and capsaicin were the main active ingredients that improves the restoration of skin temperature after cold-water stimulation test.

Kotaka et al. 2014 have found that the application of camphor to the skin has induced increases in local blood flow in the skin.

Ghita et al. 2017 using real-time *in vivo* application of reflectance confocal microscopy have proved that topical application of capsaicin induces a localized inflammatory process.

The rest active ingredients (plant oils, cannabis sativa seed oil) may improve the penetration of camphor and capsaicin into the skin and thus have beneficial auxiliary effect.

Conclusions

The single application of the new rewarming gel improves skin microcirculation determined by cold stimulation test. The method used is appropriate for objective and quantitative assessment of the effects of a single application of warming and other products.

Use of the Skin Indentometer to Evaluate Skin Stiffness in Localized Scleroderma

Z. Ivanova, T. Aleksiev, H. Dobrev

Department of Dermatology and Venereology, Medical University, Plovdiv, Bulgaria

Corresponding Author: ivanova1991@yahoo.bg

KEY WORDS: Skin firmness, indentometry

Introduction: Localized scleroderma (LS) is a rare disease of the connective tissue that manifests with localized induration of the skin. In this study, we applied a new measurement device based on indentometry to determine the skin stiffness in patients with LS.

Methodology: A total of 30 sclerodermatous plaques in 12 patients with LS were measured with Indentometer IDM 800 (Courage + Khazaka, Cologne, Germany). The device measures the penetration depth of the probe indenter (pin) into the skin in mm. We used two probes with pin diameters 3 and 5 mm, respectively. The stiffer the skin, the less deep is the displacement by the indenter. The smaller the diameter, the deeper the pin will go into the skin when using the same force. The measurements were made on diseased skin and in adjacent normal skin served as control.

Results: The sclerodermatous skin showed lower Indentometer values compared to adjacent normal skin. The depth penetration with probe 3 mm was 1.461 mm vs 1.871 mm ($P<0.0001$) and with probe 5 mm – 1.179 vs 1.489 ($P=0.0013$). This suggests that diseased skin is stiffer than healthy skin.

Conclusion: The non-invasive method used is appropriate for objective and quantitative determination of the degree of skin induration in localized scleroderma as well as for assessment the disease evaluation and treatment efficacy.

Use of the Skin Indentometer to Evaluate Skin Stiffness in Localized Scleroderma



ZL. IVANOVA, T. ALEKSIEV, H. DOBREV

DEPARTMENT OF DERMATOLOGY AND VENEREOLOGY, FACULTY OF MEDICINE, MEDICAL UNIVERSITY, PLOVDIV, BULGARIA



Introduction

Localized scleroderma (LS) is a rare disease of the connective tissue that is characterized by initial phase of inflammation followed by fibrotic and atrophic changes of the affected skin. Various methods have been used for the evaluation of disease severity and tissue damage, including clinical scores, ultrasonography, thermography, CT, MRI and durometry.

Objectives

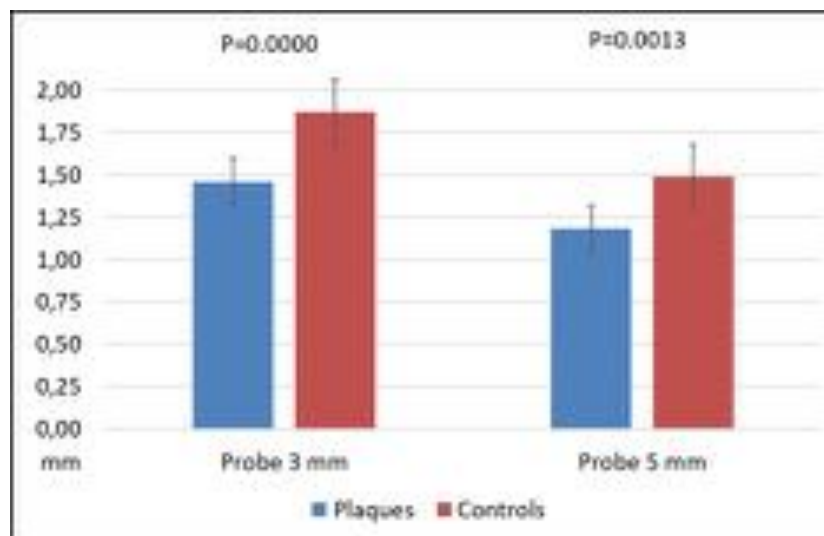
In this study, we applied a new measurement device based on indentometry to determine the skin stiffness in patients with LS.

Methodology

A total of 30 sclerodermatous plaques in 12 patients with LS were measured with Indentometer IDM 800 (Courage + Khazaka, Cologne, Germany). The device measures the penetration depth of the probe indenter (pin) into the skin in mm. We used two probes with pin diameters 3 and 5 mm, respectively. The stiffer the skin, the less deep is the displacement by the indenter. The smaller the diameter, the deeper the pin will go into the skin when using the same force. The measurements were made on diseased skin and in adjacent normal skin served as control.

Results

The sclerodermatous skin showed lower Indentometer values compared to adjacent normal skin. The depth penetration with probe 3 mm was 1.461 mm vs 1.871 mm ($P < 0.0001$) and with probe 5 mm – 1.179 vs 1.489 ($P = 0.0013$). This suggests that diseased skin is stiffer than healthy skin.



Discussion

Indentometry is a method for evaluation of skin softness/firmness.

The Indentometer IDM 800 is a quick and easy tool. The measurement principle is based on the force (by a spring) used on the small indenter of the probe to deform the skin.

The device measures how the probe indenter displaces the skin. The penetration depth of the pin (displacement) is measured in mm (0-3 mm).

Results obtained are interpreted as follow:

- The firmer/stiffer the skin, the less deep is the displacement by the pin.
- The smaller the diameter, the deeper the pin goes into the skin when using the same force as the contact area with the skin is smaller.

We found that sclerodermatous skin allows less penetration of both probes, suggesting that it is firmer than surrounding healthy skin. The degree of penetration with the small probe is greater, suggesting that it is more sensitive to skin changes.

Conclusions

We used for the first time new Indentometer device to evaluate the diseased skin in patients with LS. The results obtained suggest that the non-invasive method used is appropriate for objective and quantitative determination of the degree of skin firmness. In addition, it could be useful for monitoring the disease evolution and treatment efficacy.

Application of a Novel Finger Temperature Device in the Assessment of Subjects with Raynaud's Phenomenon

T. Aleksiev, Z. Ivanova, H. Dobrev

Department of Dermatology and Venereology, Medical University, Plovdiv, Bulgaria

Corresponding Author: t_aleksiev91@abv.bg

KEY WORDS: Skin temperature, cold-water provocation test

Introduction: Finger skin thermometry is one of the most commonly used methods for evaluating the response of the digital vessels to cold stimulation. The aim of this study is to evaluate the applicability of novel Finger skin temperature device for performing cold stimulation test in subjects with primary and secondary Raynaud's phenomenon (RP).

Methodology: A total of 155 consecutive subjects were studied. They were divided into three groups: 73 patients with primary RP (8 male, 65 female, mean age 38.5 ± 16.2), 42 patients with secondary RP (4 male, 38 female, mean age 49.6 ± 13.1 , connected with lupus erythematosus and systemic scleroderma), and 40 healthy controls (5 male, 35 female, mean age 38.8 ± 16.6). Standardized cold-water provocation test consisting of exposure of both hands to a temperature of 10°C for 5 minutes was performed. Changes in skin temperature of both wrists and 2-5 fingers were measured using a novel Finger temperature device (Courage & Khazaka). Measurements were made before and 5, 10, 15, 20, 25, and 30 min after cold stimulation. The time for recovery of baseline temperature of all fingers below 15 min was considered normal.

Results: The cold-water provocation test was normal in 6 (8.2%) of the patients with primary RP, in 7 (16.6%) of the patients with secondary RP, and in 28 (70%) of the healthy control subjects. The time of complete recovery of baseline temperature with respect to the first finger and for all 2-5 fingers in the three groups was as follows: 24.8 and 28.5 min (primary RP), 21.7 and 26.8 min (secondary RP), and 11.1 and 15.1 min (healthy subjects). Furthermore, the microcirculation was seriously disturbed (rewarming time >31 min) in 54.1%, 34.5% and 5% in the same study groups. These results suggested that microcirculation is more disturbed in patients with primary RP than in patients with secondary RP. In support of this unexpected finding, the results reported by Ruaro B. et al.¹ were. They investigate the blood perfusion (BP) by laser speckle contrast analysis (LASCA) in different skin areas of hands and found that it was significantly lower in primary RP than in secondary RP related to systemic sclerosis.

Conclusion: The new Finger temperature device used may be considered useful for performing cold stimulation test in patients with RP.

¹B. Ruaro. 2019; 10: 360. Front. Pharmacol., 2019 ; 10: 360.

Application of a Novel Finger Temperature Device in the Assessment of Subjects with Raynaud's Phenomenon

T. ALEKSIEV, ZL. IVANOVA, H. DOBREV

DEPARTMENT OF DERMATOLOGY AND VENERELOGY, FACULTY OF MEDICINE, MEDICAL UNIVERSITY, PLOVDIV, BULGARIA



Introduction

Finger skin thermometry is one of the most commonly used methods for evaluating the response of the digital vessels to cold stimulation.

Objectives

To evaluate the applicability of novel Finger skin temperature device for performing cold stimulation test in subjects with primary and secondary Raynaud's phenomenon (RP)

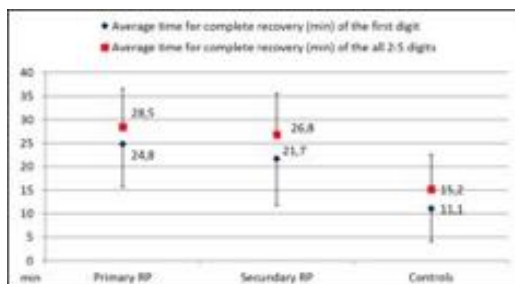
Methodology

A total of 155 consecutive subjects were studied. They were divided into three groups: 73 patients with primary RP (8 male, 65 female, mean age 38.5 ± 16.2), 42 patients with secondary RP (4 male, 38 female, mean age 49.6 ± 13.1 , connected with lupus erythematosus and systemic scleroderma), and 40 healthy controls (5 male, 35 female, mean age 38.8 ± 16.6). Standardized cold-water provocation test consisting of exposure of both hands to a temperature of 10°C for 5 minutes was performed. Changes in skin temperature of both wrists and 2-5 fingers were measured using a novel Finger temperature device (Courage & Khazaka). Measurements were made before and 5, 10, 15, 20, 25, and 30 min after cold stimulation. The time for recovery of baseline temperature of all fingers below 15 min was considered normal.

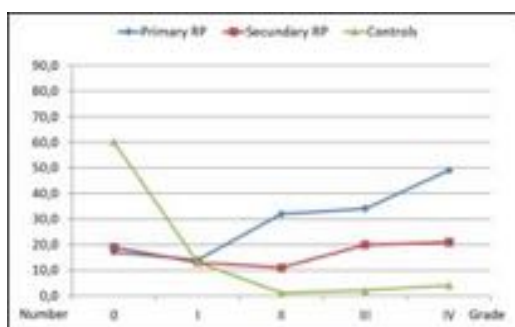
Results

The cold-water provocation test was normal in 6 (8.2%) of the patients with primary RP, in 7 (16.6%) of the patients with secondary RP, and in 28 (70%) of the healthy control subjects. The time of complete recovery of baseline temperature with respect to the first finger and for all 2-5 fingers in the three groups was as follows: 24.8 and 28.5 min (primary RP), 21.7 and 26.8 min (secondary RP), and 11.1 and 15.2 min (healthy subjects). Furthermore, the microcirculation was serious disturbed (rewarming time >31 min) in 54.1%, 34.5% and 5% in the same study groups.

Average time of complete recovery of both hands (Mean \pm SD)



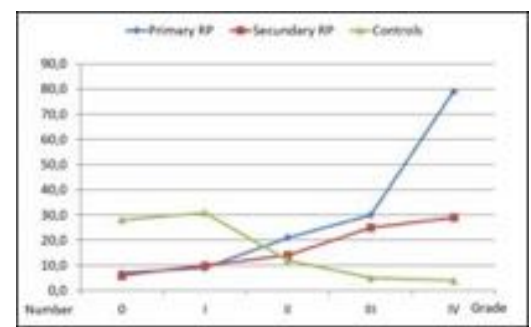
Complete rewarming time of the first digit.



Assessment scale for cold stimulation test [Kadan M. et al, 2015]

Stage	Rewarming time (min)	Assessment	Potential diagnosis
0	0-10	Normal	Healthy person
I	11-15	Mild disturbed	Otherwise healthy person
II	16-20	Moderate disturbed	Mild vasospastic disorder
III	21-30	Serious disturbed	Moderate vasospastic disorders
IV	>30	Serious disturbed	Serious vasospastic disorder

Complete rewarming time of all 2-5 digits.



Distribution of patients by groups (0-4) according to "Assessment scale for cold stimulation test"

Discussion

These results suggested that microcirculation is more disturbed in patients with primary RP than in patients with secondary RP. In support of this unexpected finding, the results reported by Ruaro B. et al. were. They investigate the blood perfusion (BP) by laser speckle contrast analysis (LASCA) in different skin areas of hands and found that it was significantly lower in primary RP than in secondary RP related to systemic sclerosis.

Conclusions

The new Finger temperature device used may be considered useful for performing cold stimulation test in patients with RP.

Use of Skin Indentometer to Measure Age-related Changes in Skin Stiffness

Z. Ivanova, T. Aleksiev, H. Dobrev

Department of Dermatology and Venereology, Medical University, Plovdiv, Bulgaria

Corresponding Author: ivanova1991@yahoo.bg

KEY WORDS: Skin firmness, indentometry

Introduction: Mechanical properties of the skin are changed with age due to intrinsic and extrinsic skin aging. In this study, we applied a new measurement device based on indentometry to determine the age-related changes in skin stiffness in healthy subjects.

Methodology: A total of 100 healthy volunteers aged 17–84 years were studied. They were divided into eight groups: 10 young men (mean age of 21.6 ± 1.6 years), 12 young women (mean age of 21.6 ± 1.8 years), 15 young men (mean age of 27.5 ± 3.4 years), 11 young women (mean age of 27.4 ± 2.9 years), 12 middle-aged men (mean age of 53.8 ± 6.9 years) and 15 middle-aged women (50.7 ± 9.7 years). 13 elderly men (mean age of 73.2 ± 7.3 years) and 12 elderly women (69.2 ± 5.2 years). The measurements were made on the forehead (center) and both volar forearms (center between wrist and elbow) with Indentometer IDM 800 (Courage + Khazaka, Cologne, Germany). The device measures the penetration depth of the probe indenter (pin) into the skin in mm. We used two probes with pin diameters 3 and 5 mm, respectively. The stiffer the skin, the less deep is the displacement by the indenter. The smaller the diameter, the deeper the pin will go into the skin when using the same force.

Results: At all study sites and with both probes, the indentometer values increased with age and there was a significant positive correlation. This suggests that the skin becomes less firm with age. On the forehead, except for the age of 21, higher values were measured in men than in women, which suggests that men's skin is less firm than female's. On both volar forearms, higher values were measured in women than in men, which suggests that women's skin is softer than the male skin. These gender differences could be explained by the greater impact of photoaging in men and the role of estrogens in women.

Conclusion: The non-invasive method used is appropriate for the objective and quantitative determination of the degree of skin stiffness in healthy people and for assessing the changes during skin aging or after external influences.

Use of Skin Indentometer to Measure Age-related Changes in Skin Stiffness



ZL. IVANOVA, T. ALEKSIEV, H. DOBREV

DEPARTMENT OF DERMATOLOGY AND VENEREOLOGY, FACULTY OF MEDICINE, MEDICAL UNIVERSITY, PLOVDIV, BULGARIA



Introduction

Mechanical properties of the skin are changed with age due to intrinsic and extrinsic skin aging.

Objectives

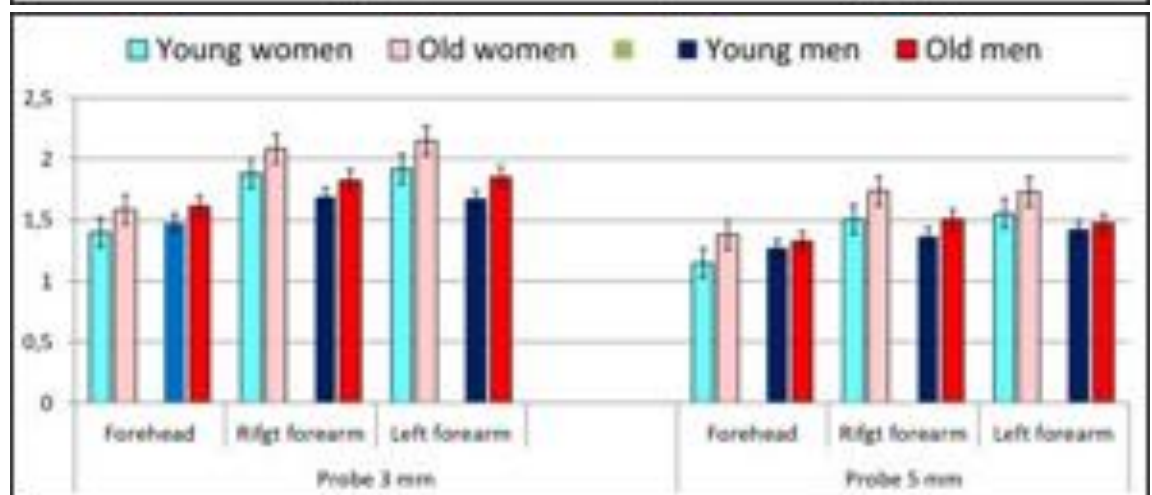
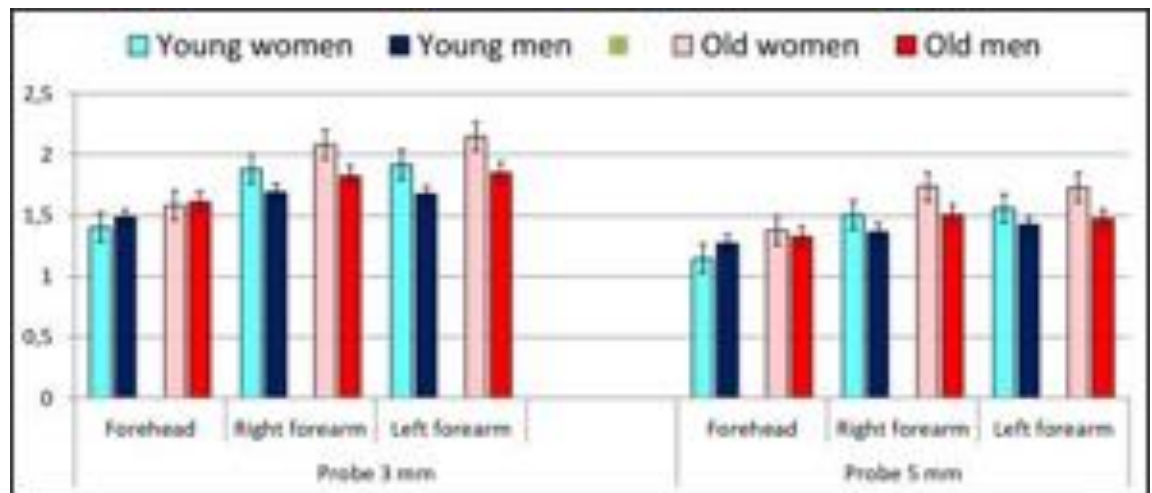
To determine the age-related changes in skin stiffness in healthy subjects using a new measurement device based on indentometry

Methodology

A total of 100 healthy volunteers aged 17–84 years were studied. They were divided into eight groups: 10 young men (mean age of 21.6 ± 1.6 years), 12 young women (mean age of 21.6 ± 1.8 years), 15 young men (mean age of 27.5 ± 3.4 years), 11 young women (mean age of 27.4 ± 2.9 years), 12 middle-aged men (mean age of 53.8 ± 6.9 years) and 15 middle-aged women (50.7 ± 9.7 years). 13 elderly men (mean age of 73.2 ± 7.3 years) and 12 elderly women (69.2 ± 5.2 years). The measurements were made on the forehead (center) and both volar forearms (center between wrist and elbow) with Indentometer IDM 800 (Courage+Khazaka, Koln, Germany). The device measures the penetration depth of the probe indenter (pin) into the skin in mm. We used two probes with pin diameters 3 and 5 mm, respectively. The stiffer the skin, the less deep is the displacement by the indenter. The smaller the diameter, the deeper the pin will go into the skin when using the same force.

Results

At all study sites and with both probes, the Indentometer values increased with age and there was a significant positive correlation. This suggests that the skin becomes less firm with age. On the forehead, except for the age of 21, higher values were measured in men than in women, which suggests that men's skin is less firm than female's. On both volar forearms, higher values were measured in women than in men, which suggests that women's skin is softer than the male skin. These gender differences could be explained by the greater impact of photoaging in men and the role of estrogens in women.



Conclusions

The non-invasive method used is appropriate for the objective and quantitative determination of the degree of skin stiffness in healthy people and for assessing the changes during skin aging or after external influences.

Skin Irritation and Inflammation – new data from an old (methylnicotinate) challenger

Sérgio Faloni de Andrade, Clemente Rocha and Luis Monteiro Rodrigues

CBIOS - Research Center for Biosciences and Health Technologies, Universidade Lusófona Lisbon, Portugal.

Corresponding Author e-mail address: sergio.andrade@ulusofona.pt

KEY WORDS: methylnicotinate, TEWL, high frequency sonography

Skin inflammation has many different expressions in clinical dermatology, with a wide variety of clinical signs and subjective symptoms. Nevertheless inflammation is a key feature in multiple dermatological problems, and at times the mechanisms involved are difficult to identify and understand. Several human models have been developed to study the impact on the skin barrier resulting from contact with various exogenous molecules, such as methylnicotinate (MN). However, skin responses to this challenger are widely varied, with no clear cause. Therefore, the aim of our work is to better understand and characterise the response(s) to the exposure of healthy caucasoid skin to this compound. Aqueous MN solution (0.5% and 1.0%) was applied in pre-defined regions (1cm²) on the skin of the anterior forearm of eight volunteers (41.37±11.32 years old) using a 5 mm diameter paper disc without occlusion. The reagent was left in contact with the skin for 1 minute before removal. A similar empty area in the same forearm was used as negative control. Immediately following MN exposure, the skin reaction was measured at 0, 30, 60 and 120 minutes by Polarised Spectroscopy (TiVi, Wheels Bridge, Sweden), Laser Doppler Flowmetry (LDF, PeriFlux System 5000, Perimed, Sweden), Transepidermal Water Loss Meter (Tewameter TM300, CK electronics, Germany) and High resolution sonography (HRS) (Dermascan C, Cortex Technology, Denmark). Direct observations of skin reactions were scored using the International Contact Dermatitis Group Research (ICDRG) scale. All procedures were approved by the institutional Ethics' Committee. Our results suggest that MN application caused a characteristic reaction on the skin 30 minutes after exposure, with an increase in the ICDRG score between 1-2. These scores are characterized by the presence of a positive reaction, including erythema, infiltration, vesicles, and possibly papules. Concomitant changes in microcirculation were detected by increases in local perfusion as monitored by LDF and TIVI, and increased dermal hypoecogenicity (edema) was detected by HRS.

An increase in TEWL was also observed. These findings indicate that under these conditions, MN induces a local and transient microinflammatory response of the skin, with highest intensity approximately 30 minutes following exposure, with a significant increase in microcirculatory variables (perfusion, flow rate, red blood cell concentration) and a significant increase in transepidermal water loss and edema.

Acknowledgments: Fundação de Ciência e Tecnologia (FCT) UIDB/04567P/2020 and UIDP/04567B/2020

1 Elawa, S., Mirdell, R., Farnebo, S., & Tesselaar, E. (2019). doi: 10.1111/srt.12807

2 Elawa, S., Mirdell, R., Tesselaar, E., & Farnebo, S. (2019). doi: 10.1016/j.mvr.2019.03.002

3 Ivens J.U. Serup K. O. (2007).doi.org/10.1111/j.1600-0846.2007.00232.x

4 Jumbelic, L., Liebel, F., & Southall, M. (2006). doi: 10.1159/000092595

Skin Irritation and Inflammation – new data from an old (methylnicotinate) challenger

Sérgio Faloni de Andrade, Clemente Rocha and Luis Monteiro Rodrigues

CBIOS - Research Center for Biosciences and Health Technologies, Universidade Lusófona Lisbon, Portugal.

Corresponding Author e-mail address: sergio.andrade@ulusofona.pt

Introduction

Skin inflammation has many different expressions in clinical dermatology, with a wide variety of clinical signs and subjective symptoms. Nevertheless inflammation is a key feature in multiple dermatological problems, and at times the mechanisms involved are difficult to identify and understand. Several human models have been developed to study the impact on the skin barrier resulting from contact with various exogenous molecules, such as methylnicotinate (MN). However, skin responses to this challenger are widely varied, with no clear cause.

Aim

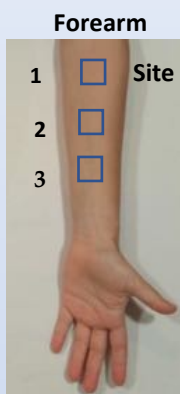
The aim of our work is to better understand and characterise the response(s) to the exposure of healthy caucasoid skin to this compound.

Methods

- Aqueous MN solution (0.5% or 1.0%)
- Negative Control

8 healthy volunteers (41.37±11.32 years old)

All procedures were approved by the institutional Ethics' Committee.



- ✓ Polarised Spectroscopy (TiVi, Wheels Bridge, Sweden)
- ✓ Laser Doppler Flowmetry (LDF, PeriFlux System 5000, Perimed, Sweden)
- ✓ Transepidermal Water Loss Meter (Tewameter TM300, CK electronics, Germany)
- ✓ High resolution sonography (HRS) (Dermascan C, Cortex Technology, Denmark)
- ✓ Variables measured before and 30, 60 and 120 min after applications.

Results

Our results suggest that MN application caused a characteristic reaction on the skin 30 minutes after exposure, with an increase in the ICDRG score between 1-2 (Fig.1). These scores are characterized by the presence of a positive reaction, including erythema, infiltration, vesicles, and possibly papules. Concomitant changes in microcirculation were detected by increases in local perfusion as monitored by LDF and TIVI, and increased dermal hypoechogenicity (edema) was detected by HRS (Figs. 2-4). An increase in TEWL was also observed (fig.5).

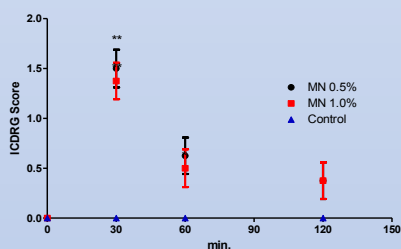


Fig. 1. Visual observation of the effects of applying MN 0.5% and 1.0% according to the score described in the ICDRG, ** p <0.05; Wilcoxon test

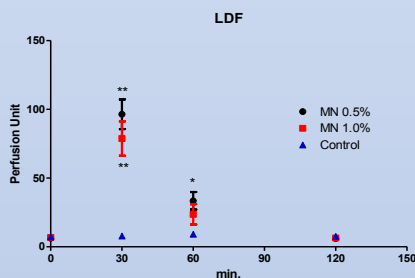


Fig. 2. Effects of the application of MN 0.5% and 1.0% on the perfusion detected by Laser Doppler. * p <0.05, ** p <0.01; Wilcoxon test

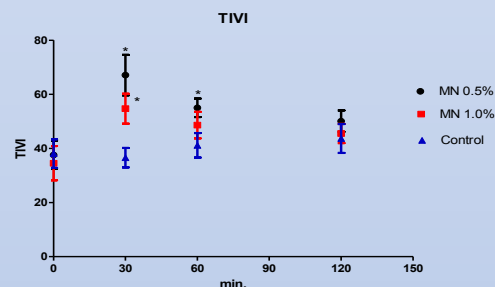


Fig. 3. Effects of the application of MN 0.5% and 1.0% on the perfusion detected by Polarized Light. * p <0.05; Wilcoxon test

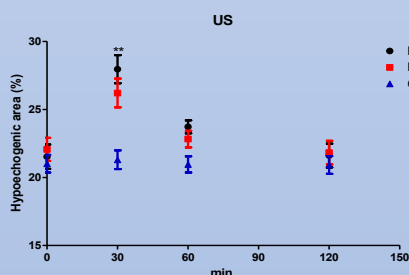


Fig. 4. Effects of the application of MN 0.5% and 1.0% on dermal hypoechogenicity. * p <0.05; Wilcoxon test

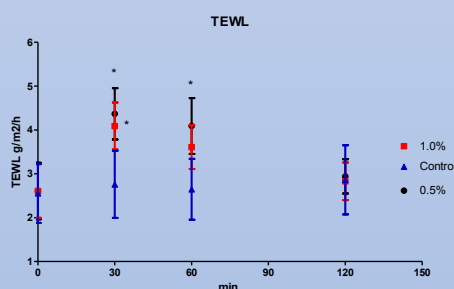


Fig. 5. Effects of the application 0.5% and 1.0% MN on transepidermal water loss. * p <0.05; Wilcoxon test

CONCLUSIONS

These findings indicate that under these conditions, MN induces a local and transient microinflammatory response of the skin, with highest intensity approximately 30 minutes following exposure, with a significant increase in microcirculatory variables (perfusion, flow rate, red blood cell concentration) and a significant increase in transepidermal water loss and edema.

References

- 1 Elawa, S., Mirdell, R., Farnebo, S., & Tesselaar, E. (2019). doi: 10.1111/srt.12807
- 2 Elawa, S., Mirdell, R., Tesselaar, E., & Farnebo, S. (2019). doi: 10.1016/j.mvr.2019.03.002
- 3 Ivens J.U. Serup K. O. (2007).doi.org/10.1111/j.1600-0846.2007.00232.x
- 4 Jumbelic, L., Liebel, F., & Southall, M. (2006). doi: 10.1159/000092595

High Resolution Sonography confirms that essential oils benefit epidermal water barrier *in vivo*

Sérgio Faloni de Andrade¹, Patricia Rijo¹, Clemente Rocha¹, Lin Zhu², Kang Chen², and Luis Monteiro Rodrigues¹

1 CBIOS - Research Center for Biosciences and Health Technologies, Universidade Lusófona de Humanidades e Tecnologias, Lisboa, Portugal.

2 Jiangxi University of Traditional Chinese Medicine, Walin, Nanchang P.R. China.

Corresponding Author e-mail address: sergio.andrade@ulusofona.pt

KEY WORDS: essential oil; skin water dynamics; skin ultrasonography

Essential oils are complex mixtures of volatile low molecular weight compounds (terpenoids and phenylpropanoids) extracted from plants responsible for their characteristic aroma. Despite the wide use of these in cosmetic and dermatological formulations, information about its mechanism of action and efficacy is still insufficient. Thus, our objective is to contribute to understanding the impact of these oils on skin's physiology in healthy volunteers using non-invasive technologies. Essential oils from *Lavandula angustifolia* (lavender) and *Salvia officinalis* (sage) were obtained by hydrodistillation of the plants' aerial parts. Commercially available almond oil (Celeiro, Portugal) was used as reference (blank) but also as the vehicle for 5% and 10% concentrations of each essential oil. Eleven healthy participants (5 men and 6 women) mean age 31.3 ± 10.0 years old were selected. All procedures were conducted in accordance to good clinical practice and previously approved by the institutional Ethics Committee (approval number 04/13). Six areas (3cm x 3cm) were drawn in both forearms to test all formulations. The application order was previously randomised, keeping one square empty as the negative control. Following application with a small spatula (2mg/cm²) formulations were left in contact with the skin for 30 minutes. Measurements involved epidermal barrier function, assessed with the Tewameter TM300 (CK electronics), epidermal hydration measured by MoistureMeter SC and D (Delphin Technologies). High resolution sonography (HRS) images were obtained with the Dermascan C (Cortex Technology). All variables were measured before and 30 min after applications. Nonparametric statistical comparisons were applied ($p < 0.05$). A significant decrease of TEWL, as well as a significant increase of superficial and deep epidermal hydration, were observed for all formulations tested. The HRS showed that epidermis is more echogenic after the application of all formulations. However, in the dermis a significant echogenicity decrease was detected for all essential oils in particular for the 5% formulations. Furthermore HRS suggests that essential oils penetrate only in the most superficial layers of the skin, reinforcing epidermal cohesion due to their lipid character. This seems to promote a statistically significant improvement of various cutaneous properties, shown by the reduction of TEWL and the increase of deep epidermal hydration.

Acknowledgments: Fundação de Ciência e Tecnologia (FCT) UIDB/04567P/2020 and UIDP/04567B/2020

1 Akdeniz, M., et al. (2018). doi: 10.1111/srt.12454

2 De Groot, A., & Schmidt, E. (2016). doi: 10.1097/der.0000000000000218

3 Patzelt, A., Lademann, J., Richter, H., Darvin, M., Schanzer, S., & Thiede, G. et al. (2011). doi: 10.1111/j.1600-0846.2011.00578.x

4 Rosado, C., Barbosa, R., Fernando, R., Antunes, F., & Rodrigues, L. (2015). doi: 10.19277/bbr.12.2.117

High Resolution Sonography confirms that essential oils benefit epidermal water barrier *in vivo*

Sérgio Faloni de Andrade¹, Patricia Rijo¹, Clemente Rocha¹, Lin Zhu², Kang Chen², and Luis Monteiro Rodrigues¹

¹CBIOS - Research Center for Biosciences and Health Technologies, Universidade Lusófona de Humanidades e Tecnologias, Lisboa, Portugal.

²Jiangxi University of Traditional Chinese Medicine, Walin, Nanchang P.R. China.

Corresponding Author e-mail address: sergio.andrade@ulusofona.pt

INTRODUCTION

Essential oils are complex mixtures of volatile low molecular weight compounds (terpenoids and phenylpropanoids) extracted from plants and are responsible for the characteristic aroma in those plants. Despite the wide use of these in cosmetic and dermatological formulations, information about its mechanism of action and efficacy is still insufficient.

OBJECTIVE

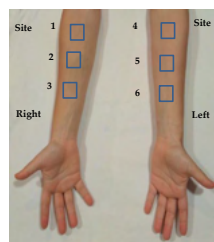
Despite the wide use of these in cosmetic and dermatological formulations, information about its mechanism of action and efficacy is still insufficient. Thus, our objective is to contribute to understanding the impact of these oils on skin's physiology in healthy volunteers using non-invasive different methodologies. Have been evaluated the essential oils from *Lavandula angustifolia* (lavender) and *Salvia officinalis* (sage) which have been obtained by hydrodistillation of the plants' aerial parts.

MATERIAL and METHODS

Treatments

- *S. officinalis* 5% and 10% in almond oil
- *L. agustifolia* 5% and 10% in almond oil
- Almond oil
- Occlusive patch

➤ 11 healthy volunteers (5 men and 6 women, mean age 31.3 ± 10.0 years old)



- ✓ Transepidermal Water Loss (TEWL) (Tewameter TM300 CK electronics GmbH, Germany)
- ✓ Epidermal hydration (MoistureMeter SC and a MoistureMeter D - Delphin Technologies, Finland)
- ✓ Skin biomechanical properties (Cutometer®MPA580 system, CK electronics GmbH, Germany).
- ✓ Variables measured before and 30 min after applications. Nonparametric statistical comparisons were applied (p<0.05).

➤ All procedures conducted according to the principles of the Declaration of Helsinki and respective amendments, approved by the Ethics Committee from the School of Sciences and Health Technologies, Universidade Lusofona (approval number 04/13).

RESULTS and DISCUSSION

A significant decrease of TEWL (Fig. 1), as well as a significant increase of superficial and deep epidermal hydration, were observed 30 min after the application of all the formulations tested (Fig.2). Regarding skin biomechanical properties, significant increase of maximum elongation amplitude, maximum relaxation, elasticity, and viscoelastic ratio (Fig.3). The ultrasonographic analysis showed a significant increase in hypoechogenicity (increase in black color) in the dermis after application of formulations containing essential oils, on the other hand, in the epidermis was observed diminishing in black color, i.e., reduction in hypoechogenicity (Fig. 4). The effects were more evident in the 5% concentration of both essential oils.

Conclusion

The findings in HRS suggest that essential oils penetrate only in the most superficial layers of the skin, where probably by reinforcing epidermal cohesion due to their lipid character promotes a statistically significant improvement of various cutaneous properties, including the reinforcement of the epidermal barrier and deep hydration.

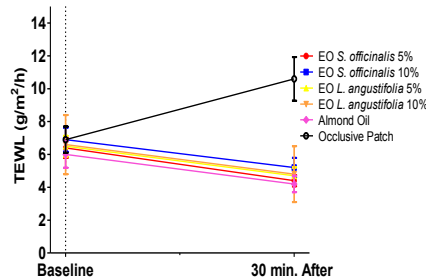


Fig. 1. Transepidermal water loss before (baseline values) and 30 min. after the application of different formulations and occlusive patch.

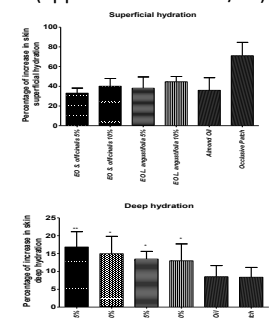


Fig. 2 – Percentage of increase in the skin hydration 30 min. after the application of different formulations and occlusive patch.

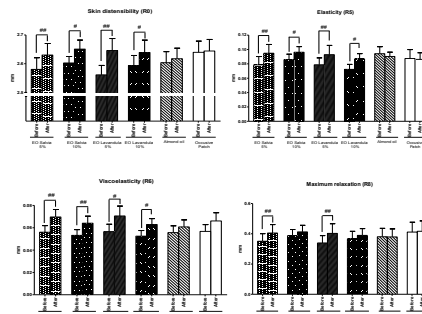
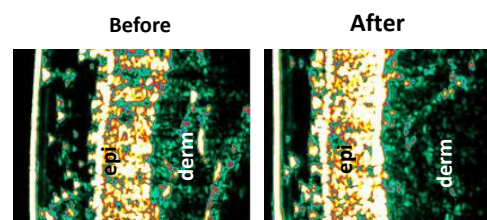


Fig. 3 – Effects on biomechanical skin properties before and 30 min. after the application of different formulations and occlusive patch.



References

- Akdeniz, M., Tomova-Simitchieva, T., Dobos, G., Blume-Peytavi, U., & Kottner, J. (2018). Does dietary fluid intake affect skin hydration in healthy humans? A systematic literature review. *Skin Research and Technology*, 24(3), 459-465. doi: 10.1111/srt.12454
- De Groot, A., & Schmidt, E. (2016). Essential Oils, Part V. *Dermatitis*, 27(6), 325-332. doi: 10.1097/der.0000000000000218
- Rosado, C., Raimundo, H., & Rodrigues, L.M. (2009). About "Deep" Skin Hydration Measurement. *Revista Lusófona de Ciências e Tecnologias da Saúde*, 6(1), 65-75.
- Rosado, C., Barbosa, R., Fernando, R., Antunes, F., & Rodrigues, L. (2015). Study of the effect of epidermal overhydration by occlusion, on the skin biomechanical behaviour assessed in vivo with the systems Cutometer®, Reviscometer® and CutiScan®. *Journal Biomedical and Biopharmaceutical Research*, 12(2), 203-213. doi: 10.19277/bbr.12.2.117

Study of skin folding in its different skin layers by coupling a folding test with LC-OCT imaging and relief morphology

M. Ayadh^{1,2}, A. Guillermin¹, M-A. Abellan¹, M. Pedrazzani³, E. Cohen³, C. Didier¹, A. Bigouret², H. Zahouani¹

1. Université de Lyon, ECL-ENISE, LTDS, 36, avenue Guy de Collongue, 69134 Ecully, France.

2. Laboratoires Clarins, 5 Rue Ampère, 95300 Pontoise, France

3. DAMAE MEDICAL, 14 Rue Sthrau, 75013 Paris, France

Corresponding Author e-mail address and URL: meriem.ayadh@ec-lyon.fr

KEY WORDS: in vivo test, skin topography, LC-OCT imaging

Knowing the evolution of the skin's response to mechanical solicitations and understanding the origin of these responses is very important in medicine, surgery, and cosmetics. Studies performed in vitro and ex vivo show that links exist between the topographic properties of the skin and the collagen and elastin fibers network in the dermis^{1,2}.

In this study we propose a combination of two experimental tests in vivo to show the link between the topographic properties of skin and the fibers network in the dermis. The first method consists in analyzing the images of skin relief of skin at rest and during a folding test. From these images we calculate the density of the furrows (or skin lines) and their orientations. The second method uses a recently developed imaging technique which allows images of human skin in vivo with very high spatial resolution: Line-field Confocal Optical Coherence Tomography (LC-OCT)³. This innovative technology allows two types of images: vertical section images and horizontal images. Thanks to these two modalities, it is possible to obtain the full 3D image of the skin. The images are taken for the skin at rest and during a folding test. From these images we extract the density of fibers and their orientation in the plan parallel to the surface of the skin. The study is carried out on 42 volunteers aged from 20 to 55 years old. The skin relief analysis and LC-OCT images are performed on the skin of the forearm. We could observe a correlation between the skin lines at the surface and the structure in depth of its layers in the volume ($0.40 < I(\text{Spearman}) < 0.57$).



Figure 1: Images of skin relief and LC-OCT images of skin at rest and during folding test

¹ M. Gasiór-Głogowska et al., “FT-Raman spectroscopic study of human skin subjected to uniaxial stress,” *J. Mech. Behav. Biomed. Mater.*, vol. 18, pp. 240–252, 2013.

² A. Delalleau, G. Josse, J. M. Lagarde, and P. F. Dermo-cosmétiques, “Un modèle hyperélastique à réorientation de fibres pour l’analyse des caractéristiques mécaniques de la peau,” <https://www.researchgate.net/publication/266492847>, no. December 2014, 2014.

³ J. Ogien, O. Levecq, H. Azimani, and A. Dubois, “Dual-mode line-field confocal optical coherence tomography for ultrahigh-resolution vertical and horizontal section imaging of human skin in vivo,” *Biomed. Opt. Express*, vol. 11, no. 3, pp. 1327–1335, 2020.

INTRODUCTION

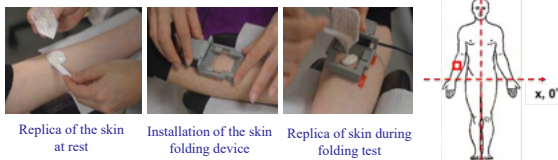
Knowing the evolution of the skin's response *in vivo* to mechanical solicitations and understanding the origin of these responses are very important in medicine, surgery, and cosmetics. In this study, we propose a combination of two experimental tests *in vivo*, replica of skin relief and LC-OCT, to show the link between the topographic properties of skin and the fibers network in the dermis. We thus compare the orientation of the skin lines at the skin surface to the orientation of the dermal fibers.

MATERIAL & METHODS

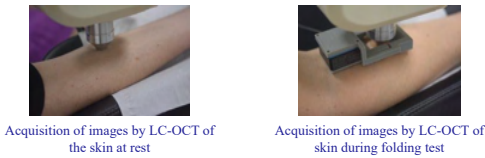
Panel and Test zone

Group	Age	Number	Body area
Young	[20 - 30] years old	21	Forearm (3 × 8 cm), 12 cm above the wrist of the hands
Elderly	[45 - 55] years old	21	

Skin relief and Folding test

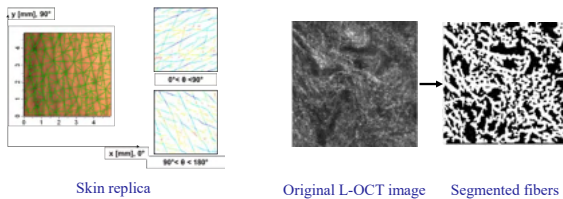


Line-field Confocal Optical Coherence Tomography imaging and Folding test



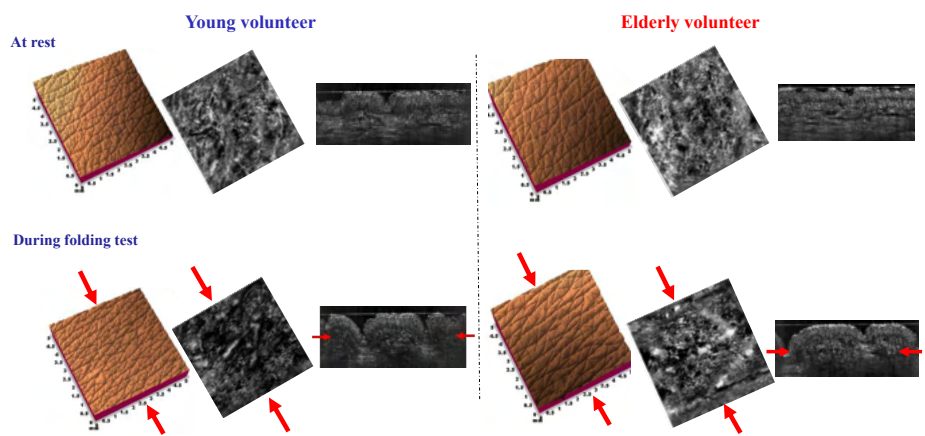
Data extraction by segmentation

Density of skin lines and skin fibers at rest and during folding tests are extracted according to 9 intervals of directions ranging from 0° to 180° with a step of 20°.

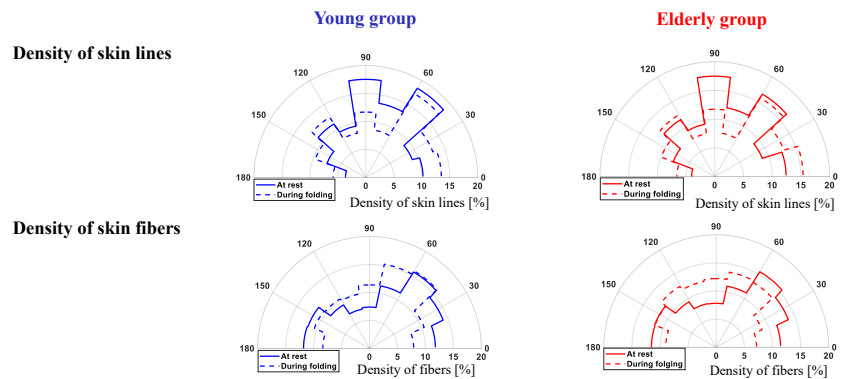


RESULTS

Images of skin relief and LC-OCT images



Distribution of skin lines and skin fibers



DISCUSSION & CONCLUSION

Age group	Condition	Directions of maximum density of skin lines	Directions of maximum density of skin fibers
Young	At rest	[40° - 90°]	[40° - 60°]
	During folding	[40° - 60°]	[40° - 60°]
Elderly	At rest	[40° - 90°]	[40° - 60°]
	During folding	[40° - 60°]	[40° - 60°]

The results of statistical analysis (ANOVA) show no difference in density of skin lines and skin fibers between the two age groups for the forearm. During folding test, a reorientation of the skin lines and skin fibers occurs. We could observe a correlation between the skin lines at the surface and the structure in depth of its layers in the volume ($0.40 < r(\text{Spearman}) < 0.57$).

The orientation of the skin lines on the surface is due to the reorganization of the collagen and elastin fibers in the dermis following the applied stress.

Multiphoton tomography combined with artificial intelligence for automatic diagnosis of skin conditions

Ana Batista, PhD^{1,2}, Pedro Guimarães, PhD^{1,3}, Michael Zieger, Dr.rer.nat.⁴, Martin Kaatz, PD Dr med. habil.⁴, Karsten Koenig, Prof.^{2,5}

¹CIBIT – Coimbra Institute for Biomedical Imaging and Translational Research, University of Coimbra, 3030-548 Coimbra, Portugal; ²Saarland University, Department of Biophotonics and Laser Technology, Saarland University, 66123 Saarbruecken, Germany; ³Chair for Clinical Bioinformatics, Saarland University, 66123 Saarbruecken, Germany; ⁴SRH Wald-Klinikum Gera, Strasse des Friedens 122, 07548 Gera, Germany; ⁵JenLab GmbH, Johann-Hittorf-Strasse 8, 12489 Berlin, Germany
ana.baptista@uc.pt

KEY WORDS: Artificial intelligence, Multiphoton tomography, Skin disease diagnosis

The potential of multiphoton tomography (MPT) for skin diagnosis is clear. However, it has not yet been fully realized. Deep learning as an end-to-end approach can integrate both morphologic and metabolic information, broadening the application of MPT. In this study, we combine MPT and convolutional neural networks (CNNs) to automatically diagnose atopic dermatitis (AD).

MPT measurements were performed in ten subjects (six AD patients and four healthy volunteers) of both sexes with ages ranging from 19 to 78 years old participating in a clinical study conducted by JenLab GmbH and SRH Wald-Klinikum Gera. Autofluorescence (AF) intensity was acquired and concatenated with the computed mean AF lifetime and ratio between the short and long relative contributions of two AF lifetime components to create 3,663 images from 21 z-stacks covering multiple layers of the skin. Preliminary fluorescence lifetime analysis was performed to identify morphologic and metabolic changes induced by AD. CNNs were trained and tuned to detect the presence of living cells in these images, and if so, to diagnose AD, independently of imaged layer or position. Accuracy, sensitivity, specificity, F-score and area under both the receiving operating characteristics and precision-recall curves were used to assess the performance of the proposed algorithm. Relevance propagation by deep Taylor decomposition was used to enhance the interpretability of the proposed approach.

The preliminary analysis identified the perinuclear accumulation of mitochondria and a tendency for a lower metabolic activity, although statistical significance was not achieved. The proposed deep-learning algorithm correctly diagnosed AD in 97.0±0.2% of all images where living cells were present. The area under the receiver operating characteristic and precision-recall curves was 0.994±3.8×10⁻⁴ and 0.996±2.2×10⁻⁴, respectively. The diagnosis was obtained with a sensitivity of 0.966±0.003, specificity of 0.977±0.003 and F-score of 0.964±0.002. Relevance heatmaps show what aspects of the images are important for the classification. Both the morphological mitochondria pattern and metabolic status of the cells appear to be key for the model's decision process.

The obtained results show that MPT imaging can be combined with artificial intelligence to successfully discriminate AD. The proposed approach serves as a framework for the automatic diagnosis of skin disorders using MPT.

Multiphoton tomography combined with artificial intelligence for automatic diagnosis of skin conditions



A. Batista^{a,b}, P. Guimarães^{a,c}, M. Zieger^d, M. Kaatz^d, and K. König^{b,e}
^aCIBIT – Coimbra Institute for Biomedical Imaging and Translational Research, University of Coimbra, 3030-548 Coimbra, Portugal; ^bBLT – Department of Biophotonics and Laser Technology, Saarland University, 66123 Saarbruecken, Germany; ^cChair for Clinical Bioinformatics, Saarland University, 66123 Saarbruecken, Germany; ^dSRH Wald-Klinikum Gera, Strasse des Friedens 122, 07548 Gera, Germany; ^eJenLab GmbH, 12489 Berlin, Germany



Purpose

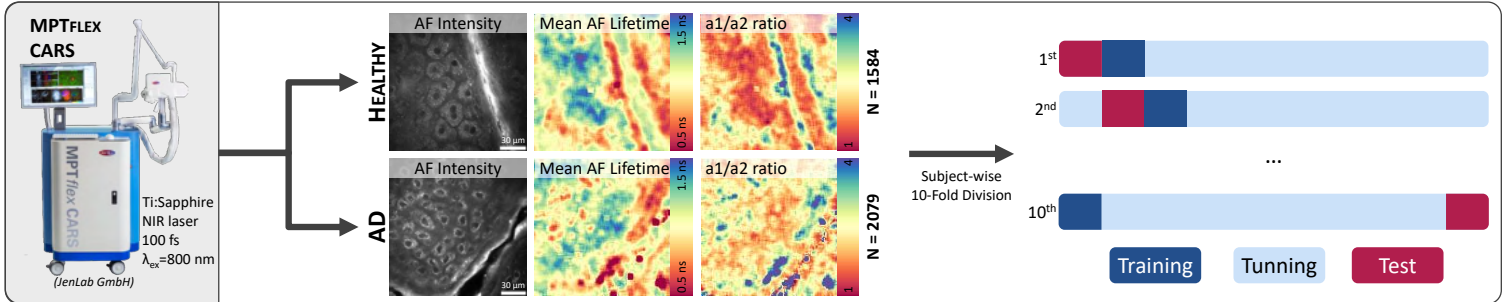
To demonstrate the potential multiphoton tomography (MPT) combined with deep learning for operator independent diagnosis of skin conditions.

Introduction

The potential of MPT for skin diagnosis is clear and has been demonstrated for several conditions including carcinomas and melanomas.¹ Nevertheless, it has not yet been fully realized. Deep learning, namely convolutional neural networks (CNNs), as an end-to-end approach can integrate both morphologic and metabolic information, broadening the application of MPT. In this study, we introduce an accurate and reliable CNN model for atopic dermatitis (AD) diagnosis, removing any operator dependency. This initial work serves as framework for other skin diseases.

Data

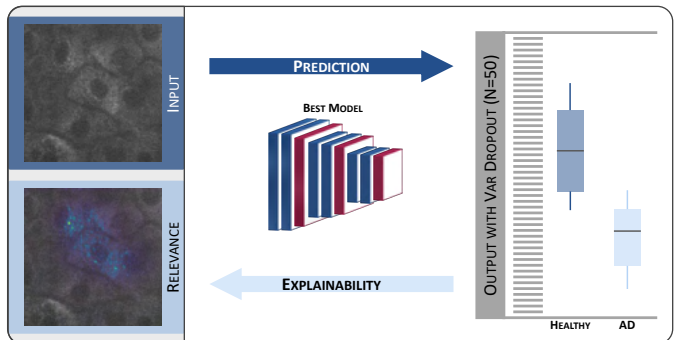
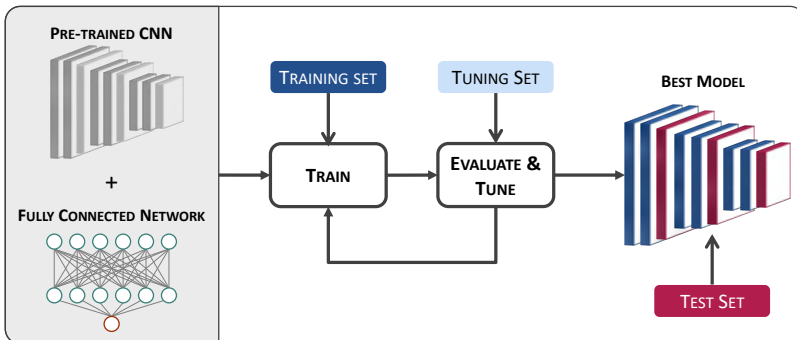
Autofluorescence (AF) intensity, mean AF lifetime, and the NAD(P)H a_1/a_2 ratio were obtained from the skin of healthy volunteers and AD patients using the multiphoton tomograph MPTflex-CARS. A total of 3663 image patches were divided into train, tune, and test sets.



Methods

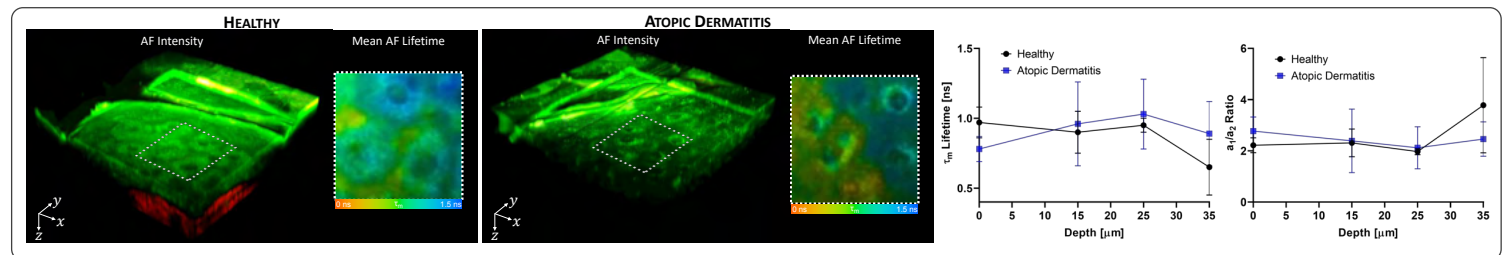
Classification workflow. Training, tuning, and testing sets are all independent. Each subject could not ever be simultaneously in the testing and training sets.

Deep Taylor decomposition for interpretability improvement, and variational dropout for uncertainty estimation.

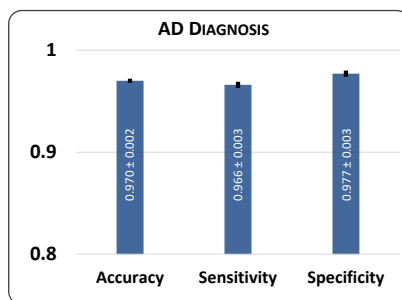


Results

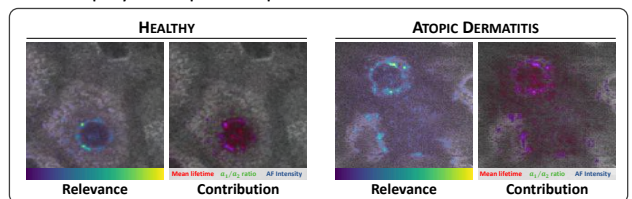
Using MPT, an accumulation of mitochondria around cell's nucleus in the outermost cell layers of AD patients was observed. This has been previously associated with cell inflammation.^{2,3} No significant changes were observed in the mean AF lifetime and NAD(P)H a_1/a_2 ratio.



With the implemented approach, 97% of all images containing living cells were correctly diagnosed with AD with high sensitivity and specificity, independent of the skin layer. Results were consistent between z-stacks and subjects as shown by the low inter-subject and inter-stack accuracy standard deviations (0.053 and 0.032, respectively).



Relevance heatmaps were computed to better understand how the classification is reached. Cell's AF intensity and mean AF lifetime play an important part in the model's decision.



Conclusion

We successfully trained and validated a CNN-based algorithm to discriminate AD in MPT images with high accuracy, sensitivity, and specificity.



Funding from the European Union's Horizon 2020 research and innovation program under grant agreement No 726666 (LASER-HISTO), FEDER Funds through the Operational Program for Competitiveness Factors - COMPETE and by Portuguese National Funds through FCT - Foundation for Science and Technology under the PTDC / EMD-EMD / 32162/2017 project.

High Frequency Ultrasound Skin Tumors Invasion Depth and Margins Assessment. Basal Cell Carcinoma Clinical Forms Differentiation with 30 and 75 MHz Ultrasound.

A. Bezugly¹, A. Khlebnikova², T. Sedova³, E. Selezneva².

1- Academy of Postgraduate Education of the Russian Federal Medical Biological Agency.

2- M.F. Vladimirsky Moscow Regional Scientific Research Clinical Institute, Scientific-Practical Center of Dermatovenerology and Cosmetology.

3- E.A. Vagner Perm State Medical University, Moscow, Russia.

KEY WORDS: basal cell carcinoma (BCC); high-frequency ultrasound skin imaging; micromorphological measurement.

Introduction:

High frequency ultrasound (HFUS) skin imaging was announced as the accurate and objective instrument for the basal cell carcinoma (BCC) and melanoma preoperative measurements. Basal cell carcinoma (BCC) is the most common malignant skin tumor among the white-skinned population. The skin tumors treatment methods should ensure the complete elimination of malignant cells and the acceptable cosmetic result in compliance with tissue and organ-preserving principles. The tumor invasion depth and its clinical-morphological form are some of the most important factors for the adequate treatment choice.

Aim:

Different BCC clinical forms ultrasonographic features evaluation at 30 and 75 MHz frequencies. BCC spread depth measured with the histological examination and high-frequency ultrasound imaging comparison.

Materials and methods:

HFUS examination of the 62 BCCs was provided. High resolution imaging system DUB (TPM GmbH, Germany) with 75-MHz and 30-MHz probes was used. After HFUS scanning, the BCCs biopsy samples were collected for the morphological examination. Based on the histomorphology results obtained, the tumors were divided into thin (≤ 1 mm invasion depth) and thick (> 1 mm invasion depth). Each BCC spread depth was measured during the HFUS examination with 75-MHz and 30-MHz ultrasound probes and morphological examination.

Results:

The surface (thin) BCCs most often had elongated contours, clear margins, and hypoechoic structure, while the nodular BCC had round or oval outlines and diffusely hypo-heterogeneous structure with clear margins. Sclerodermiform BCCs were visualized as hypoechoic areas of irregular shape penetrating in the dermis, with wavy, fuzzy margins. High, statistically significant correlation was founded between histological and HFUS measurements. The BCC's treatment choice algorithm, based on HFUS measurement results, was proposed.

Conclusion:

HFUS is valuable instrument for the BCC's clinical-morphological forms differentiation. In cases of BCCs with a thickness of ≤ 1 mm, was a high correlation ($r=0.870$) of the tumor spread depth measured with histomorphometry and HFUS. In cases of BCCs with a thickness of > 1 mm, a very high correlation ($r=0.951$) of the tumor spread depth was observed between histomorphology and 30 MHz HFUS measurements.

Basal cell carcinoma invasion depth measurement with 30 and 75 MHz high-frequency ultrasound.

A. Bezugly¹, A. Khlebnikova², T. Sedova³, E. Selezneva².

1-Academy of Postgraduate Education of the Russian Federal Medical Biological Agency. 2-M.F. Vladimirsky Moscow Regional Scientific Research Clinical Institute. 3-E.A. Vagner Perm State Medical University.

Aim: To compare the depth spread of basal cell carcinoma (BCC) measured by histological examination and high-frequency ultrasound (HFUS) imaging with 30-MHz and 75-MHz probes.

Materials and methods: 27 BCCs examined with 30 and 75 MHz HFUS. Following biopsy (punch or surgical), samples were examined histologically.

Based on the histomorphology results obtained, the tumors were divided into thin (≤ 1 mm invasion depth) and thick (>1 mm invasion depth). Each BCC invasion depth was measured with 75-MHz and 30-MHz HFUS and morphological examination.

Results: Thin BCCs (Figure 1) average invasion depth measured histologically was 0.494 ± 0.212 mm. Its average depth obtained with 75-MHz and 30-MHz HFUS was 0.591 ± 0.265 and 0.734 ± 0.123 mm, respectively.

A high, statistically significant correlation between the histological and 75 MHz HFUS measurements was obtained ($r=0.870$). The correlation between 30 MHz HFUS and histology was weak ($r=0.290$).

The average thick BCC (Figure 2) invasion depth values obtained with the histological examination and 30 MHz HFUS scanning were 1.845 ± 0.718 mm and 1.995 ± 0.699 mm.

A high, statistically significant ($r=0.951$) correlation between the thick BCC spread depth measured with 30 MHz, HFUS and histomorphological examination were obtained.

Conclusion: In cases of BCCs with a thickness of ≤ 1 mm, there was a high correlation ($r=0.870$) of the tumor spread depth between micromorphological measurements and the results obtained using a 75 MHz transducer and in cases of BCCs with the thickness of >1 mm, a very high correlation ($r=0.951$) of the tumor spread depth was observed between histomorphometry and 30 MHz transducer measurements. The 22-33 MHz HFUS could be recommended for BCCs measurement of thickness ≥ 1 mm, and 50-75 MHz HFUS for BCCs with thickness ≤ 1 mm.

Keywords: basal cell carcinoma (BCC); high-frequency ultrasound skin imaging; micromorphological measurement

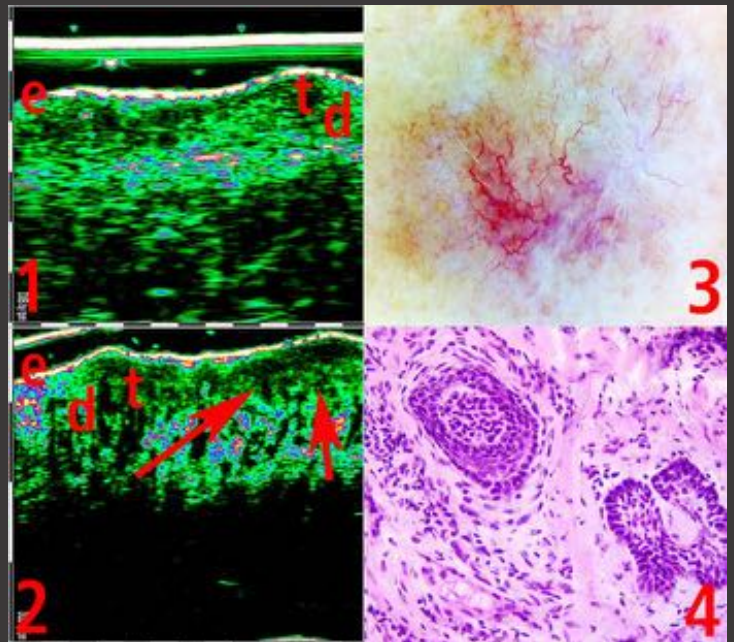


Figure 1. Thin micronodular invasive BCC B-mode 30 (1) and 75 MHz (2) scans, videodermoscopy (3), and histology (4), e-epidermis, d- dermis, t - tumor

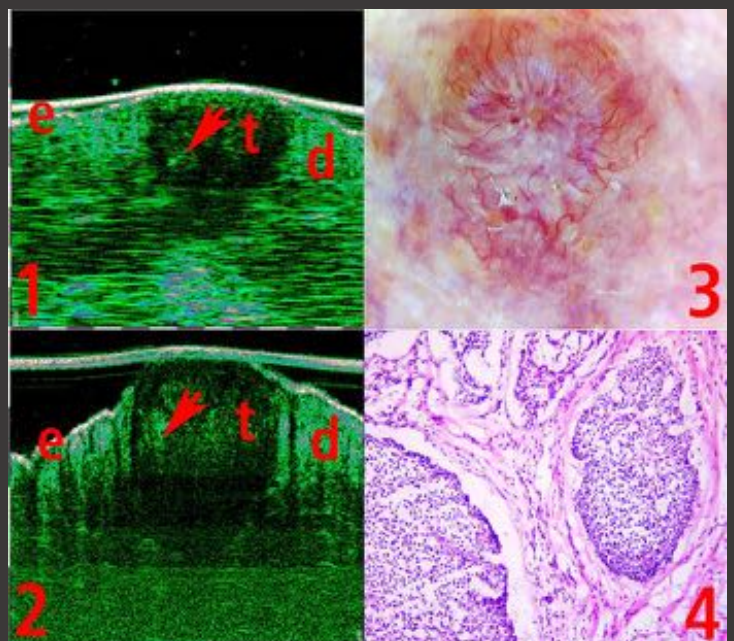


Figure 2. Nodular BCC. B-mode 30 (1) and 75 MHz (2) scans, videodermoscopy (3), and histology (4), e-epidermis, d- dermis, t - tumor

Connected Beauty- Digitalization Devices for Claim Substantiation

C Bonnaud-Rosaye¹, I Bonnet¹, W Chan², V Andre¹

1-BASF Beauty Care Solutions France, 32, rue Saint Jean de Dieu, Lyon, France
2-BASF Corporation, 540 White Plains Road, Tarrytown, NY 10591-9005, United States
catherine.bonnaud-rosaye@basf.com

KEY WORDS: clinical protocol, hydration, connected device

Consumer trends and behaviors are changing rapidly with advanced technology. Nowadays, consumers want to know how technology can provide them a better personal experience and make them feel connected. Today's personal devices can empower the connected consumer to self-diagnose beauty issues and respond accordingly to imperfections. Moreover, such devices provide scientists tools to quantify consumers' skin conditions at home usage situation.

We have designed a clinical/consumer study with a specific connected sensor to validate the consumer home use experience and data collection. Connected to the smartphone, the personalized device measures consumers own skin moisturization level at any time. The skin moisture degree is evaluated by measuring the impedance of a high frequency current. We conducted the double blinded placebo controlled clinical study on 23 female volunteers self-declaring to have dry skin. Each volunteer applied a placebo formula and a formula containing a bioactive on each hemi-face twice daily for 15 days. Real-time moisturization was measured by the volunteers using the personalized device each day during the treatment time and 7 days after the treatment.

This study demonstrated that we can efficiently use a personalized device to measure the moisturization effectiveness of a bioactive versus a placebo, particularly at different time in the day, such as at the wake-up time which is not easily measurable in an institute. Furthermore, the measures were easily and directly done by the consumer at home and in general, the consumers loved to use such connected device. Measures showed that compared to placebo, the bioactive provided a better hydration in the morning, throughout the day and even after the regression period.

This is important to find new way to measure the effectiveness of a bioactive in real conditions. To be closer to skin care habits of consumers at home better reflects the final efficacy of cosmetic products.

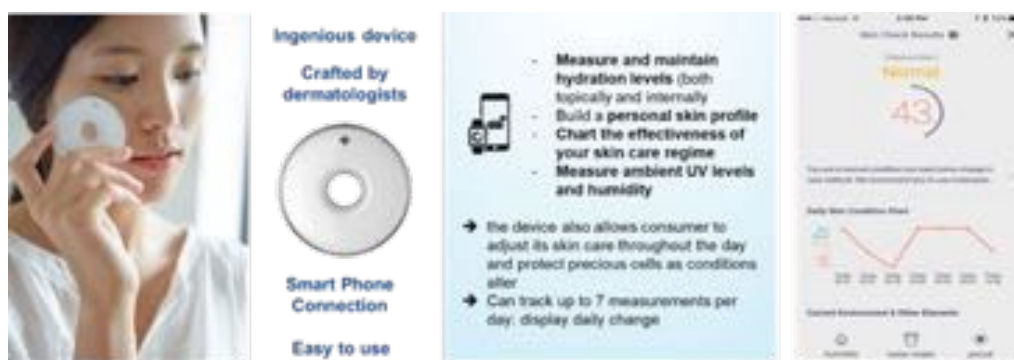


Fig 1:Skin hydration device characteristics

Connected Beauty- Digitalization Devices for Claim Substantiation

C Bonnaud-Rosaye¹, I Bonnet¹, W Chan², A Courtois¹

1-BASF Beauty Care Solutions France, 32, rue Saint Jean de Dieu, Lyon, France

2-BASF Corporation, 540 White Plains Road, Tarrytown, NY 10591-9005, United States

catherine.bonnaud-rosaye@basf.com

Introduction

Consumer trends and behaviors are changing rapidly with advanced technology. Nowadays, consumers want to know how technology can provide them a better personal experience and make them feel connected. Today's personal devices can empower the connected consumer to self-diagnose beauty issues and respond accordingly to imperfections. Moreover, such devices provide scientists tools to quantify consumers' skin conditions at home usage situation.

Objective

We designed a clinical/consumer study with a specific connected sensor to validate the consumer home use experience and data collection. Connected to the smartphone, the personalized device measures consumers own skin moisturization level at any time. The skin moisture degree is evaluated by measuring the impedance of a high frequency current.

Clinical test protocol

Volunteer panel

- 23 females
- 18-65 years old
- Self-declared dry skin

Tested products

- Placebo
- + 3% **Molecular patch**

Application

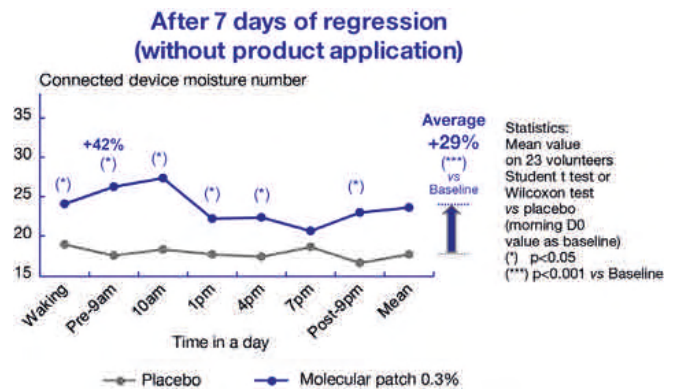
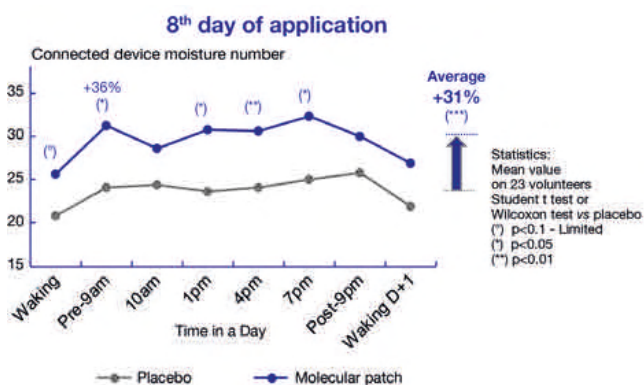
- Randomized, split face, twice daily for 15 days
- Regression for 7 days

Evaluation

- Day -1, 0, 7, 14 & 21:**
Seven (7) Connected Device measurements @ wake up, (after product application); 10am, 1pm, 4pm, 7pm and before bedtime
- All other days:**
Two (2) Connected Device measurements @ wake up and before bedtime



Results



- The skin was more moisturized in the morning with the bioactive product application than with the Placebo.
- The skin was maintained more moisturized throughout the day than with the Placebo.
- Such moisturization efficacy even lasts into the regression period when volunteers stopped using the products. Meanwhile, consumers felt the efficacy of the bioactive and the impact of real-time moisturization measurement on their daily skin care habits.

Conclusion

This study demonstrated that we can efficiently use a **personalized device to measure the moisturization effectiveness** of a bioactive versus a placebo, particularly **at different time in the day**, such as at the **wake-up time** which is not easily measurable in an institute. Furthermore, the measures were easily and directly done by the consumer at home and in general, the consumers loved to use such connected device. Measures showed that compared to placebo, the bioactive provided a better hydration in the morning, throughout the day and even after the regression period.

Assessment of a new transformative texture massage product in a pediatric population: effect on child, parent and child-parent interaction

Gaëtan Boyer¹, Clarence de Belilovsky¹, Pedro Pinto², Gaëlle Bellemère¹, Caroline Baudouin¹

1 Laboratoires Expanscience, Innovation R&D Direction, rue des Quatre Filles, 28233 EPERNON, FRANCE

2 PhDTrials, Av. Maria Helena Vieira da Silva, LISBOA, PORTUGAL

gboyer@expanscience.com

KEY WORDS: massage, emotion, well-being

Massage is used for several centuries with well-known therapeutic benefits. Positive effects of massage on pediatric population are well documented for example on sleep disturbances, parent-child interaction and parental stress¹. The aim of this work was to evaluate the effects of massage in a pediatric population using a new transformative texture product: study on the child, the parent and the parent-child interactions.

We conducted a mono-centric open-label study under dermatological and pediatric controls. 75 subjects were recruited aged from 7 days to 24 months. Massage has been performed daily by parents during 21 days at home after toilet and before sleep with a new transformative texture “gel to oil” massage balm. No instructions for the massage method were given. Tolerance evaluation was performed. Assessments of the effects of the massage just after the first application (performed on the study site), after 7 days (telephone questionnaire) and after 21 days have been performed using clinical scoring (redness, dryness, roughness and suppleness) and questionnaires related to the efficacy and cosmetic qualities of the product, the child well-being and sleep, the parent-child interaction and the mood and stress of the parent. Video recording of the parent face has been performed during the first massage and percentages of time of Joy and Disgust emotions detected using an artificial intelligence algorithm based on deep learning have been calculated.

Tolerance of the massage product was very good. Improvement of redness, dryness roughness and suppleness were observed immediately after the first application and after 21 days. After 21 days, parents perceived effects on moisturizing and nourishing of the child skin. The transformative texture was well appreciated for the massage and considered as a sensorial texture. Effect of the massage with the product on the child well-being has been positively perceived immediately and after 21 days. Improvement of the time for getting asleep has been observed. Parents perceived an improvement of the interaction, the complicity and the emotional bonds with their child. Effects on parent’s mood and stress were also observed. During the first massage, Joy emotion was identified during $35.3\pm 21.6\%$ of the massage time and Disgust emotion during only $4.8\pm 5.4\%$.

This study demonstrated that a “real-life” massage without any specific instructions has positive effects on the child well-being, the parent mind and the parent-child interaction. The transformative texture of the product was well perceived for the massage and the product improved child skin. Emotions assessment method used gave convincing results for a massage application.

¹ T. Field. Pediatric Massage Therapy Research: A Narrative Review. Children 2019, 6, 78

Assessment of a new transformative texture massage product in a pediatric population: effect on child, parent and child-parent interaction

Gaëtan Boyer¹, Clarence de Belilovsky¹, Pedro Pinto², Gaëlle Bellemère¹, Caroline Baudouin¹

1- Laboratoires Expanscience, Innovation R&D Direction, rue des Quatre Filles, 28233 Epemon, France
2- PhDTrials, Av. Maria Helena Vieira da Silva, Lisboa, Portugal
*gboyer@expanscience.com

Introduction

Massage is used for several centuries with well-known therapeutic benefits and other positive impacts as relaxing effect, social interaction and well-being improvement¹. Positive effects of massage on pediatric population are well documented for example on sleep disturbances, parent-child interaction and parental stress². The aim of this work was to evaluate the effects of massage in a pediatric population using a new transformative texture product: study on the child, the parent and the parent-child interactions.

Materials and Methods

We conducted a mono-centric open-label study under dermatological and pediatric controls. 75 subjects were recruited aged from 7 days to 24 months. Massage has been performed daily by parents during 21 days at home after toilet and before sleep with a new transformative texture "gel to oil" massage balm. No instructions for the massage method were given. Tolerance evaluation was performed. Assessments of the effects of the massage just after the first application (performed on the study site), after 7 days (telephone questionnaire) and after 21 days have been performed.

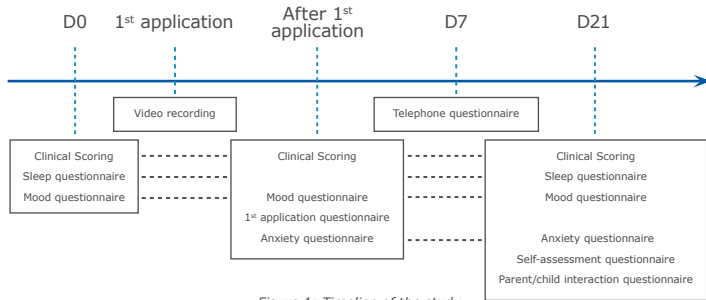


Figure 1: Timeline of the study

Assessments included clinical scorings (redness, dryness, roughness and suppleness) and questionnaires related to the efficacy and cosmetic qualities of the product, the child well-being and sleep, the parent-child interaction and the mood and stress of the parent. Different scales have been used:

- 5 points Likert scale (Totally agree – Agree – Neither agree or disagree – Disagree – Totally disagree) interpreted by comparison of the percentage of positive answers (sum of Totally agree and Agree related to the total number of answers) to the minimum percentage calculated to have a significant difference with a "random" percentage of 50%.
- 9 points scale from 0 (None/Disagree) to 9 (Important/Agree). Results obtained with this scale are expressed as mean \pm standard deviation and processed by comparison of answer groups at each time using a statistical test. Normality of data is tested using Shapiro-Wilk test. Paired t-test (normal data) or Wilcoxon signed rank test (non-normal data) is then used with a significance level $\alpha < 0.05$.
- Quantitative scale. Some questions involve a quantitative answer (for example: sleep duration). Results obtained with this scale are expressed as mean \pm standard deviation and processed by comparison of answer groups at each time using a statistical test. Normality of data is tested using Shapiro-Wilk test. Paired t-test (normal data) or Wilcoxon signed rank test (non-normal data) is then used with a significance level $\alpha < 0.05$.

Statistical analysis was performed using the R software version 4.0.3³.

Video recording of the parent face has been performed during the first massage. Set up is illustrated figure 2. Face tracking and facial landmarks estimation was performed to evaluate the emotions of the parent by an artificial intelligence algorithm based on deep learning⁴. We considered the percentages of time of Joy and Disgust emotions detected during the massage as valence indicators.



Figure 2: Set up for recording the parent face during the first application

Results

Tolerance of the massage product was very good. Clinical scorings demonstrated an improvement of redness, dryness, roughness and suppleness immediately after the first application and after 21 days (table 1).

	% of variation after 1 st application compared to D0	% of variation after 21 days compared to D0
Redness	-32.1%*	-67.9%*
Dryness	-69.7%*	-93.9%*
Roughness	-64.1%*	-92.4%*
Suppleness	1.60%*	10.5%*

Table 1: Clinical scores variations after 1st and 21 days of application * : $p < 0.05$

After 21 days, parents perceived effects on moisturizing (94.7%) and nourishing (98.7%) of the child skin. The transformative texture was well appreciated for the massage (94.7%) and considered as a sensorial texture (86.7%).

Effect of the massage with the product on the child well-being has been positively perceived immediately (93.3%) and after 21 days (82.3%). Improvement of the time for getting asleep has been observed (-22.9%).

Parents perceived an improvement of the interaction (98.7%), the complicity (86.7%) and the emotional bonds (80.0%) with their child. The massage with the product was considered as a tenderness moment with their child (97.3%) and a source of shared well-being (93.3%).

Effects on parent's mood and stress were also observed. Immediately and after 21 days of application, parents feel less tired and also more calm (table 2).

After this 1 st / 21 days of application, would you say that you feel:	% of variation after 1 st application compared to D0	% of variation after 21 days
Tired	-23.0%*	-30.0%*
Calm	8.2%*	8.0% ^o

Table 2: Mood variations of parents after 1st and 21 days of application * : $p < 0.05$ / ^o: $p < 0.1$

During the first massage, mean massage time was 5.52 ± 2.35 min. During this time, the exploitable time for emotion assessment (face of the parent correctly detected) was 2.78 ± 1.5 min ($50.5 \pm 16.5\%$ of the total massage time).

After image processing by the artificial intelligence algorithm, Joy emotion was identified during $35.3 \pm 21.6\%$ of the exploitable time and Disgust emotion during only $4.8 \pm 5.4\%$.

Individual percentages of Joy and Disgust emotions are illustrated figure 3. For all subjects, time of Joy emotion was always higher than time of Disgust emotion.

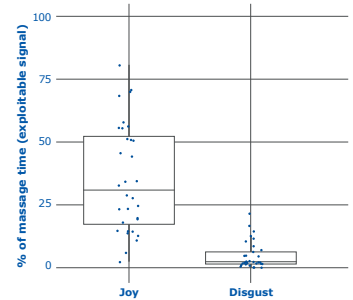


Figure 3: Emotions detected during the first massage

Conclusion

This study demonstrated that a "real-life" massage without any specific instructions has positive effects on the child well-being, the parent mind and the parent-child interaction. The transformative texture of the product was well perceived for the massage and the product improved child skin. Emotions assessment method used gave convincing results for a massage application.

References

1. S. Iorio et al. Healing bodies: the ancient origins of massages and Roman practices. *Medicina Historica* 2018; Vol. 2, N. 2: 58-62.
2. T. Field. *Pediatric Massage Therapy Research: A Narrative Review*. Children 2019, 6, 78.
3. R Core Team (2020). R: A language and environment for statistical computing. R Foundation for Statistical Computing, Vienna, Austria. URL <https://www.R-project.org/>
4. <https://blog.affectiva.com/emotion-ai-101-all-about-emotion-detection-and-affectivas-emotion-metrics>

Mapping of the biophysical properties of pregnant women abdomen skin: a pilot study

G. Boyer¹, G. Bellemère¹, C. de Belilovsky¹, C. Baudouin¹

1 Laboratoires Expanscience, rue des Quatre Filles, 28233 EPERNON, FRANCE
gboyer@expanscience.com

KEY WORDS: pregnancy, mapping, skin properties

During pregnancy mechanical stretching of abdomen skin due to baby growth is very important and could lead to skin breakage (also known as striae distensae or stretch mark). Recent work demonstrated that biomechanical properties of healthy abdomen skin change drastically during pregnancy and that these properties remain altered 4 months after delivery¹. It remains unclear if these observed modifications are homogeneous on the abdomen area or if a specific area is more affected. The aim of this pilot study is to perform a mapping of abdomen skin properties of a woman at 8 months of pregnancy using various non-invasive techniques in order to evaluate if gradient or specific pattern of these properties exist.

25 measurement points have been defined on one half of the abdomen. Assessments performed included hydration (Corneometer CM825), Transepidermal Water Loss (TEWL, Vapometer SWL-5), mechanical properties (Cutometer SEM 575) and thickness and echogenicity of the skin (Dermascan 20 MHz). Mapping of each property has been performed by interpolation algorithm using Octave software.

Results obtained show that skin biophysical parameters were not homogeneous on abdomen as illustrated by figure 1 with skin thickness. Moreover, specific locations exhibited particular properties. High variations of the measurements between the 25 points were observed: 104% for hydration, 40% for TEWL, 134% for echogenicity, 47% for thickness and 30% to 160% for biomechanical properties. Study of the relationships between all measured parameters demonstrated that some skin properties are significantly correlated while others are independent.

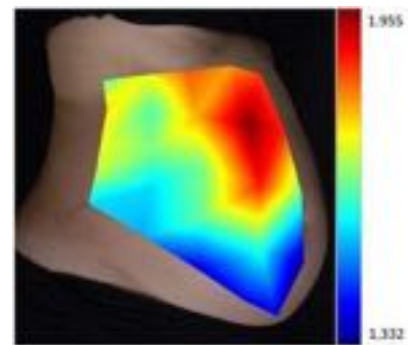


Figure 1: skin thickness mapping.

This pilot study demonstrated that the skin properties of women at 8 months of pregnancy are not homogeneous on the abdomen, tending to show that specific area could be more affected and therefore more subjected to stretch mark formation. A future study will compare women at different stages of pregnancy to quantify the variations of skin properties on the abdomen along pregnancy time.

¹ G. Boyer, N. Lachmann, G. Bellemère, C. De Belilovsky and C. Baudouin. Effects of pregnancy on skin properties: A biomechanical approach. *Skin Res Technol.* 2018 Nov;24(4):551-556.

Mapping of the biophysical properties of pregnant women abdomen skin: a pilot study

G. Boyer^{1*}, G. Bellemère¹, C. de Belilovsky¹, C. Baudouin¹

1- Laboratoires Expanscience, Centre IRD, Epernon, France * gboyer@expanscience.com

Introduction

During pregnancy mechanical stretching of abdomen skin due to baby growth is very important and could lead to stretch mark (also known as striae distensae). Recent work demonstrated that biomechanical properties of healthy abdomen skin change drastically during pregnancy and that these properties remain altered 4 months after delivery¹. It remains unclear if these observed modifications are homogeneous on the abdomen area or if a specific area is more affected.

Hypothesis

The aim of this pilot study is to evaluate if gradient or specific pattern of abdomen skin properties exist during pregnancy.

Methods

A pilot study has been conducted. A healthy 28 years old woman at 8 months of pregnancy has been recruited. 25 measurement points have been defined on one half of the abdomen as illustrated figure 1. Non-invasive assessments performed were:

- Hydration using Corneometer CM825 (Courage + Khazaka, Germany),
- Barrier function via Transepidermal Water Loss (TEWL) using Vapometer SWL-5 (Delfin Technologies, Finland),
- Mechanical properties using Cutometer® SEM 575 (Courage + Khazaka, Germany),
- Thickness and echogenicity using Dermascan 20 MHz (Cortex Technology, Denmark).

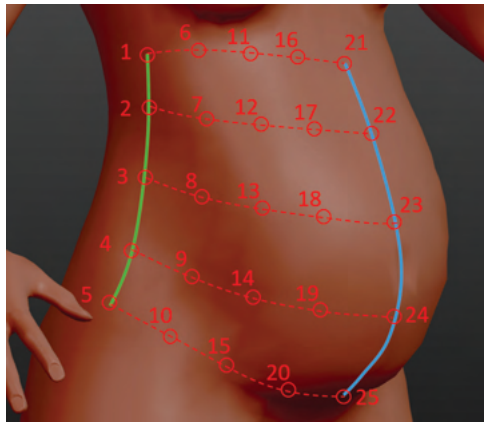


Figure 1: Positioning of the 25 measurement points.

Mapping of each property has been performed by interpolation algorithm using Octave software². Evaluation of correlation between measured parameters has been performed using R³.

Results

Results obtained show that skin biophysical parameters were not homogeneous on abdomen.

Figure 2 to figure 6 illustrate respectively hydration, TEWL, echogenicity, thickness and biomechanical properties interpolated from the 25 measurement points. Specific locations exhibited particular properties. High variations of the measurements between the 25 points were observed: 104% for hydration, 40% for TEWL, 134% for echogenicity, 47% for thickness and 30% to 160% for biomechanical properties.

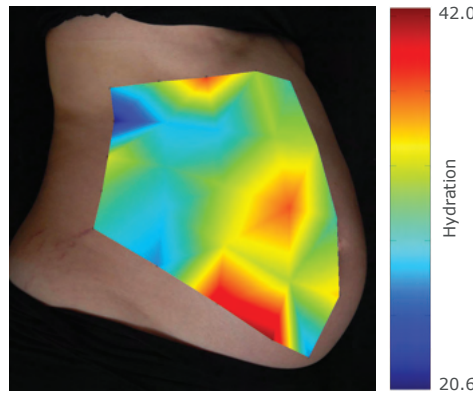


Figure 2: Interpolated hydration measured using Corneometer CM825 on 8 months pregnant woman abdomen.

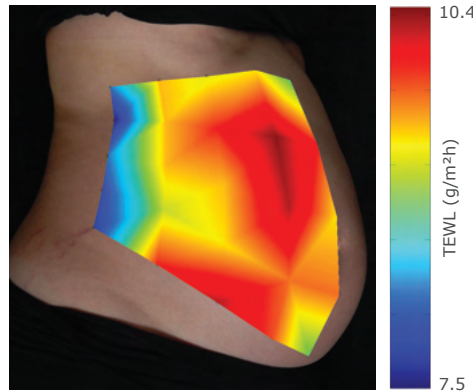


Figure 3: Interpolated TEWL measured using Vapometer SWL-5 on 8 months pregnant woman abdomen.

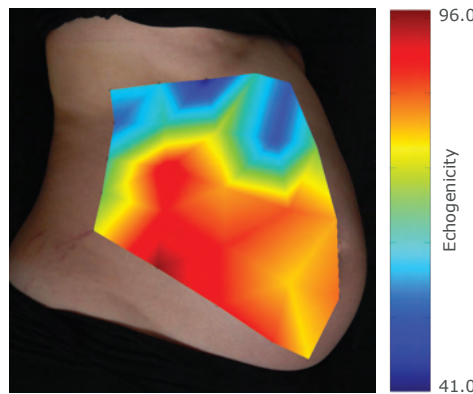


Figure 4: Interpolated echogenicity measured using echography on 8 months pregnant woman abdomen.

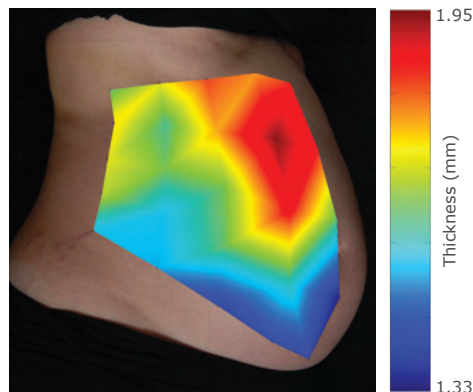


Figure 5: Interpolated thickness measured using echography on 8 months pregnant woman abdomen.

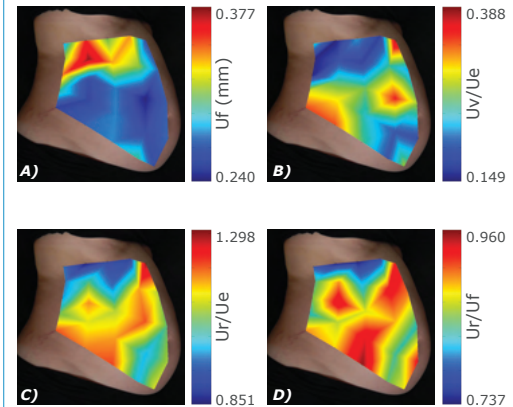


Figure 6: Interpolated biomechanical properties measured on 8 months pregnant woman abdomen
A) Firmness: Uf (mm) B) Ratio of viscoelastic to elastic distension: Uv/Ue
C) Net elasticity: Ur/Ue and D) Elastic recovery: Ur/Uf

Relationships between all measured parameters are illustrated in the correlation matrix figure 7. Positive correlations are in blue and negative correlations in red. Pearson correlation coefficient is indicated in each circle. Non significant coefficients are strikethroughs. Results show that some skin properties are significantly correlated while others are independent.

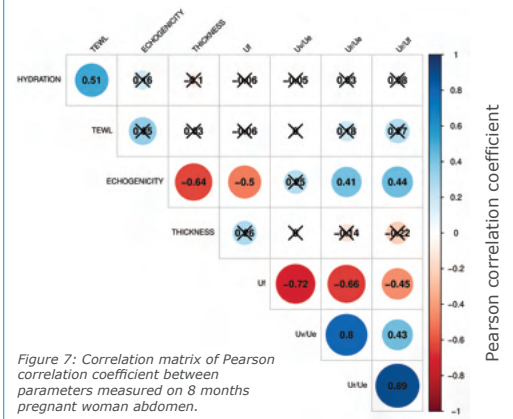


Figure 7: Correlation matrix of Pearson correlation coefficient between parameters measured on 8 months pregnant woman abdomen.

Conclusion

This pilot study demonstrated that the skin properties of women at 8 months of pregnancy are not homogeneous on the abdomen, tending to show that specific area could be more affected and therefore more subjected to stretch mark formation. A future study will compare women at different stages of pregnancy to quantify the variations of skin properties on the abdomen along pregnancy time.

References

- 1 G. Boyer, N. Lachmann, G. Bellemère, C. De Belilovsky and C. Baudouin. Effects of pregnancy on skin properties: A biomechanical approach. Skin Res Technol. 2018 Nov; 24(4):551-556.
- 2 J.W. Eaton, D. Bateman, S. Hauberg, R. Wehbring (2019). GNU Octave version 5.1.0 manual: a high-level interactive language for numerical computations. URL <https://www.gnu.org/software/octave/doc/v5.1.0/>
- 3 R Core Team (2020). R: A language and environment for statistical computing. R Foundation for Statistical Computing, Vienna, Austria. <https://www.R-project.org/>



A PIONEER AND EXEMPLARY CSR STRATEGY ADOPTED IN 2004

EXPANSCIENCE®
LABORATOIRES

Mustela®

Characterization of sensitive skin in a pediatric population

G. Boyer¹, G. Bellemère¹, C. de Belilovsky¹, C. Baudouin¹

1 Laboratoires Expanscience, rue des Quatre Filles, 28233 EPERNON, FRANCE
gboyer@expanscience.com

KEY WORDS: sensitive skin, children, skin properties

Sensitive skin affects about 50% of adult population¹. In children, prevalence of sensitive skin is over 30% under 6 years old². The differences between a “normal” immature skin of infant and a “specific” sensitive skin remained unclear. In this study, we aimed to investigate the sensitive skin syndrome in a pediatric population.

We developed a parent-reported questionnaire to identify sensitive skin in infants and children. We subjected parents to this questionnaire in order to recruit infant with sensitive and non-sensitive skin. This questionnaire was also submitted to adult with sensitive and non-sensitive skin to further validate questionnaire relevance. In order to characterize sensitive skin properties in infants and adults, we performed clinical, instrumental and non-invasive evaluations. We recruited 77 children (including 33 with sensitive skin) of different age groups (3-6 months, 6-12 months, 24-48 months) and 20 adults (aged 18–20 years, including 10 with sensitive skin). All measurements were performed on the face. Skin sensitivity was identified by parents or adult subjects according to questionnaire responses. Dryness of the skin was evaluated clinically on the face using the SRRC score³. Hydration and Transepidermal water Loss (TEWL) have been instrumentally measured using Corneometer and Aquaflex devices. Key inflammatory biomarkers have been quantified from noninvasive skin surface samples (cytokines and polyunsaturated fatty acids (PUFA)) as well as Naturals Moisturizing Factors (NMFs) and ceramides.

Results show that, in sensitive skin children, skin is clinically dryer and had more scaling, roughness, and redness than the non-sensitive skin subjects. Hydration measured instrumentally confirmed the skin dryness in sensitive skin subjects in children but not in adults. TEWL as well as levels of ceramides and NMFs were similar in both sensitive and non-sensitive groups. Interestingly, a specific profile of cytokines and PUFA has been observed in sensitive skin subjects. All these findings were also observed in adults, further demonstrating the relevance of the questionnaire developed to recruit infants with sensitive skin in our study.

To our knowledge, this is the first study showing that clinical sensitive skin exists in a pediatric population. Results show that this syndrome can be observed early, within the first months of life. Clinical, instrumental and biological approaches have been successfully used to identify the key specific characteristics of sensitive skin in children.

¹ Misery L. et al. . Sensitive skin in Europe. *J Eur Acad Dermatol Venereol* 2009; 23: 376–381

² C. de Belilovsky et al. . PRO investigation: PRevalence and Origins of Hypersensitive skin among more than 8 000 children. *Am Acad of Dermatol*, 68th Annual Meeting, March 5–9, 2010, Miami, Florida

³ Serup J. EEMCO guidance for the assessment of dry skin (xerosis) and ichthyosis: clinical scoring systems. *Skin Research and Technology*. 1(3), 109–114 (1995)

Investigation of Pediatric Sensitive Skin: Characterization by *in vivo* approach and development of an *in vitro* model

G. Boyer¹, S. Brédif¹, G. Bellemère¹, C. De Belilovsky¹, C. Baudouin¹

¹ Innovation R&D Direction, Laboratoires Expanscience, Epernon, France

Introduction & Objectives

Skin sensitivity is a self-reported syndrome which affects about 50% of adult population [1]. Recently, a group of expert defined sensitive skin as "A syndrome defined by the occurrence of unpleasant sensations (stinging, burning, pain, pruritus, and tingling sensations) in response to stimuli that normally should not provoke such sensations. These unpleasant sensations cannot be explained by lesions attributable to any skin disease. The skin can appear normal or be accompanied by erythema. Sensitive skin can affect all body locations, especially the face" [2]. There are therefore two kinds of signs that defined sensitive skin, objective signs characterized by erythema and subjective

signs characterized by sensations like stinging, burning or tingling. Concerning children, previous work indicates a prevalence of sensitive skin over 30% under 6 years old [3]. The differences between a "normal" immature skin of infant and a "specific" sensitive skin remain unclear.

A clinical study was performed to investigate the sensitive skin syndrome in a pediatric population. Based on clinical findings, an *in vitro* skin model mimicking the features of pediatric sensitive skin was developed.

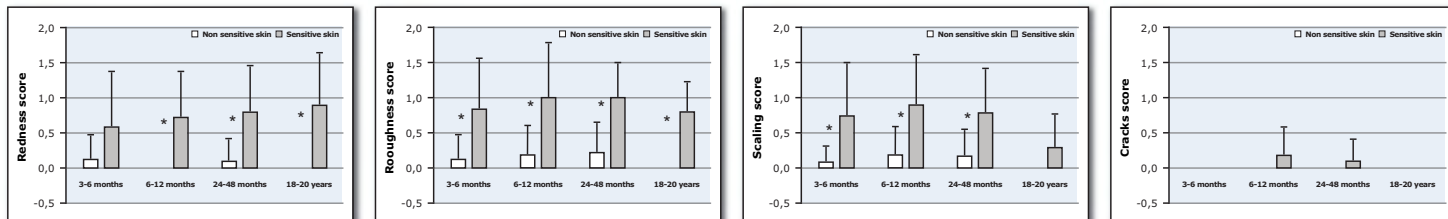
Clinical study

Two panels (non sensitive and sensitive skin) each composed of three groups of children (3-6 months, 6-12 months, 24-48 months) have been recruited using a specifically developed questionnaire. Two control groups of adults (18-20 years) have also been enrolled. Each group was composed of 10 subjects. Measurements were performed on the face (cheek). This area is considered to be the most exposed to external stimuli and the most relevant to observe differences between non sensitive and sensitive skin. Dryness of the skin has been evaluated clinically using the SRRC score. This score includes four characteristics: Scaling, Roughness, Redness and Cracks with 4 grades for each characteristic.

Hydration measurement has been performed using Corneometer. Transepidermal Water Loss has been measured using Tewameter. Biological assays using swab technique have also been performed on the face in order to analyze Natural Moisturizing Factors (NMFs) by means of LC/UV, Ceramides by means of GC/MS, Cytokines (IL1 α and IL8) by means of ELISA and Polyunsaturated fatty acids (PUFA) C18:2 and C20:5 by means of GC/MS.

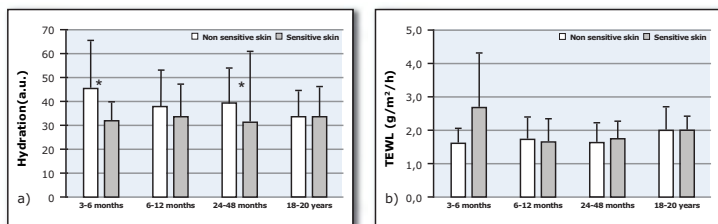
Clinical results show that the sensitive skin is clinically drier, more squamous, rougher and more erythematous than non sensitive skin in children for each age group as well in adults (figure 1).

Figure 1: SRRC score parameters for non sensitive and sensitive skin. *: $p < 0.05$.



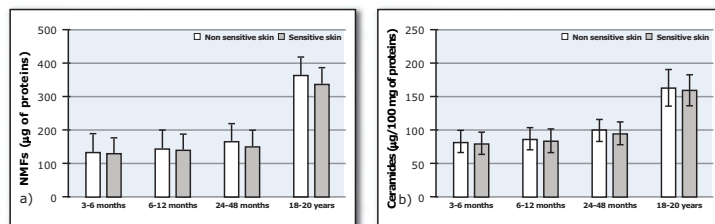
Measurement of *stratum corneum* hydration further showed that sensitive skin was drier than non sensitive skin (figure 2). No differences in TEWL have been found between sensitive and non sensitive skin. All the findings observed on children groups were confirmed on the adult panel demonstrating the relevance of the questionnaire developed for inclusion of children with sensitive skin.

Figure 2: a) Hydration and b) TEWL measured on non sensitive and sensitive skin. *: $p < 0.1$.



The amount of NMF and Ceramides have been quantified in subjects with non sensitive and sensitive skin (figure 3). No statistical differences in the amounts of ceramides and NMFs have been observed between non sensitive and sensitive skin. Interestingly, a higher quantity of both NMF and Ceramides in adult group than in child group has been measured, which may reflect the immaturity of infant skin.

Figure 3: Quantification of a) NMFs and b) ceramides in the skin of sensitive and non sensitive subjects.



A particular profile of cytokine expression in the sensitive skin has been observed (figure 4) showing a higher inflammatory background. Interestingly, polyunsaturated fatty acids confirmed this observations (figure 5). Pro-inflammatory marker C18:2 is higher in sensitive skin whereas anti-inflammatory marker C20:5 is lower.

Figure 4: Quantification of a) IL1 α and b) IL8 in the skin of sensitive and non sensitive subjects. *: $p < 0.05$.

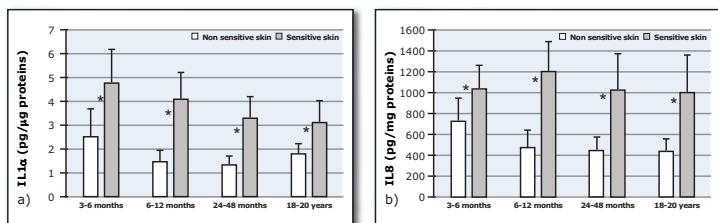
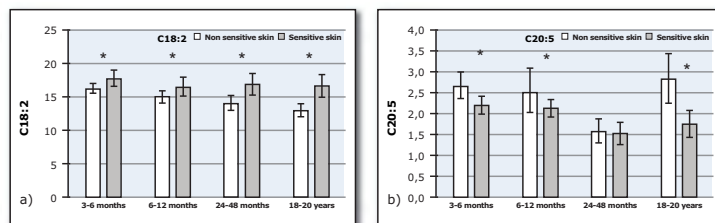


Figure 5: Quantification of a) C18:2 and b) C20:5 in the skin of sensitive and non sensitive subjects. *: $p < 0.05$.



In vitro model

Reconstructed epidermis was topically treated by lactic acid. The production of inflammatory cytokines and mediators (IL1-alpha, IL1-RA, IL8, VEGF and PGE2) was measured in the supernatants and in the cell lysates by ELISA assay. A screening of polyunsaturated fatty acids (PUFA) expressed by the epidermis was realized by GC/MS analysis.

Lactic acid induced an increased production of inflammatory cytokines IL1-alpha, IL1-RA, IL8, PGE2 and VEGF, as well as the IL1RA/IL1alpha ratio, a sensitive marker of cutaneous inflammation (Tables 1 and 2). The screening of PUFA revealed an induction of pro-inflammatory fatty acids belonging to arachidonic acid pathway (Table 3).

The *in vitro* observations based on this lactic acid-treated epidermal model thus mimicked the features of pediatric sensitive skin observed in the clinical study.

Table 1: Intracellular levels of inflammatory mediators

	Control	Lactic acid 0.6%	Evolution vs control
IL8 (pg/mg of proteins)	10.6	52.1	+390%
IL1-alpha (pg/mg of proteins)	88	794	+806%
IL1-RA (pg/mg of proteins)	2328	31243	+1242%
Ratio IL1-RA/IL1-alpha	26.6	39.3	+48%

Table 2: Released production of inflammatory mediators

	Control	Lactic acid 0.6%	Evolution vs control
IL1-alpha (pg/ml)	7 ± 1	23 ± 7	+221% ns
IL8 (pg/ml)	65 ± 4	120 ± 18	+84% $p < 0.05$
PGE2 (pg/ml)	48 ± 4	149 ± 36	+207% $p < 0.05$
VEGF (pg/ml)	433 ± 17	1109 ± 45	+156% $p < 0.001$

Table 3: PUFA level (quantity normalized by C16:0)

	Control	Lactic acid 0.6%	Evolution vs control
C18 :2 LA	0.181	0.216	+19%
C20 :4 AA	0.035	0.050	+42%

Conclusion

To our knowledge, this is the first study characterizing sensitive skin in a pediatric population. Results show that this syndrome starts from the first months of life. Clinical, instrumental and biological approaches have been successfully used to identify the key differences between a non sensitive and a specific sensitive skin in a pediatric population. Based on these findings, we were able to develop an *in vitro* model reproducing the main features of pediatric sensitive skin. This model may be of peculiar interest to screen interesting active ingredients or topical products designed for the management of pediatric sensitive skin.

REFERENCES:

- Misery et al. Sensitive skin in Europe. *J Eur Acad Dermatol Venereol* 2009; 23: 376-381
- Misery et al. Definition of sensitive skin: an expert Position paper from the special interest group on sensitive skin of the international forum for the study of itch. *Acta Derm Venereol.* 2017 Jan 4; 97 (1): 4-6
- C. de Belilovsky et al. PRO investigation: Prevalence and Origins of Hypersensitive skin among more than 8 000 children. *Am Acad of Dermatol, 68th Annual Meeting, March 5-9, 2010, Miami, Florida*

Multimodal CARS tomography of human skin *in vivo*

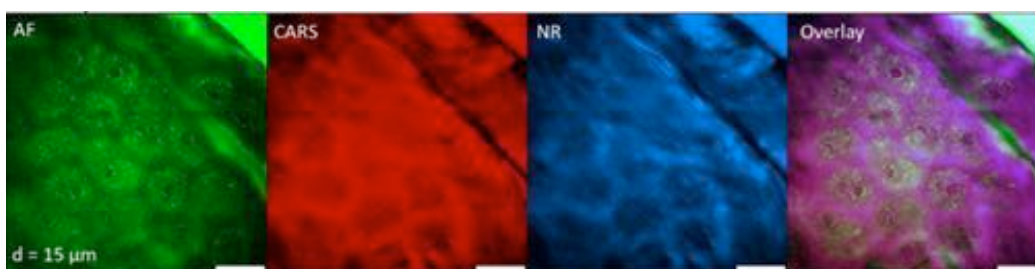
H. G. Breunig, K. König

JenLab GmbH, Johann-Hittorf-Str. 8, 12489 Berlin, Germany

breunig@jenlab.de, www.jenlab.de

KEY WORDS: CARS microscopy, label-free imaging, skin imaging, multiphoton imaging

Laser microscopy provides a non-invasive view of the surface and inside of the skin. In particular by using near infrared laser radiation to excite signals from endogenous skin molecules and structures, detailed, high-contrast, and substance-specific *in-vivo* imaging is possible even without any labelling. With simultaneous two-wavelength excitation, even non-fluorescent molecules can be detected because they specifically scatter the incoming light, a process which is associated with the generation of new wavelengths. This so-called Raman scattering is caused by the light interaction with the molecular bonds which enables in particular the detection of lipids and water which are invisible to solely fluorescence imaging. The extension of optical imaging by including Raman techniques, for label-free detection of non-fluorescent molecules, has been an active area of research in the last decades. However, in contrast to multiphoton tomography, which has been utilized in many medical studies for *in vivo* as well as *ex vivo* imaging, the combination with Raman imaging and its variants, like coherent anti-Stokes Raman scattering (CARS)¹, has only recently found its way into clinical practice², although, a manifold of excitation setups and light sources has been described in the literature and the method has technically matured. However, costs and complexity are intrinsically higher than for sole fluorescence imaging which still limits a wide-spread use by non-imaging experts. We present multimodal skin imaging, including fluorescence, second harmonic generation and CARS imaging with a commercial skin imaging device and discuss possibilities and limitations.



Microscopic label-free autofluorescence and CARS imaging provides complementary information on the skin composition *in vivo*. Scale bar: 30 μm .

¹ M. Weinigel, et al., J. Med Imaging., 2(2015)016003.

² K. König, et al., J. Biomed. Opt. 25.1 (2020)014515.

Multimodal CARS Tomography of Human Skin *in vivo*

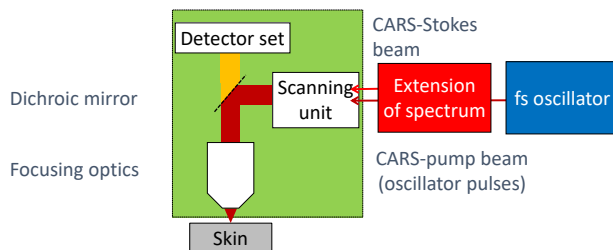


Hans Georg Breunig and Karsten König
 JenLab GmbH, Johann-Hittorf-Strasse 8, 12489 Berlin, Germany
 Biophotonics and Laser Technology, Saarland University, 66125 Saarbrücken, Germany
breunig@jenlab.de, www.jenlab.de

Abstract

By using near-infrared laser radiation to generate signals from endogenous skin molecules and structures, detailed, high-contrast, and substance-specific *in vivo* imaging is possible without any labelling. With simultaneous two-beam excitation, even non-fluorescent molecules can be detected because they specifically scatter the incoming light which generates new substance-characteristic signal wavelengths. This so-called Raman scattering is caused by the light interaction with the molecular bonds and enables in particular the detection of lipids and water which are both undetectable by fluorescence imaging. The extension of optical imaging by including Raman techniques, for label-free detection of non-fluorescent molecules, has been an active area of research in the last decades. However, in contrast to multiphoton tomography, which has been utilized in many medical studies for *in vivo* as well as *ex vivo* imaging, the combination with Raman imaging and its variants, like coherent anti-Stokes Raman scattering (CARS), has only recently found its way into clinical practice. The multimodal "optical biopsies" provide a novel view of healthy as well as disease-affected skin on a sub-cellular level with the potential for new future diagnosis procedures of skin conditions and the investigation of skin diseases based on multimodal CARS imaging.

Methods and setup



The multimodal CARS imaging is based on a laser-scanning setup. Excitation pulses are generated by a femtosecond oscillator and split in two parts. One part is spectrally extended with a photonic crystal fiber to provide the necessary wavelength for the CARS excitation. Both parts are then spatially and temporally overlapped on the sample. Several multimodal signals can be excited (see table below) which are detected in reflection and provide a depth-resolved microscopic view of the skin composition.

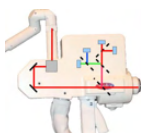
Type of signal	Excitation modality	What can be seen?
Fluorescence	Single beam	Endogenous fluorophores (keratin, NAD(P)H, melanin, collagen, elastin)
SHG (second harmonic generation)	Single beam	Collagen
CARS (coherent anti-Stokes Raman scattering)	Two beam	Lipids, Water

Imaging system



Multiphoton Tomograph MPTflex CARS

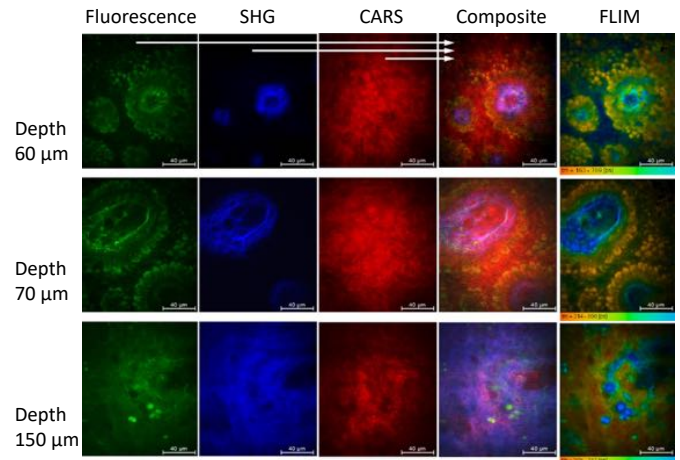
Parameters	
Excitation wavelengths	800 nm + 1040 nm
Optical resolutions	0.5 μ m lateral 1.5 μ m axial
Imaging time per frame	6 - 10 s
Max imaging depth	200 μ m



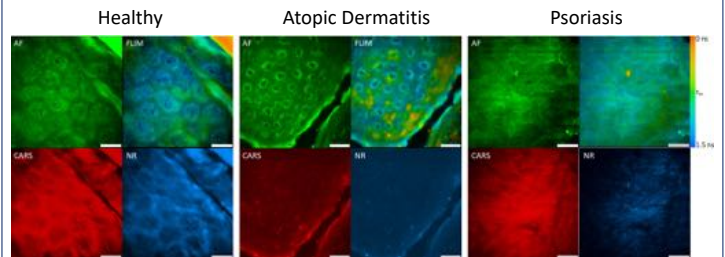
Scan head with four- Skin measurement procedure detector setup



Results



Multimodal CARS imaging of healthy human skin *in vivo*. The horizontal sections show fluorescence, SHG, CARS signals, and overlays of the three signals (composite). The FLIM images represent the color-coded fluorescence decay.



In-vivo multimodal optical biopsies of healthy skin and from patients suffering from atopic dermatitis or psoriasis. The lesion affected by atopic dermatitis exhibits enhanced fluorescence signals close to the nuclei. This could result from intercellular edema and perinuclear accumulation of the NAD(P)H-containing mitochondria. In the psoriasis-affected lesion, the thickening of the epidermal layer, i.e., in particular the enlarged stratum corneum prevented reaching the cellular layers at the recorded depth of 15 μ m; no cells are visible. The psoriasis-affected skin also exhibits strong CARS signals which indicate the hexagonal shape of cells the stratum corneum which is also visible in the healthy skin. Scale bar: 30 μ m. Imaging depth: 15 μ m

AF: auto fluorescence
 CARS, NR: Raman signals
 FLIM: color-coded fluorescence decay

Conclusion

- Multimodal CARS imaging offers label-free microscopic *in-vivo* imaging of human skin.
- The different imaging modalities simultaneously reveal the microscopic distributions of endogenous skin fluorophores (fluorescence), collagen (fluorescence and second harmonic generation) and lipids (CARS).
- Multimodal CARS imaging is suitable for the investigation of human skin morphology and the study of skin diseases with subcellular resolution.

References

- König, Breunig et al., "Translation of two-photon microscopy to the clinic: multimodal multiphoton CARS tomography of *in vivo* human skin", *J Biomed Opt* **25**(1), 014515 (2020).
- Guimarães, Batista et al., "Artificial intelligence in multiphoton tomography: Atopic dermatitis diagnosis", *Sci rep* **10**(1), 1-9 (2020).
- Weinigel, Breunig et al., "Clinical multimodal CARS imaging", in: K. König (ed.) *Multiphoton microscopy and fluorescence lifetime imaging*. De Gruyter (2018).
- Weinigel, Breunig et al., "Multipurpose nonlinear optical imaging system for *in vivo* and *ex vivo* multimodal histology", *J Med Imaging* **2**, 016003 (2015).
- Breunig, Weinigel et al., "Clinical coherent anti-Stokes Raman scattering and multiphoton tomography of human skin with a femtosecond laser and photonic crystal fiber", *Laser Phys Lett* **10**, 025604 (2013).
- König, Breunig et al., "Optical skin biopsies by clinical CARS and multiphoton fluorescence/SHG tomography", *Laser Phys Lett* **8**, 1-4 (2011).

Ex-vivo biomarker assessment of multifunctional moisturizing formulations

M. De Marco¹, B. Lu¹, E. Peltier², L. Peno-Mazzarino³

¹ Bayer HealthCare 33 rue de l'Industrie 74240 Gaillard, FR; ² Bayer Consumer Care AG Peter Merian Straße 84, Basel CH-4052; ³ Laboratoire BIO-EC, Chemin de Saulxier, 91160 Longjumeau, FR
Corresponding Author e-mail address and URL: marine.demarco@bayer.com

KEY WORDS: Moisturizer, Biomarkers, Ceramides

Introduction: Dry, xerotic skin is the most common dermatological disorder impacting up to around 50% of the world's population¹. Its development is complex and during the past decade there has been considerable scientific progress in understanding the dry skin condition at the molecular level. In the context of developing skin care products to address xerotic skin needs, it is fundamental to investigate the effects of the different actives on the stratum corneum skin barrier. The aim of this study was to evaluate the effects of a variety of combinations of actives: Vitamins (B5, B3, E), Lipids (including shea butter and argan oil at different concentrations), cf table 1, on a range of skin barrier related biomarkers.

Materials and Methods: Assessments were carried out ex-vivo using human living skin explants. The explants (average diameter of 12mm±1mm) came from an abdominoplasty from a 55-year-old Caucasian woman. Test products (2µl per explant) were applied on day 0, day 2, day 3 and day 6. After application the following biomarkers were evaluated: cell viability, Ceramide and Filaggrin, Involucrin, Loricrin, SPRR1a (Small Proline-Rich Proteins 1a) and Aquaporin-3, using an immunostaining assessment technique after 7 days.

Product	Base	Vitamins B5, B3, E	Lipids %
Base chassis	X		
Combination 1	X	X	
Combination 2	X		lowest
Combination 3	X		medium
Combination 4	X		highest
Combination 5	X	X	lowest
Combination 6	X	X	medium
Combination 7	X	X	highest

Table 1: Ingredient combinations tested.

These biomarkers are all important in the development of dry skin and were chosen due to their importance in defining the formation of the stratum corneum lipid barrier and natural moisturizing factor production, cornification of the corneocyte cell envelope and its mechanical resistance, the keratinocyte terminal differentiation process and skin hydration.

Results: At the end of the experiments the base chassis showed improvements vs control in Involucrin (+268%), Loricrin (+221%) and Aquaporin-3 (+63%), while adding vitamins (Combination 1) showed additional significant positive effects on ceramide production (+27%), and SPRR1a (+214%). Addition of vitamins and lipids (Combination 5) increased Ceramide (+59%) along with Involucrin (+243%), Loricrin (+458%) SPRR1a (+193%) and Aquaporin-3 (+94%). Addition of medium and high levels of lipids (Combinations 3,4,7) improved filaggrin (up to +17%).

Conclusion: Ex-vivo testing with skin explants is a valuable tool to provide mechanistic understanding of the biochemical effects of multifunctional topical skin formulations on barrier related biomarkers in relation to the treatment of xerotic skin.

¹ M.A. Farage, *Frontiers in Medicine*, 6(2019)98. <https://doi.org/10.3389/fmed.2019.00098>.

EX-VIVO BIOMARKER ASSESSMENT OF MULTIFUNCTIONAL MOISTURIZING FORMULATIONS

Marine DE MARCO¹, Bailu LU¹, Erwan PELTIER², Laurent PENO-MAZZARINO³,

¹Bayer HealthCare 33 rue de l'Industrie 74240 Gaillard, FR; ²Bayer Consumer Care AG Peter Merian Straße 84, Basel CH-4052; ³Laboratoire BIO-EC, Chemin de Saulxier, 91160 Longjumeau, FR.

INTRODUCTION

Dry, xerotic skin is the most common dermatological disorder impacting up to around 50% of the world's population. Its development is complex and during the past decade there has been considerable scientific progress in understanding the dry skin condition at the molecular level. In the context of developing skin care products to address its xerotic skin needs, it is fundamental to investigate the effects of the different actives on the stratum corneum (SC) skin barrier. The aim of this study was to evaluate the effect of a variety of combinations of actives: Vitamins (B5, B3, E), Lipids (including shea butter and argan oil at different concentrations), on a range of skin barrier related biomarkers.

MATERIALS AND METHODS

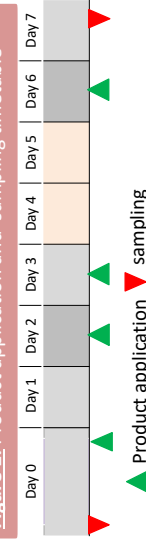
- Test products are a range of oil-in-water emulsions containing different concentrations of Vitamins (B5, B3, E) and Lipids (including shea butter and argan oil), Table 1.

Table 1: Test formulation comparison

Products	Code	Base	Vitamins (B3, B5, E)	Lipids %
Base chassis	E	X		
Combination 1	P1	X	X	
Combination 2	P2	X	X	Lowest
Combination 3	P3	X	X	Medium
Combination 4	P4	X	X	Highest
Combination 5	P5	X	X	Lowest
Combination 6	P6	X	X	Medium
Combination 7	P7	X	X	Highest

- Assessments were carried out *ex-vivo* using human living skin explants. The explants (average diameter of 12mm±1mm) came from an abdominoplasty from a 55-year-old Caucasian woman. Test products (2 mg/cm² per explant) were applied on day 0, day 2, day 3 and day 6. Product application and sampling timetable shown in Figure 1.

Figure 1: Product application and sampling timetable



- After sampling the following biomarkers were evaluated: cell viability, Ceramide and Filaggrin, Involucrin, Loricrin, SPRR1a (Small Proline-Rich proteins 1a) and Aquaporin-3, using an immunostaining assessment technique after 7 days.

DISCUSSION / CONCLUSIONS

- The biomarkers assessed in the study presented here are all important in the development and treatment of dry skin and are chosen due to their importance in defining the formation of the SC lipid barrier and natural moisturizing factor production, cornification of the corneocyte cell envelope and its mechanical resistance, the keratinocyte terminal differentiation process and skin hydration. While the base chassis itself provided improvements to a range of biomarkers, addition of vitamins and lipids also improved ceramide, involucrin, Loricrin, SPRR1a and Aquaporin-3 levels.
- *Ex-vivo* testing with skin explants is an important tool for the mechanistic understanding of the biochemical effects of topical skin formulations on barrier related biomarkers in relation to the treatment of xerotic skin, providing valuable insights to support clinical observations.

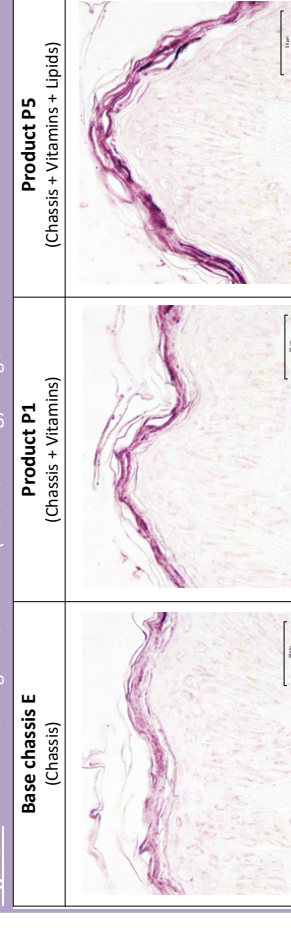
RESULTS

Table 2: Biomarker variations at day 7 (T7) compared with untreated control

Biomarkers	E	P1	P2	P3	P4	P5	P6	P7
Ceramides	-52%**	+27%**				+59%**		
Filaggrin	+2%^{NS}	+4%^{NS}	+10%^{NS}	+17%**	+17%**	+4%^{NS}	+6%^{NS}	+13%**
Involucrin	+268%**	+254%**				+243%**		
Loricrin	+221%**	-22%^{NS}				+458%**		
SPRR1 a	+6%^{NS}	+214%**				+193%**		
Aquaporin-3	+63%**	+19%^{NS}	+137%**	+107%**	-7%^{NS}	+94%**	+164%**	+26%^{NS}

NS: non significant *: $p < 0.05$ (95%) **: $p < 0.01$ (99%) Student t-test statistical analysis
Note: results from image analysis

Figure 2: Immunostaining of ceramides (violet staining) images



- The skin contains a wide range of biomarkers associated with barrier and hydration, including Ceramides (component of SC barrier lipids), Filaggrin (natural moisturizing factor formation), Involucrin (cornified cell envelope component and marker of differentiation), Loricrin (important for cornified envelope mechanical integrity), SPRR1a (marker for keratinocyte differentiation) and Aquaporin-3 (water transport).
- At the end of the experimental period the base chassis (E) showed improvements vs control in Involucrin (+268%), Loricrin (+221%) and Aquaporin-3 (+63%) levels, while adding vitamins (P1) showed additional significant positive effects on SPRR1a (+214%). Addition of vitamins and lipids (P5) increased Involucrin (+243%), Loricrin (+458%) SPRR1a (+193%) and Aquaporin-3 (+94%) (cf Table 2).
- Addition of medium and high levels of lipids (P3, P4 and P7) improved Filaggrin by up to +17%.
- Regarding the impact of the different combinations (E, P1, P5) after seven days of treatment, Ceramides were moderately observed in the SC with product E. Treatment with Product P1 induced a clear increase in Ceramides. An even stronger increase was observed after treatment with Product P5 (Figure 2). Products P1 and P5 induced a significant increase in Ceramides by +27% ($p < 0.05$) and +59% ($p < 0.01$) respectively, moreover addition of vitamins and lipids demonstrated an even larger increase in Ceramides vs vitamins alone (P1), +25% ($p = 0.007$). (Figure 2.)
- Compared with base chassis (E) significant improvements were seen for SPRR1a levels (P1, +197% and P5, +177%), Loricrin (P5, +74%) and Filaggrin (P3, +14% and P4, +14%).

Do you know the CBright?

- ✓ Unique and innovative photo positioning device
- ✓ Standardization and reproducibility over 180-degree
- ✓ Professional photographic quality
 - ❖ Diffuse and polarized LED illumination (4 200 °K)
 - ❖ Positioning device with laser line
 - ❖ Support for color chart
 - ❖ Professional Canon camera
- ✓ Ergonomic and compact bench
 - ❖ Simplifies the forensic obligations of professionals
 - ❖ Creating a unified photo library for scientific publications, panelist data and illustrations
- ✓ Ergonomic:
 - ❖ 180-degree shooting angles (0, 30, 45, 60 and 90°)
 - ❖ Ease and simple of use
 - ❖ Movies are possible "travelling"
- ✓ Compact:
 - ❖ Support on the floor with a small footprint
 - ❖ Grey background unfolding as a folding triptych
 - ❖ Solidity and quality of materials CE marked

Contact us at info@eotech.fr
Eotech Skin Team

New approach for hair keratin characterization: use of the confocal Raman spectroscopy to assess the effect of a thermal stress on human hair fiber

M. ESSENDOUBI¹, N. ANDRE², B. GRANGER², C. CLAVE², C. GIBIELLE², M. MANFAIT¹, I. THUILLIER², O. PIOT¹, J. GINESTAR²

1. EA 7506 Biospectroscopie Translationnelle (BioSpectT), Faculty of Pharmacy, University of Reims
Champagne-Ardenne

2. CFEB SISLEY 3-5 avenue de Friedland 75008 Paris

Confocal Raman spectroscopy (CRS) is a powerful laser optical technique that provides structural and molecular information throughout human hair fiber. This technique has the advantage of being non-destructive, label free and can detect molecular information at various depths in the cortex and cuticle levels. Thereby Raman spectra constitute highly specific spectroscopic fingerprints by providing molecular information about disulfide bands and conformational organization of keratin. In order to assess the thermo-protective effect of a cosmetic finished product, CRS has been used to assess the molecular changes in keratin fibers after thermal damages. To achieve this goal, the present work aims to evaluate *ex-vivo* the thermo-protective effect of an hair care product by applying CRS on treated and untreated hair samples. The *ex-vivo* results show that the Raman spectral signature of the hair treated and heated is very close to the untreated and unheated sample. This shows that the keratin spectral signature is preserved by hair product after thermal stress with straightening process. This suggests that the hair care promotes the α helix keratin conformation and preserves the S-S disulfide keratin bands. Scanning electronic microscopy has been also used to assess the morphological changes of the heat damaged hair fibers and correlated the Raman results. The in use test results confirmed the good perception for the consumers as regards the hair protection against heat. According to our results, CRS is a technique with a great analytical and structural potential to evaluate the molecular effect after hair heat stress.

Keywords: Confocal Raman spectroscopy, Human hair fiber, keratin, thermal stress, scanning electron microscopy, thermo-protective effect, hair care, cosmetics.

NEW APPROACH FOR HAIR KERATIN CHARACTERIZATION: USE OF THE CONFOCAL RAMAN SPECTROSCOPY TO ASSESS THE EFFECT OF A THERMAL STRESS ON HUMAN HAIR FIBER

M. ESSENDUBI¹, N. ANDRE², B. GRANGER², C. CLAVE², M. MANFAIT¹, I. THUILLIER², O. PIOT¹, J. GINESTAR²

1) EA 7506 Biospectroscopie Translationnelle (BioSpectT), Faculty of Pharmacy, University of Reims Champagne-Ardenne mohammed.essendoubi@univ-reims.fr
2) CFEBS SISLEY 3-5 avenue de Friedland 75008 Paris nada.andre@sisley.fr / berengere.granger@sisley.fr



INTRODUCTION

The hair, like the skin, undergoes various internal and external aggressions. The use of heat styling devices can reach extremely high temperature and cause significant stress on hair at the morphological and molecular levels. Heating is known to damage cumulatively the hair fiber in surface and depth. In order to assess the thermo-protective effect of a cosmetic finished product, several methods were used such as scanning electronic microscopy (SEM, ref. 1) on *ex vivo* hair tresses and satisfaction questionnaire during a clinical study. A new microspectroscopic approach consisted on using the Confocal Raman spectroscopy (CRS) (ref. 2) to assess the structural and molecular changes in keratin fibers after thermal damages on the hair. It has the advantage of being non-destructive, label free and can detect information at various depths in the cortex and cuticle levels. Thereby Raman spectra constitute highly specific spectroscopic fingerprints by providing molecular information about disulfide bands and conformational organization of keratin.

METHODS

HAIR SAMPLES



- ❖ Tresses of natural blond human hair in order to limit fluorescence interference during Raman measurements

HAIR SAMPLES TREATMENT

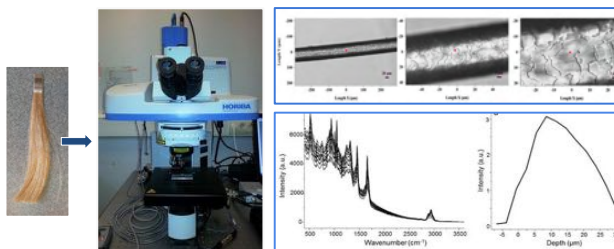
- ❖ Leave-on care product application: 10% of the tresses weight for 5 minutes of application
- ❖ Heating cycle: 5 seconds at 235°C followed by 15 seconds of cooling at room temperature

SEM OBSERVATIONS



- ❖ FEG ZEISS GeminiSEM 300
- ❖ Coating: 2nm of gold
- ❖ Working distance: 6.2-6.5mm
- ❖ Electron High Tension: 2-8 kV

CONFOCAL RAMAN SPECTROSCOPY



- ❖ Laser wavelength: 785 nm, Objective: 100 X, Acquisition time: (50 x s 1), spectral range: 400 to 4000 cm⁻¹, Axial resolution: 2 μm
- ❖ Choice of the mapping zone of the hair fiber with the microscope camera
- ❖ Raman axial (Z) profile: in-depth scanning through the hair fiber at different focus points, from the surface Z=0 μm to 30 μm of depth

IN VIVO STUDY

23 Caucasian subjects included
Use of the heat protective hair treatment, 3 times a week, before using the straightening iron

- ❖ **Raman analysis**
On 5 subjects before and after one month of use
Calculation of mean ± standard error of the molecular keratin spectral markers
Statistical analysis with Student t test and Mann-Whitney (p < 0.05)

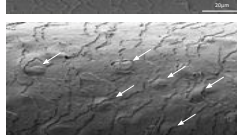
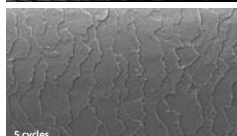
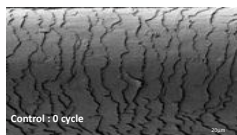
- ❖ **Satisfaction questionnaire** after one month of use

RESULTS

PREPARATORY STUDY

Evaluation of heat threshold stress

SEM images (x1000) of hair fibers subjected to several cycles of thermal stress (0, 5, 10) were taken using a hair iron straightener at 235°C.



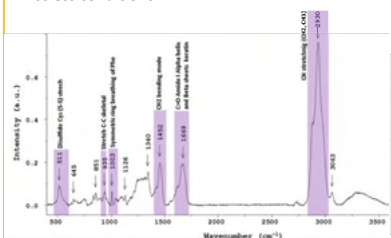
- ★ 10 heat stress cycles are too aggressive on the hair structure and cause significant morphological alteration of the fibers (bubbles and cracks)

- ★ The study was conducted with a heat stress of 5 cycles in order to preserve the morphological integrity of the hair fibers

Raman analysis

For *ex-vivo* evaluation, we analyzed 4 hair samples: S1: untreated and unheated (Control), S2: treated and unheated (T UH), S3: untreated and heated (5X) (UT H) and S4: treated and heated (5X) hair sample (T H)

- ★ The first step of this work was to determine the reference Raman spectra of each hair sample and assignment of keratin molecular bands in thermal stress conditions

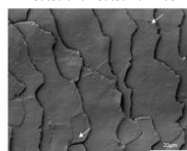
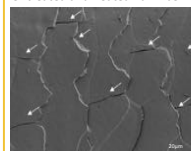


Raman spectrum of human hair fiber showing keratin molecular markers detected after thermal stress

- ★ In the spectra, we can distinguish several peaks specific to the keratin molecule and sensitive to thermal stress

SEM observations

Untreated and heated hair fiber Treated and heated hair fiber

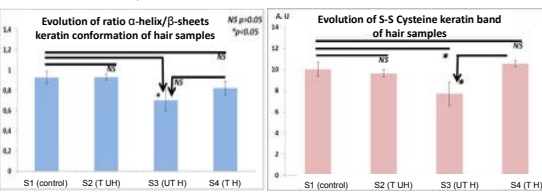


- ★ The hair care clearly shows protective properties with respect to heat damage (less bubbles & cracks)

EX VIVO STUDY

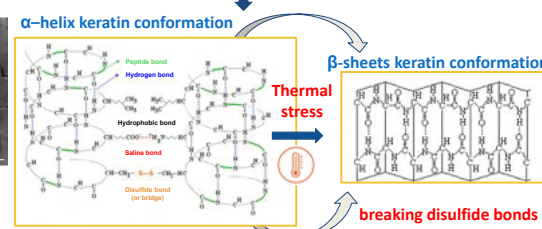
- ★ The second step was to evaluate the influence of treatment and thermal stress on hair fibers. For this two molecular spectral markers were calculated:

- The ratio of α-helix (1640-1660 cm⁻¹) to β-sheets (1660-1685 cm⁻¹) on amide I region.
- Disulfide S-S cysteine keratin cross-links bands (510 cm⁻¹)



T: Treated, UT: Untreated, H: Heated and UH: Unheated

- ★ The hair care provides heat protection of the hair fibers by promoting the α-helix keratin conformation and inhibits the transition to the β-sheets keratin conformation
- ★ The hair care also preserves the (S-S) disulfide keratin bands from heat damage and stabilizes the tertiary structure of keratin hair fiber

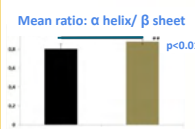


The figures of keratin chemical structures are taken from website: technocoff/biologie/bio6.htm

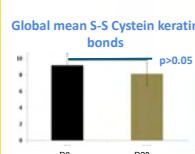
IN VIVO STUDY

Raman analysis

- ★ Heat protection by promoting the α-helix conformation of keratin



- ★ Stabilization of disulfide bonds



Satisfaction

- 83% anti-split end action
- 78% anti-brittle action
- 87% softer, shinier and beautiful hair
- 96% more supple hair

CONCLUSION

- ❖ The *ex-vivo* and *in-vivo* results show that the keratin molecular structure is preserved by hair care product after thermal stress
- ❖ The hair care product promotes the α-helix keratin conformation and preserves the S-S disulfide keratin bonds
- ❖ SEM images show clearly the morphological protective properties of the hair care product from heat damages and confirm the obtained Raman spectroscopy results
- ❖ The in use test results confirmed the good perception for the consumers as regards the hair protection against heat
- ❖ CRS is a technique with great molecular potential to investigate the effect of cosmetic ingredients on keratin structure in human hair fibers under external stress conditions such as heat
- ❖ CRS offers the opportunity to study other important aspects related to the effectiveness of hair cosmetics such as hydration, oxidative and UV stress or active penetration.



Visualization and quantification of pigmentation spots on facial skin by 3D LC-OCT

Mélanie Pedrazzani¹, Gabriel Koeller², Magalie Daniel³, Simon Aubailly⁴, Arnaud Dubois⁵, Clara Tavernier¹, Emmanuel Cohen¹, Elian Lati³, Jean-Jacques Servant², Catherine Heusèle^{4*}

¹ DAMAE Medical, Paris, France, ² Eotech, Marcoussis, France, ³ Laboratoire BIO-EC, Longjumeau, France, ⁴ LVMH Recherche, Saint Jean de Braye, France, Université Paris-Saclay, ⁵ Institut d'Optique Graduate School, Laboratoire Charles Fabry, Palaiseau, France

*cheusele@research.lvmh-pc.com

KEY WORDS: LC-OCT, pigmentation, dermo-epidermal junction, skin

Pigmentation spots such as actinic lentigos are one of the most visible and undesirable signs of photoaging on the skin. Histology on skin biopsies has revealed the melanin patterns leading to these color changes. Non-invasive techniques are of interest to quantify on any skin location the melanin content and organization to diagnose pigmented spots and evaluate cosmetic products.

Line-field confocal optical coherence tomography (LC-OCT) is an imaging technique that non-invasively provides images of the skin in real-time. The new version of the technology allows 3D image acquisition with enhanced visualization and quantification of skin structures. In this work, we investigate the cutaneous structure and melanin pattern in spotted area of the face of Caucasian and Asian women in comparison to a non-spotted area.

Two groups of healthy women aged 37 - 64 presenting actinic lentigo on the face were recruited (12 Caucasian, 10 Asian). 3D LC-OCT images were acquired on a spotted area over a field-of-view of 1.2 x 0.5 mm² on a 0.5 mm depth with an isotropic spatial resolution of about 1 μm. The same images were obtained on a non-spotted area in the vicinity of the lentigo. Stratum corneum thickness, epidermal thickness, and dermo-epidermal junction (DEJ) length were measured using a semi-automatic segmentation tool on 2D vertical optical sections. Melanin distribution pattern was qualified by observation of the 3D images and melanin density was determined according to the depth.

Most of the investigated lentigos were located on the cheek mainly on the cheekbone. On the whole panel, the stratum corneum and the epidermis were significantly thicker on the spotted area. The DEJ length reported to scanned length was significantly much greater in the spotted area.

Two main types of melanin and DEJ associated configurations were observed. Half of the analyzed spots were presenting a diffuse pattern of bright points associated to melanin. In the other half of the spots, DEJ was much more undulated than in the non-spotted area. Horizontal optical sections showed either well-defined round papillae surrounded with bright melanin loaded cells either a complex papilla network. For all the patterns, image analysis showed a large increase of melanin density in the pigmented spots and an increase of the epidermal height where melanin is detected.

This study confirmed melanin patterns with epidermal and DEJ modification observed in spotted area previously described by histology on biopsies. 3D LC-OCT allows real time visualization of the melanin pattern in the pigmented spots and further quantification of the epidermal morphological characteristics and an evaluation of the melanin content.

Visualization and quantification of pigmentation spots on facial skin by 3D LC-OCT

Mélanie Pedrazzani¹, Gabriel Koeller², Magalie Daniel³, Simon Aubailly⁴, Arnaud Dubois⁵, Clara Tavernier¹, Emmanuel Cohen¹, Elian Lati³, Jean-Jacques Servant², Catherine Heusèle⁴

¹ DAMAE Medical, Paris, France, ² Eotech, Marcoussis, France, ³ Laboratoire BIO-EC, Longjumeau, France, ⁴ LVMH Recherche, Saint Jean de Braye, France, Université Paris-Saclay, ⁵ Institut d'Optique Graduate School, Laboratoire Charles Fabry, Palaiseau, France

INTRODUCTION

Pigmentation spots such as actinic lentigos are one of the most visible and undesirable signs of photoaging of the skin. Histology on skin biopsies has revealed the melanin patterns that leads to these color changes. Non-invasive techniques are of interest to quantify the melanin content and organization in any location of the skin to diagnose pigmented spots and evaluate cosmetic products.

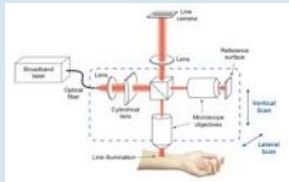
Line-field confocal optical coherence tomography (LC-OCT) is an imaging technique that provides non-invasive images of the skin in real time (1). The latest version of the technology allows 3D image acquisition with enhanced visualization and quantification of skin structures. In this work, we studied the skin structure and melanin pattern on a spotted area of the face of Caucasian and Asian women in comparison with a non-spotted area.

METHODS

Image acquisition

Two groups of healthy women aged 37 to 64 with solar lentigo on the face were recruited (12 Caucasian, 10 Asian).

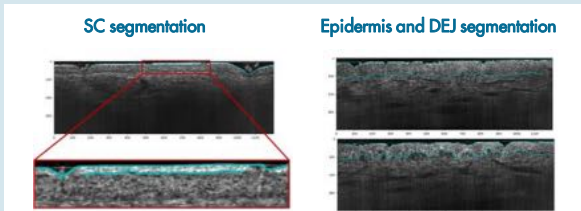
3D LC-OCT images were acquired over a field-of-view of 1.2 x 0.5 mm² at a depth of 0.5 mm with an isotropic spatial resolution of approximately 1 μm.



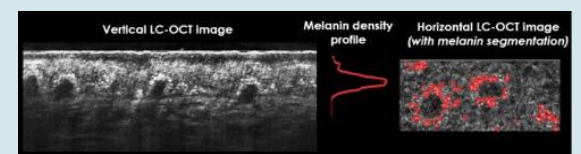
Images were acquired on a spotted area as well as on a non-spotted area adjacent to the spot. Most of the lentigos investigated were located on the cheek, mainly on the cheekbone.

Image analysis

Stratum corneum (SC) thickness, epidermal thickness, and dermo-epidermal junction (DEJ) length were measured using a semi-automatic segmentation tool on 2D vertical optical sections. DEJ length was expressed relative to the length of the ROI (region of interest), with a zero value corresponding to a flat DEJ.



The melanin distribution pattern was qualified by observation of 3D images. Melanin was quantified on ROI of size 250 x 100 μm². Melanin density was calculated on each horizontal image and a profile was obtained by plotting melanin density versus distance from the bottom of the papilla. The maximum distance where melanin was observed (melanin thickness) and the area under the density curve (total melanin) were then computed.



CONCLUSION

This study confirmed melanin patterns with epidermal and DEJ modification observed in the spotted areas previously described by histology on biopsies and the 2 types of pattern present on the face (2,3). 3D LC-OCT allows real time visualization of the melanin pattern in pigmented spots and quantification of the epidermal morphological characteristics and melanin content.

RESULTS

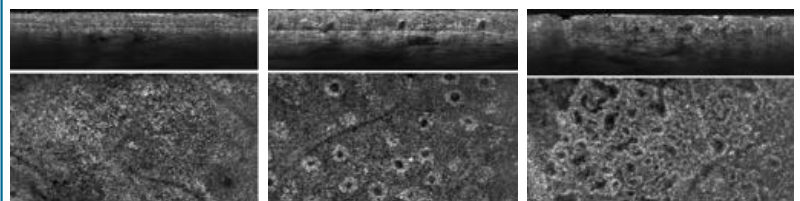
Epidermal metrics on pigmented spots vs. control

	Pigmented spot	Control	Significance
Stratum corneum thickness (μm)	12.0 +/- 2.3	10.3 +/- 1.9	*
Epidermal thickness (μm)	62.8 +/- 11.5	56.1 +/- 7.5	*
DEJ length/ROI length (%)	17.8 +/- 9.5	10.7 +/- 3.7	***

*p<0.05, ***p<0.001

On the whole panel, the stratum corneum and the epidermis were significantly thicker on the spotted area and the DEJ length relative to the length of the ROI was significantly greater.

Melanin Patterns



Two main types of melanin/DEJ patterns were observed. Half of the analyzed spots had a diffuse pattern of melanin bright points. In the other half of the spots, DEJ was much more undulated than in the non-spotted area. Horizontal optical sections showed either well-defined round papillae surrounded with bright melanin loaded cells either a complex papillae network.

	All types		Type I		Types II and III	
	Spots	Control	Spots	Control	Spots	Control
SC thickness (μm)	12.0 +/- 2.3 *	10.3 +/- 1.9	11.0 +/- 2.1	10.3 +/- 1.9	13.1 +/- 2.0 *	10.2 +/- 2.1
Epidermal thickness (μm)	62.8 +/- 11.5 *	56.1 +/- 7.5	55.5 +/- 6.7	54.7 +/- 6.2	68.7 +/- 11.8 *	56.8 +/- 8.9
DEJ length/ROI length (%)	17.8 +/- 9.5 ***	10.7 +/- 3.7	12.5 +/- 3.3 *	9.1 +/- 3.4	22.2 +/- 11.3 **	12.5 +/- 3.4
Maximal melanin (%)	15.3 +/- 2.5 ***	6.5 +/- 3.8	15.1 +/- 2.0 ***	6.4 +/- 2.0	16.0 +/- 2.5 **	7.1 +/- 4.8
Melanin thickness (μm)	38.1 +/- 15.8 **	26.5 +/- 9.1	26.5 +/- 7.8	21.9 +/- 5.9	50.2 +/- 11.9 ***	31.1 +/- 9.7
Total melanin	479 +/- 229 ***	93.1 +/- 77	319 +/- 96 ***	77 +/- 40	650 +/- 190 ***	116 +/- 97

*p<0.05, **p<0.01, ***p<0.001, p values correspond to comparison between spotted and control areas

Quantification of epidermal and DEJ morphology confirmed the visual classification according two types of melanin repartition in the pigmented spots.

(1) Ogjen, J., Daurès, A., Cazalas, M., Perrot, J. L., and Dubois, A. (2020) Frontiers in Optoelectronics 13 381-92
 (2) Andersen, W. K., Labadie, R. R., and Bhowan, J. (1997) Journal of the American Academy of Dermatology 36, 444-7
 (3) Yonei, N., Kaminska, C., Kimura, A., Furukawa, F., and Yamamoto, Y. (2012). Dermatol. 39, 829-32

JenLab GmbH

Experts for Biomedical Femtosecond Laser Technology

JenLab GmbH

Campus Adlershof, Johann-Hittorf-Strasse 8, 12489 Berlin, Germany
info@jenlab.de and www.jenlab.de

KEY WORDS: femtosecond laser, two-photon microscopy, multiphoton tomography, laser transfection, cryomicroscopy, FLIM, confocal reflection, SHG, CARS

JenLab was founded in Jena in 1999. First products included the miniaturized cell chamber MiniCeM™ for microscopy and cell manipulation as well as the immunohistochemistry kit Jenfluor™ for the fluorescence detection of alkaline phosphatase and endogenous peroxidase.

In 2002/2003, the first multiphoton tomograph DermaInspect™ was developed by JenLab, tested in the Department of Dermatology of the Friedrich Schiller University Jena and sold to the Beiersdorf AG in Hamburg. The DermaInspect™ became the first CE-certified medical product for multiphoton tomography. Signals are based on fluorescent coenzymes, melanin, keratin and elastin as well as on second harmonic generation (SHG) by collagen.

JenLab developed also the compact two-photon FLIM microscope TauMap™ for fluorescence lifetime imaging based on time-correlated single photon counting (TCSPC) with an 80 MHz titanium:sapphire laser.

Further Jenlab femtosecond laser microscopes include 2PM™ for two-photon imaging with the additional option of cryo-imaging and FemtOgene™ for femtosecond laser transfection and optical reprogramming.

The second generation of multiphoton tomographs, the MPTflex™, was validated in the clinical environment in 2010 and became JenLab's second CE-certified medical product.

The two-beam multiphoton CARS tomographs DermaInspect-CARS and MPTflex-CARS™ based on a photonic crystal fiber (PCF) were launched in 2010 and 2014. The tomographs provide additional information on intratissue lipids and water by Coherent Anti-Stokes Raman Scattering (CARS).

The latest product MPTcompact™ was clinically tested in 2020. The ultracompact femtosecond fiber laser head is located inside the 360° measurement head. The multimodal tomograph provides optical biopsies based on (i) autofluorescence AF, (ii) SHG, (iii) FLIM, (iv) confocal reflection, and (v) dermoscopy with white light LEDs and CMOS camera.

Johann Wilhelm Ritter Award for Innovative Skin Imaging

K. König

JenLab GmbH, Johann-Hittorf-Strasse 8, 12489 Berlin
info@jenlab.de, www.jenlab.de

KEY WORDS: Johann Wilhelm Ritter, Award, UV

The JWR Award for innovative skin imaging is given during the World Conference of the International Society for Biophysics and Imaging of the Skin ISBS. The JWR Award is sponsored by JenLab GmbH.

The first JWR award was presented at the World ISBS2016 conference in Lisbon to *Rainer Voegeli* from DSM Nutritional Products Ltd., Switzerland. The second JWR award was presented to *Pegah Kharazmi* from British Columbia University (Canada) conference in San Diego 2018. The third JWR award will be presented at the World ISBS2022 conference in Berlin.

When he was just 24 years old, Johann Wilhelm Ritter discovered the ultraviolet radiation in 1801. Becoming increasingly in the crossfire of critical opinions, he lost his reputation as a genius of physics and electrochemistry and died aged 33 as a poor man.

Johann Wilhelm Ritter started to study medicine at the University of Jena but focused more on self-experiments on galvanic phenomena. He became the pioneer of scientific electrochemistry and a member of the German Romantic movement. Influenced by its philosophy of “polarities and symmetries in nature” and after the discovery of „heat rays“ (infrared radiation) by Herschel in 1800, Ritter started to search for opposite rays beyond the violet. He found in 1801 that silver chloride was transformed into black when it was placed beyond the violet end of the visible part. This was the discovery of „chemical rays“, later on called ultraviolet radiation.

The Jena university gave him the permission to give lectures on galvanism but did not provide him with a regular income. He moved to Munich in 1804 and got married. However, suffering from financial difficulties and weak health likely due his self-experimentation on galvanism, he died as father of four young children too young on Jan 23, 1810.



Johann Wilhelm Ritter – discoverer of the ultraviolet radiation

1

¹ K. König. *Dermatol. Mon. schr.* 174 (1988) 493-497.

Johann-Wilhelm-Ritter Award for Innovative Skin Imaging



Karsten König
JenLab GmbH, Johann-Hittorf-Strasse 8, 12489 Berlin, Germany
koenig@jenlab.de, www.jenlab.de

The discoverer of the ultraviolet radiation



Johann-Wilhelm Ritter (Dec 16, 1776 Samitz/Silesia – Jan 23, 1810 Munich)

Johann Wilhelm Ritter

When he was just 24 years old, Johann Wilhelm Ritter discovered the ultraviolet radiation in 1801.

Becoming increasingly in the crossfire of critical opinions, he lost his reputation as a genius of physics and electrochemistry and died aged 33 as a poor man.

Johann Wilhelm Ritter started to study medicine at the University of Jena but focused more on self-experiments on galvanic phenomena. He became the pioneer of scientific electrochemistry.

Ritter was a member of the German Romantic movement. Influenced by its philosophy of “polarities and symmetries in nature” and after the discovery of „heat rays“ (infrared radiation) by Herschel in 1800, Ritter started to search for opposite rays beyond the violet. He found in 1801 that silver chloride was transformed into black when it was placed beyond the violet end of the visible part. This was the discovery of „chemical rays“, later on called ultraviolet radiation.

The Jena university gave him the permission to give lectures on galvanism but did not provide him with a regular income.

Therefore he moved to Munich in 1804 and got married. However, suffering from financial difficulties and weak health likely due his self-experimentation on galvanism, he died as father of four young children too young on Jan 23, 1810.

The JWR Award

The JWR Award for innovative skin imaging is given during the World Congress of the International Society for Biophysics and Imaging of the Skin ISBS.

The JWR Award is sponsored by JenLab GmbH.

The first JWR Award was presented at the World ISBS Congress 2016 in Lisbon to *Rainer Voegeli* from DSM Nutritional Products Ltd., Switzerland. The second JWR Award was presented to *Pegah Kharazmi* from British Columbia University (Canada) at the World ISBS Congress 2018 in San Diego. The third JWR Award will be presented at the World ISBS Congress 2022 in Berlin.

The JWR award includes:

- a personal honorary certificate
- a 1,000 Euro Scientific Research Award
- ISBS membership for one year
- invitation as plenary talk speaker at the next World ISBS Congress including 900 Euro travel support

Further information can be find on the websites:

jwr-award.org
isbs-congress.com
isbskin.org

First and Second JWR Award

Johann-Wilhelm Ritter Award 2016



Stacy Hawkins, Karsten König, Pegah Kharazmi, Bernard Querleux, Joachim Fluhr

Johann-Wilhelm Ritter Award 2018



References

- [1] K. Richter (ed.). Der Physiker des Romantikerkreises Johann Wilhelm Ritter in seinen Briefen an den Verleger Carl Friedrich Ernst Frommann. 1988. Hermann Böhlau Nachfolger Weimar
- [2] K. König. Johann Wilhelm Ritter-der Entdecker der UV-Strahlung. Dermatol. Mon. schr. 174 (1988) 493-497.

Optical Metabolic Skin Imaging with two-wavelength femtosecond laser

Karsten König and Wolfgang Becker

JenLab GmbH and Becker&Hickl GmbH, Berlin, Germany

Corresponding Author e-mail address and URL: koenig@jenlab.de and www.jenlab.de

KEY WORDS: OMI, two-photon imaging, skin, femtosecond laser, FLIM

The fluorescence of the coenzymes NAD(P)H and flavins (FAD, FMN) can be used to evaluate cell metabolism. Of high interest is the information on the metabolism of intratissue cells of pathological skin compared to healthy skin and on the impact of cosmetics.

Intratissue NAD(P)H in its free and bound form can be detected by Multiphoton FLIM Tomography with a femtosecond laser excitation wavelength of 800 nm or shorter. Intratissue flavins / flavoproteins can be also excited at a longer NIR wavelength such as 880 nm.

Here we report on a tomograph MPTflex with a two-wavelength fiber femtosecond laser emitting two femtosecond laser beams at 780 nm and 880 nm with a temporal shift of a few nanoseconds in combination with a low-noise two-detection-channel hybrid PMT detector for multiplex time-correlated single photon counting (TCSPC). Using an acousto-optical modulator (AOM), the image recording laser beams are switched permanently. The tomograph provides simultaneously four high-resolution autofluorescence images within a single six second scan of a 0.3x0.3 mm² tissue area. The tissue depth can be varied with an accuracy of about 1 µm. One image depicts the autofluorescence of NAD(P)H when excited with 780 nm light. The second image depicts collagen as SHG-signal of the 880 nm beam. The third image provides a 780nm excited NAD(P)H + flavin image, and the fourth image the 880 nm excited flavin image. All four images can be depicted as false color images where the color represents the subnanosecond/nanosecond autofluorescence lifetime. Information on the cells metabolism can be obtained by NAD(P)H/flavin ratios as well as by the ratio free to bound coenzyme.

We acknowledge financial support from the Federal Ministry of Education and Research under the OMOXI project (Grant# 13N14505).

OPTICAL METABOLIC SKIN IMAGING WITH TWO-WAVELENGTH FEMTOSECOND LASER



Karsten König¹, Wolfgang Becker²

¹JenLab GmbH, Johann-Hittorf-Strasse 8, 12489 Berlin, Germany

²Becker&Hickl GmbH, Berlin

koenig@jenlab.de, www.jenlab.de

Abstract

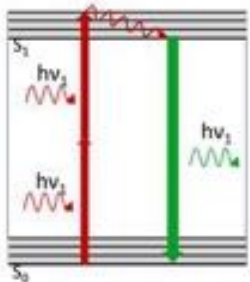
The fluorescence of the coenzymes NAD(P)H and flavins (FAD, FMN) can be used to evaluate cell metabolism. Of interest is the metabolism of intratissue cells of pathological skin compared to healthy skin and the impact of cosmetics. Intratissue NAD(P)H in its free and bound form can be detected by Multiphoton FLIM Tomography with a femtosecond laser excitation wavelength of 800 nm or shorter. Intratissue flavins / flavoproteins can be also excited at a longer NIR wavelength such as 880 nm. We report on a tomograph MPTflex™ with a two-wavelength fiber fs laser emitting two laser beams at 780 nm and 880 nm in combination with a low-noise two-detection-channel hybrid PMT detector for multiplex

time-correlated single photon counting (TCSPC). Using an acousto-optical (AOM) modulator, the beams are switched permanently. The tomograph provides simultaneously four high-resolution autofluorescence images within a 6 s scan of 0.3 x 0.3 mm² tissue. Image 1 depicts NAD(P)H when excited with 780 nm light. Image 2 depicts collagen as SHG-signal of the 880 nm beam. Image 3 provides a 780nm excited NAD(P)H + flavin image, and image 4 the 880 nm excited flavin. All 4 images can be depicted as false color images where the color represents the sub-nanosecond autofluorescence lifetime. Information on the cells metabolism can be obtained by NAD(P)H/flavin ratios as well as by the ratio free to bound coenzyme.

Materials and Methods

Two-photon excitation principle

Two near infrared photons are absorbed simultaneously to excite the autofluorescence of cells and elastin. Collagen provides an intrinsic signal by second harmonic generation SHG.



FLIM based Oxygen Metabolic Index (OMI)

The fluorescence decay per pixel can be measured by the detection of the arrival time of the photon using TCSPC. OMI is based on coenzyme imaging using the so called fluorescence lifetime redox ratio (FLIRR). It is calculated from the FLIM based intensity ratios of bound NAD(P)H and free FAD⁺[3]:

$$FLIRR = \frac{NAD(P)Ha_2\%}{FAD^+a_1\%}$$

Experimental setup

MPTflex™

- **Multiphoton Tomograph**
Non-invasive imaging by multiphoton excitation
- **Maximum Field of View**
350 μm x 350 μm
- **Spatial resolutions**
< 0.5 μm (lateral)
< 2 μm (axial)
- **Power**
max 50 mW at skin
- **Laser pulse parameters**
Repetition rate 80 MHz,
pulse width <160 fs

80 MHz Femtosecond Laser

1. MaiTai, tunable 690-960nm
2. Fiber laser at 780 nm / 880 nm

Detector

FLIM-PMT or Hybrid-PMT

FLIM/PLIM Module

SPC 150 with multiplexer



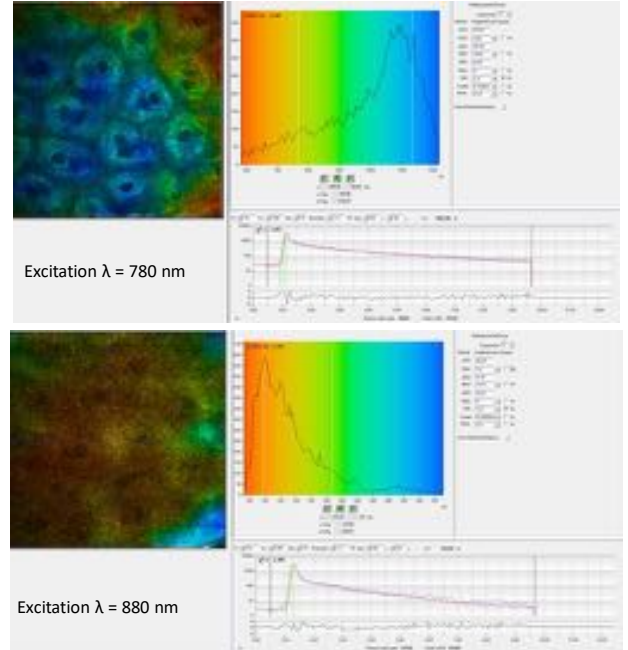
Hybrid Photo Detector by Becker & Hickl GmbH

- Extremely fast response
- Instrument response function (IRF) down to 18 ps FWHM
- High detection efficiency
- Large active area
- No afterpulsing background
- Clear IRF: No tails or secondary peaks



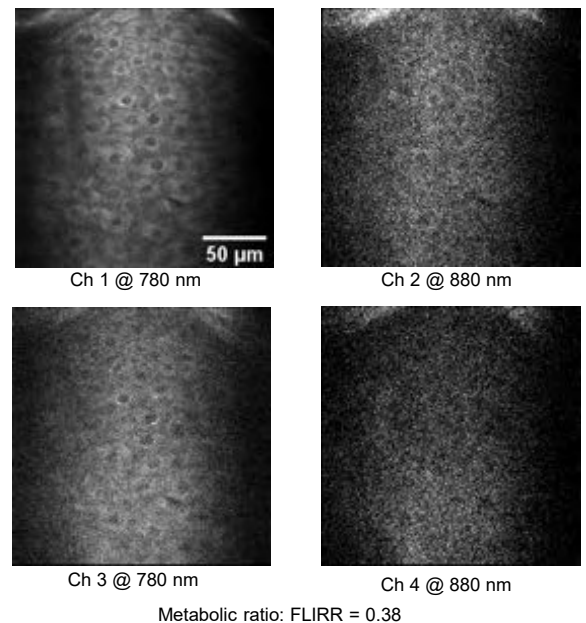
Results

Multiphoton Tomography with the tunable Ti:sapphire laser MaiTai



Metabolic ratio: FLIRR = 0.34

Multiphoton Tomography with the two-wavelength laser OMOXI



Metabolic ratio: FLIRR = 0.38

Conclusion

- OMI can be performed with a 2-wavelength-FLIM-tomograph
- Flavins without NAD(P)H background can be imaged using 880nm excitation
- Flavin fluorescence photons << NAD(P)H fluorescence photons -> therefore FLIM analysis difficult, high binning required

Acknowledgement

We acknowledge financial support from the Federal Ministry of Education and Research under the OMOXI project (Grant# 13N14505).

References

- [1] K. König (ed.) Multiphoton microscopy and fluorescence lifetime imaging. De Gruyter (2018).
- [2] K. König. Review: Clinical in vivo multiphoton FLIM tomography. Methods Appl. Fluoresc. 8 (2020) 034002.
- [3] S. Alam et al.: Scientific Reports, Vol. 7, 10451 (2017)

***Ex vivo* evaluation of endogenous hyaluronic acid in human skin**

L. R. Paula¹, L. P. M. Neto^{2,3}, G. C. da Silva^{2,3}, A. A. Martin^{2,3*}

¹Natura Cosméticos S/A, Rod. Anhanguera, Km 30,5, Cajamar, SP - Brazil, 07750-000; ²Science and Technology Institute, University of Brazil, 235 R. Carolina Fonseca, Sao Paulo, SP, Brazil; ³Dermo PROBES – Skin and Hair Technology, Av. Cassiano Ricardo, 601, Sao Paulo, SP, Brazil
*airton.a.martin@gmail.com; probes.com.br/dermoprobes

KEY WORDS: Raman spectroscopy, hyaluronic acid, human skin.

Introduction: Hyaluronic acid (HA) is a glycosaminoglycan present in connective tissues and is related to tissue hydration¹⁻³, being of great interest, since it can lead to the development of products and therapies in minimizing skin aging. Thus, this study evaluated the presence of endogenous HA in human skin *ex vivo* by confocal Raman spectroscopy (CRS) and immunofluorescence (IF). **Methods:** Six skin biopsies from plastic surgery were evaluated using both techniques. A Rivers Diagnostic system (Model 3510 Skin Composition Analyzer) and specific markers for the presence of HA on the skin (AB53842) were used. The spectral evaluation was carried out by comparing the average spectra of each region of the skin with the standard spectrum of the HA, besides the evaluation of the data by the method of classic Least Squares Calibration (CLS), to obtain the concentration of the HA in the skin. **Results:** It was possible to verify, through the CRS technique, in all samples, the presence of HA, specifically in the Raman peaks of 1047, 1098, 1125, 1205 and 1654 cm^{-1} , being verified that the HA concentration was higher in the dermis region when compared to the epidermis region (Figure 1 A-B). Through the IF analysis, it was possible to detect the presence of HA in all samples, corroborating with the Raman results. **Conclusion:** CRS has been proved to be an excellent tool in the evaluation of endogenous HA, enabling the obtaining of useful information for the development of more effective products, as well as for a better understanding of the component in human skin.

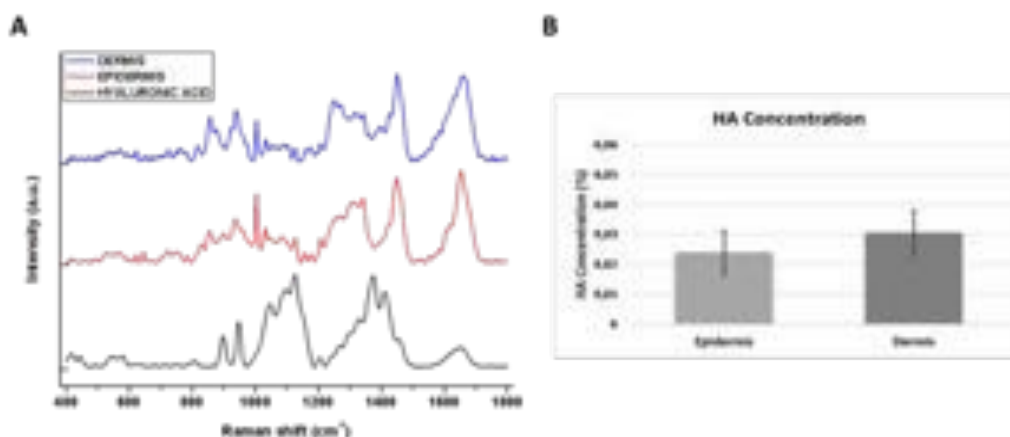


Figure 1: A: Raman spectra of the epidermis and dermis compared to the HA spectrum; B: Concentration of HA on the skin.

¹Tammi, M. I., Day, A. J. and Turley, E. A., J. Biol. Chem. 277(2002)4581- 4584.

²Weindl, G., Schaller, M., Schafer-Korting, M. and Korting, H. C., Skin Pharmacol Physiol. 17(2004)207-213.

³Coleman, S. R. and Grover, R., Aesthet. Surg. J. 26(2006) S4-9.

Ex vivo evaluation of endogenous hyaluronic acid in human skin: confocal Raman spectroscopy

L. R. Paula¹, L. P. Medeiros Neto², G. C. da Silva², A. A. Martin^{2,3*}



¹Natura Cosméticos S/A, Rod. Anhanguera, Km 30,5, Cajamar, SP - Brazil, 07750-000

²Science and Technology Institute, University of Brazil, 235 R. Carolina Fonseca, Sao Paulo, SP, Brazil

³DermoPROBES – Skin and Hair Technology, Av. Cassiano Ricardo, 601, Sao Paulo, SP, Brazil

*airton.a.martin@gmail.com; probes.com.br/dermoprobes



Introduction

Hyaluronic acid (HA) is a glycosaminoglycan present in connective tissues and is related to tissue hydration¹⁻³, being of great interest, since it can lead to the development of products and therapies in minimizing skin aging.

Thus, this study evaluated the presence of endogenous HA in human skin *ex vivo* by the techniques of confocal Raman spectroscopy (CRS) and immunofluorescence (IF).

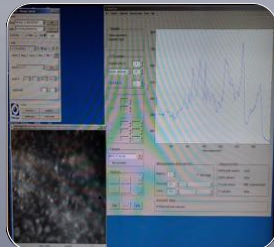
Methodology

Ethics committee: 19038719.9.0000.5494



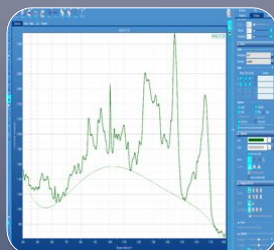
Samples

- 6 skin biopsies
- Slices 16 μm – CRS
- Slices 3 μm – IF



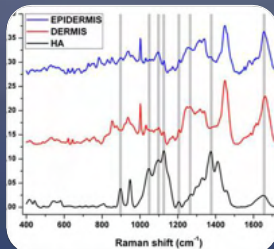
Spectra Acquisition

- Confocal Raman
- Laser 785 nm
- 20 - 30 mW
- Epidermis / Dermis



Data pre-processing

- Baseline
- Smoothing
- Vector Normalization



Statistical Analysis

- Average
- Classic Least Squares Calibration (CLS)

Results

It was possible to verify, through the CRS technique, in all samples, the presence of HA, specifically in the peaks of 1047, 1098, 1125, 1205 and 1654 cm^{-1} .

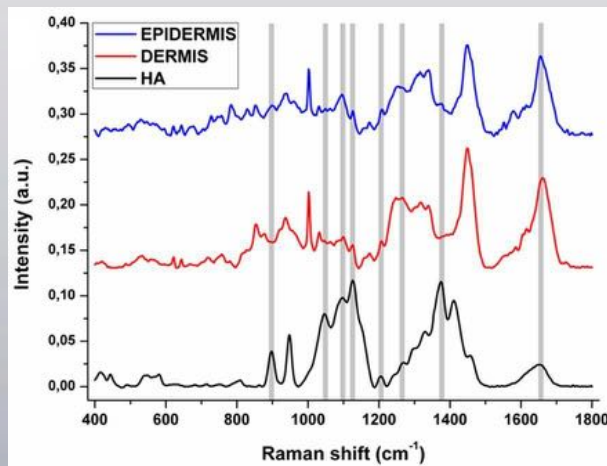


Figure 1. Raman spectra of the epidermis and dermis compared to the HA spectrum.

Regarding the HA concentration, a greater amount was found in the dermis (0.0303 a.u.) when compared to the epidermis (0.0239 a.u.).

Through the IF analysis, it was possible to detect the presence of HA in all samples, corroborating with the results found by the spectroscopy technique.

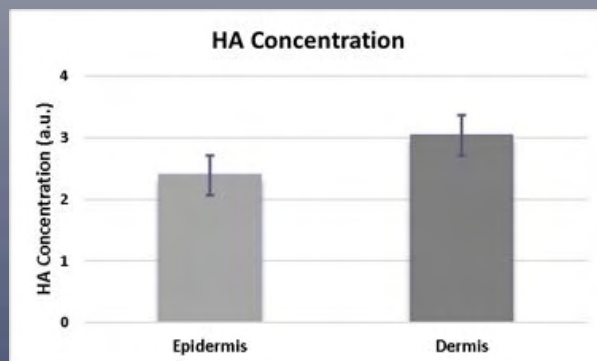


Figure 2. Concentration of HA on the skin.

Conclusion

The CRS has proven to be an excellent tool in the evaluation of endogenous HA, enabling the obtaining of useful information for the development of more effective products, as well as for a better understanding of the component in human skin.

¹Tammi, M. I., Day, A. J. and Turley, E. A., J. Biol. Chem. 277(2002) 4581- 4584.

²Weindl, G., Schaller, M., Schafer-Korting, M. and Korting, H. C., Skin Pharmacol Physiol. 17(2004) 207-213.

³Coleman, S. R. and Grover, R., Aesthet. Surg. J. 26(2006) S4-9.

A portable and compact multiphoton tomograph for in vivo and ex vivo imaging

Dmitry Pankin and Karsten König

JenLab GmbH and Becker&Hickl GmbH, Berlin, Germany

Corresponding Author e-mail address and URL: koenig@jenlab.de and www.jenlab.de

KEY WORDS: multiphoton tomograph, two-photon imaging, skin, femtosecond laser, FLIM, Reflection, confocal, dermoscopy

Multiphoton tomographs can be employed for rapid high-resolution label-free tissue imaging with subcellular resolution (“optical biopsies”). They are based on the detection of femtosecond laser induced autofluorescence of cells and elastin as well as of collagen by second harmonic imaging. Cell cultures, tumor spheroids, biopsies, small animals, humans and even diamonds and solar cells have been investigated.

Here we report on the portable multiphoton tomograph *MPTcompact* with an ultracompact fiber laser at 780 nm. The laser head is positioned inside the measurement head that includes also a scanning unit and photon detectors for time-resolved single photon counting, confocal reflectance microscopy, and wide-field white light imaging for dermoscopy. The system can also be operated in the field by battery power.

The *MPTcompact* has been evaluated in a multicenter clinical trial to image *in vivo* malignant pigmented skin lesions of 100 patients as well as to test anti-ageing strategies in the Japanese cosmetic industry by measurement of the intratissue NADH level and the ratio elastin to collagen in the upper dermis as skin age parameter that can be influenced by cosmetics.

K. König, A. Batista, A. König, HG. Breunig. Invited paper: Multimodal multiphoton tomograph using a compact femtosecond fiber laser. SPIE-Proceed. Vol. 10882 (2019) 108821A

K. König, A. Batista, M. Zieger, M. Kaatz, H. Hänssle. Clinical multimodal multiphoton tomography of pigmented skin lesions with an ultracompact femtosecond fiber laser. SPIE-Proceed. Vol 11211 (2020) 112110E

K. König, D. Pankin, A. Paudel, H. Hänßle, J. Winkler, M. Zieger, M. Kaatz: Invited paper: Skin cancer detection with a compact multimodal fiber laser multiphoton FLIM tomograph. SPIE-Proceed. Vol 116480 (2021) 116480A

MULTIMODAL MULTIPHOTON TOMOGRAPH



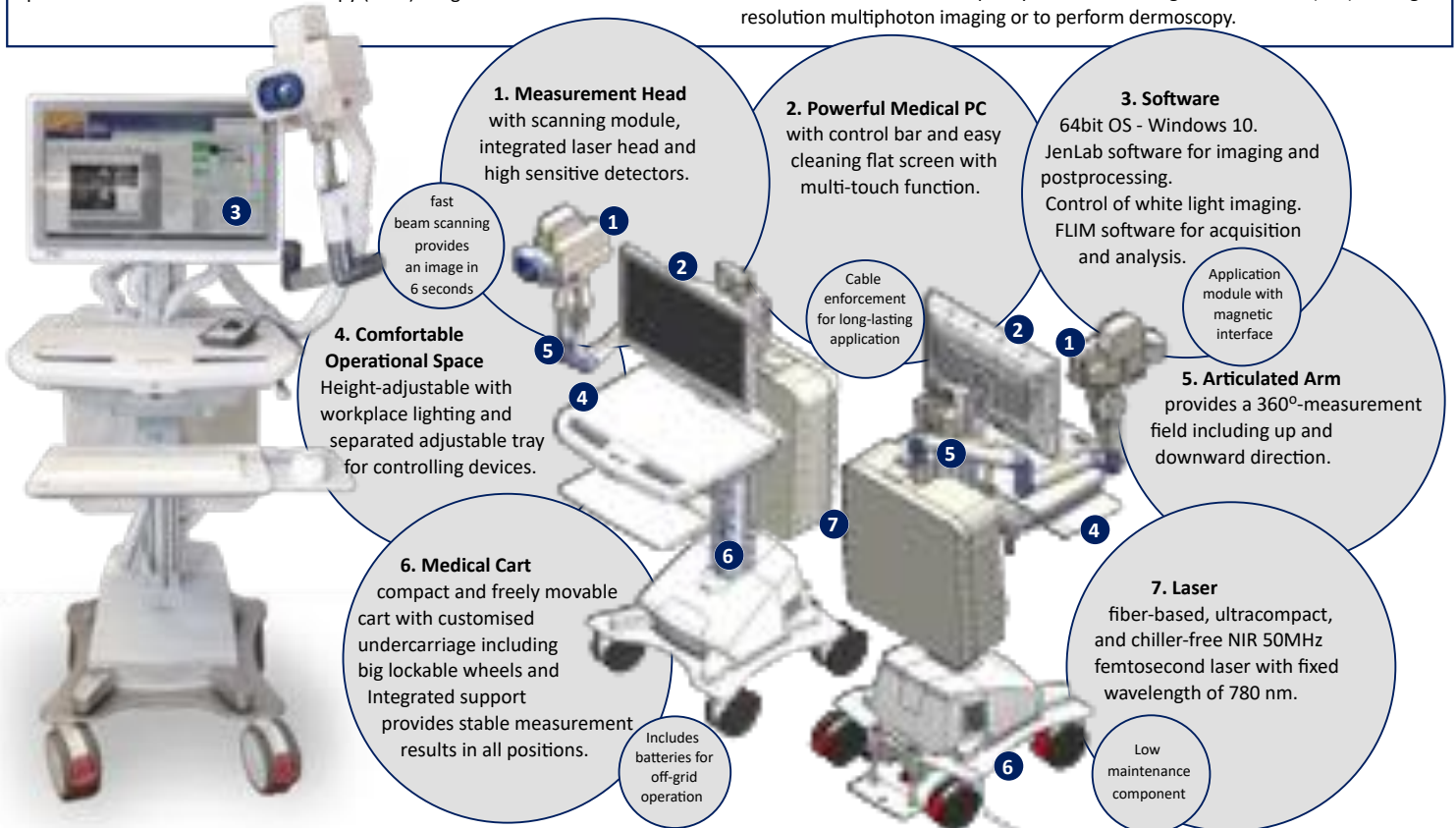
MPTcompact

Karsten König and Dmitry Pankin
 JenLab GmbH, Johann-Hittorf-Strasse 8, 12489 Berlin, Germany
 koenig@jenlab.de, www.jenlab.de

Modules, Components and Technical Highlights of MPTcompact

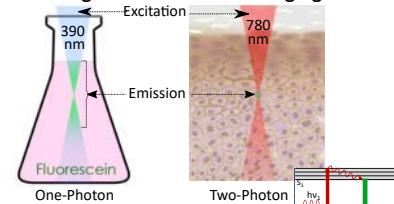
The MPTcompact is a multiphoton tomograph based on femtosecond laser technology. It is able to perform five imaging modalities: The autofluorescence (AF) of biomolecules such as NAD(P)H, flavins, porphyrins, elastin, and melanin is imaged with submicron resolution. The extracellular matrix protein collagen can be identified by its second harmonic generation (SHG). An integrated module provides confocal reflection microscopy (RCM) images.

FLIM images can be generated based on time-correlated single-photon counting (TCSPC) with 200 ps temporal resolution and bi-exponential fitting. This enables optical metabolic imaging (OMI) by recording the fluorescence decay of the coenzymes NAD(P)H and flavins. AF, SHG, RCM and FLIM are simultaneously provided in one scan. Finally, a CMOS camera can be used to image suspicious skin lesions on a mm scale to quickly determine a region of interest (ROI) for high-resolution multiphoton imaging or to perform dermoscopy.



Technologic Background

Advantages of Two-Photon Imaging

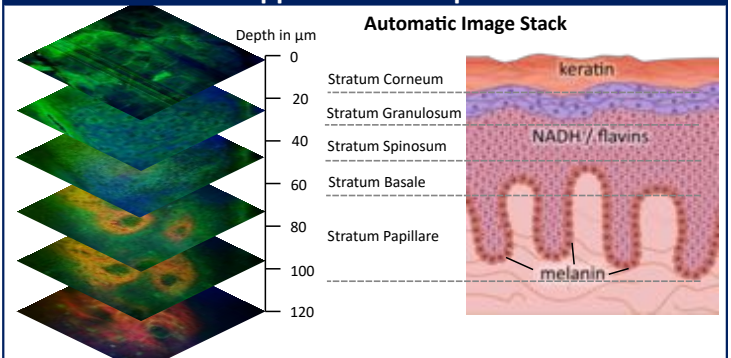


With two-photon excitation the formation of fluorescence is limited to the focus. Additionally the IR-Laser source provides deeper penetration into tissue.

Endogenous Skin Fluorophores

Fluorophore	Emission λ (nm)	Lifetime τ (ns)
NADH(P)H free	460	0.3
NADH(P)H-protein	440	2.0-2.3
Flavines	530	5 (bound: < 1)
Elastin	420-460	0.3/ 2
Collagen	420-460	0.3/ 2
Melanin	> 440	< 0.15
PPIX	635, 710	10-12

Application Examples



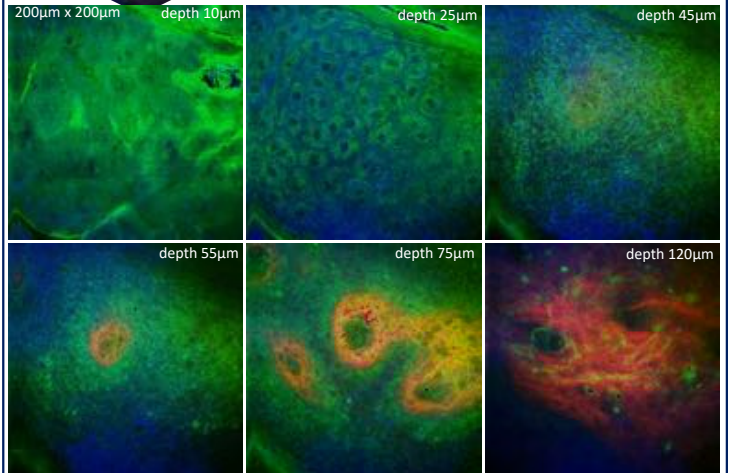
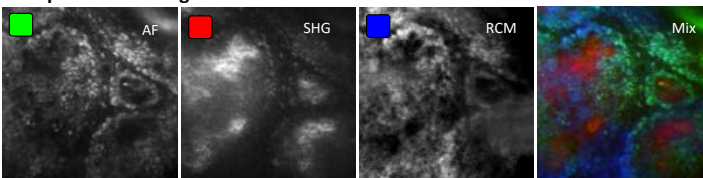
Types of Imaging

White Light Imaging: An integrated CMOS camera produces dermatoscopic pictures (area size 10 x 10mm, picture size 800 x 800 px).

Beam Scanning: Four images from AF, SHG, confocal and FLIM channels are simultaneously generated during beam scanning. 512 Lines, 512 Rows.

FLIM: Free / bound molecules can be discriminated in FLIM images by pseudo-coloring their fluorescence decay times.

Composite from single channels



White Light Module for Dermoscopy with a Multiphoton Tomograph MPTcompactTM

M. Warzecha¹, P. Prinke², J. Haueisen², Ł. Piątek³, G. Lisowicz⁴, K. König^{1,5}

¹JenLab GmbH, Johann-Hittorf- Straße 8, 12489 Berlin
info@jenlab.de

²Institute of Biomedical Engineering and Informatics, Technische Universität Ilmenau, 98693 Ilmenau, Germany

³Faculty of Applied Information Technology, University of Information Technology and Management, Suchbarskiego
2, 35-225 Rzeszów, Poland

⁴Info-Projekt IT Sp. z. o.o., Ul. Zaleska 63b, 35-332 35-225 Rzeszów, Poland

⁵Department of Biophotonics and Laser Technology, Saarland University, Campus A5.1, 66123 Saarbrücken,
Germany

KEY WORDS: Skin cancer diagnosis, dermoscopy, deep learning, artificial intelligence

To minimize the mortality rate for skin cancer, early diagnosis of pigmented lesions is essential. Early inspection is usually supported by total body dermoscopy which provides magnification as well as nondestructive and noninvasive scanning of the skin region. The three most popular procedures for visual inspection of the skin nevi are the ABCD rule^{1,2}, the 7-point checklist³ and Chaos and Clues⁴. Computer-aided diagnosis systems for supporting recognition of skin nevi evaluation can be issued for general practitioner's offices. Multiphoton tomography (MPT) by using femtosecond laser pulses provides in vivo access to the skin with subcellular resolution due to optical sectioning.

In this study we use the MPTcompactTM with a flexible measuring head, giving the possibility to detect two photon excited autofluorescence (2P-AF) and second harmonic generation (SHG) of light⁵. Fluorescence lifetime imaging (FLIM) provides cell-typical time-resolved fluorescence decay. A white light imager tool consisting of four light-emitting diodes and a camera allows an illumination and pre-scan imaging of the pigmented skin region. The aim of this project is to create a database of dermoscopic images and image stacks consisting of suspicious pigmented lesions. This database forms the basis for discovering malignant melanoma using deep learning algorithms and feature-based approaches following the requirements of the three classification criteria mentioned above. Finally, artificial intelligence-based tools are used to support the medical specialists during the skin cancer diagnosis. Due to the multiphoton tomograph with the additional white light camera, both skin surface classification and deep skin analysis can be carried out with this unique multimodal device, resulting in less physically taken skin biopsies.

We acknowledge financial support from the Federal Ministry of Education and Research under the DigiSkinDia-project (project number 01DS19012B).

¹ Stolz, W., Reimann, A. and Cognetta, A. B. : "ABCD rule of dermatoscopy: A new practical method for early recognition of malignant melanoma." *European Journal of Dermatology*, Vol. 4, No. 7, pp. 521 – 527, (1994).

² Stolz, W., et al.: *Farbatlas der Dermatoskopie*. Stuttgart: Thieme Verlagsgruppe, 2004.

³ Argenziano, G., et al.: "Epiluminescence Microscopy for the Diagnosis of Doubtful Melanocytic Skin Lesions", *Archives of Dermatology*, Vol. 134, No.12, pp. 1563 – 1570, (1998).

⁴ Rosendahl, C. (2014) "Dermatoscopy: Chaos and Clues". *Practical Dermatology*.

⁵ K. König, "Multiphoton Tomography (MPT)," in *Multiphoton Microscopy and Fluorescence Lifetime Imaging*, De Gruyter, 2018.

White Light Module for Dermoscopy with the Multiphoton Tomograph MPTcompact



M. Warzecha¹, P. Prinke², J. Hauelsen², Ł. Piątek³, G. Lisowicz⁴, K. König^{1,5}

¹JenLab GmbH, Johann-Hittorf- Straße 8, 12489 Berlin
info@jenlab.de

²Institute of Biomedical Engineering and Informatics, Technische Universität Ilmenau, 98693 Ilmenau, Germany

³Faculty of Applied Information Technology, University of Information Technology and Management, Suchbarskiego 2, 35-225 Rzeszów, Poland

⁴Info-Projekt IT Sp. z o.o., Ul. Załęska 63b, 35-332 35-225 Rzeszów, Poland

⁵Department of Biophotonics and Laser Technology, Saarland University, Campus A5.1, 66123 Saarbrücken, Germany

Abstract

To minimize the mortality rate for skin cancer, early diagnosis of pigmented lesions is essential. Early inspection is usually supported by total body dermoscopy which provides magnification as well as nondestructive and noninvasive scanning of the skin region. The three most popular procedures for visual inspection of the skin nevi are the ABCD rule [1,2], the 7-point checklist [3] and Chaos and Clues [4]. Computer-aided diagnosis systems for supporting recognition of skin nevi evaluation can be issued for general practitioner's offices.

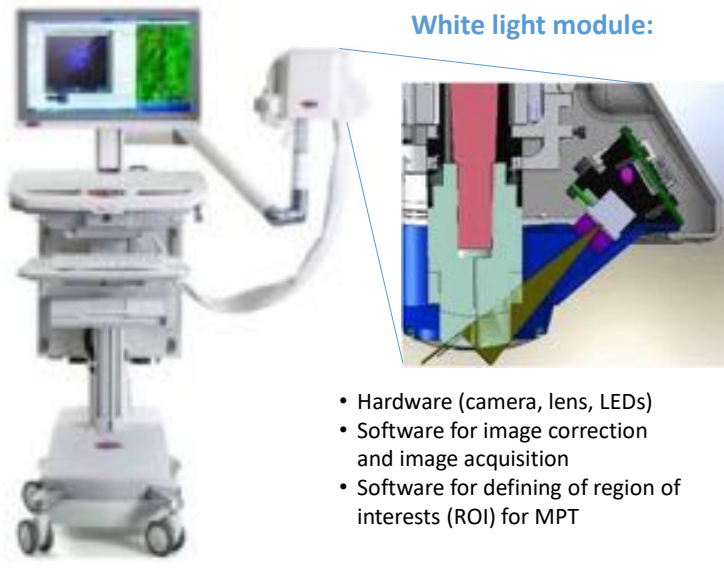
3D-Multiphoton tomography (MPT) by using femtosecond laser pulses provides in vivo access to the deep skin with subcellular resolution due to optical sectioning.

In this study we use the MPTcompact with a flexible measuring head, giving the possibility to detect two photon excited autofluorescence (2P-AF) and second harmonic generation (SHG) of light [5].

Fluorescence lifetime imaging (FLIM) provides information on time-resolved fluorescence decay per pixel. A white light imager tool consisting of four light-emitting diodes and a camera allows an illumination and pre-scan imaging of the pigmented skin region. The aim of this project is to create a database of dermoscopic images and image stacks consisting of suspicious pigmented lesions. This database forms the basis for discovering malignant melanoma using deep learning algorithms and feature-based approaches following the requirements of the three classification criteria mentioned above. Finally, artificial intelligence-based tools are used to support the medical specialists during the skin cancer diagnosis. Due to the multiphoton tomograph with the additional white light camera, both skin surface classification and deep skin analysis can be carried out with this unique multimodal device, resulting in fewer physically taken skin biopsies.

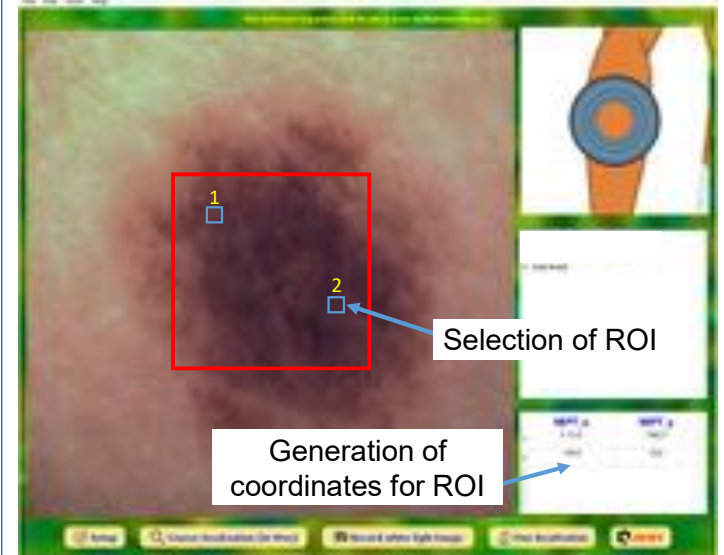
Concept

MPTcompact



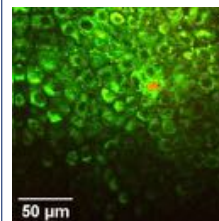
Localization

Software JenLab localizer with white light image:

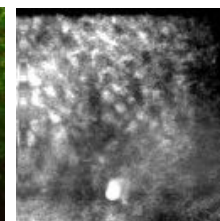


- White light image (10 x 10 mm²) recording in bmp-format
- Accessible region for high resolution MP imaging up to 4 x 4 mm² (red square)

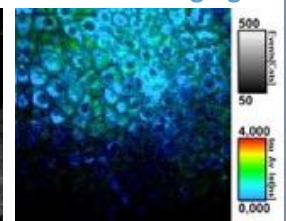
Autofluorescence/SHG



Confocal reflection



Fluorescence lifetime imaging



Conclusion

- Compact MPT with a camera module for white light recordings of skin lesions realized and tested.
- Selection of ROI for MP acquisition by clicking with a computer mouse on a recorded white light image is possible.
- Evaluation of lesions from white light images using algorithms for cancer determination is in progress.
- Building of data base from clinical studies to support deep learning algorithms for cancer forecast is underway.

Acknowledgement

We acknowledge financial support from the Federal Ministry of Education and Research under the DigiSkinDia-project (project number 01DS19012B).

References

- [1] Stolz, W., Reimann, A. and Cagnetta, A. B.: "ABCD rule of dermatoscopy: A new practical method for early recognition of malignant melanoma". *European Journal of Dermatology*, Vol. 4, No. 7, pp. 521 - 527 (1994).
- [2] Stolz, W., et al.: *Farbatlas der Dermatologie*. Stuttgart: Thieme Verlagsgruppe (2004).
- [3] Argenziano, G., et al.: "Epiluminescence Microscopy for the Diagnosis of Doubtful Melanocytic Skin Lesions", *Archives of Dermatology*, Vol. 134, No.12, pp. 1563 - 1570 (1998).
- [4] Rosendahl, C.: "Dermatoscopy: Chaos and Clues". *Practical Dermatology*, no. July, pp. 23 - 24 (2014).
- [5] König, K.: "Multiphoton Tomography (MPT)", in *Multiphoton Microscopy and Fluorescence Lifetime Imaging*, De Gruyter (2018).

Project partners

Project partner	Company / Institution logo
JenLab GmbH, Germany	
Technische Universität Ilmenau, Institute for Biomedical Engineering and Informatics, Germany	
University of Information Technology and Management In Rzeszów, Poland	
Info-Projekt IT, Poland	

AquaFlux and Epsilon: Precision Skin Condition Measurement

P Xiao, LI Ciortea, S Bahman and EP Berg

We present our latest study on precision measurement of skin condition using AquaFlux and Epsilon instrumentation. The AquaFlux is a patented, condenser-based, closed chamber evaporimeter for skin transepidermal water loss (TEWL) measurement. The Epsilon uses novel capacitance-based permittivity imaging technology to represent and measure stratum corneum water content. Both devices are fully calibrated and exhibit high accuracy, high repeatability, and low noise. We will present the technical background, then the results and discussion, showing that precise measurement of TEWL and skin hydration reveal otherwise undistinguishable changes in skin condition.

Introduction

Stratum corneum (SC) hydration is important for its cosmetic properties and barrier function. SC hydration and transepidermal water loss (TEWL) are two key indices used for SC characterisation. Previous studies have shown that capacitance-based fingerprint sensors, originally designed for fingerprint imaging, can be adapted for skin hydration imaging, surface analysis, 3-D surface profile and skin micro-relief measurements [1-3]. In this paper, we present our latest study on precision measurement of skin condition using AquaFlux and Epsilon instrumentation. The AquaFlux is a patented, condenser-based, closed chamber evaporimeter for skin transepidermal water loss (TEWL) measurement. The Epsilon uses novel capacitance-based permittivity imaging technology to represent and measure stratum corneum water content. Both devices are fully calibrated and exhibit high accuracy, high repeatability, and low noise. We will present the technical background, then the results and discussion, showing that precise measurement of TEWL and skin hydration reveal otherwise undistinguishable changes in skin condition.

Below, we present our latest SC barrier function study, using the Epsilon capacitance-array sensor to measure hydration and AquaFlux condenser-chamber instrument for TEWL [4,5]. With the Epsilon, we can measure skin surface hydration dynamically during occlusive contact, to generate time-dependent grey-scale occlusion curves. With the AquaFlux, we can accurately measure TEWL. Our previous studies have shown that skin occlusion measurements can be used with both techniques to give further information about skin properties [6]. The purpose of this study is to develop a new SC barrier characterisation method by using occlusion with both fingerprint imaging and TEWL measurement.

Apparatus

Figure 1 shows photos and schematic diagrams of the Epsilon permittivity imaging system and the AquaFlux TEWL instrument (BioX Systems Ltd). The Epsilon is based on a Fujitsu fingerprint sensor, which has 256x300 pixels with 50µm spatial resolution and 8-bit grey-scale capacitance resolution per pixel. The AquaFlux uses the closed condenser-chamber measurement method. Its cylindrical measurement chamber is open at the end placed onto the skin surface, and closed at the other end by means of a condenser cooled below the freezing point of water. This design provides a controlled measurement environment, which enhances the repeatability and accuracy of the measurements. An alternative TEWL device, the VapoMeter from Delfin, Finland, is also used in the study.

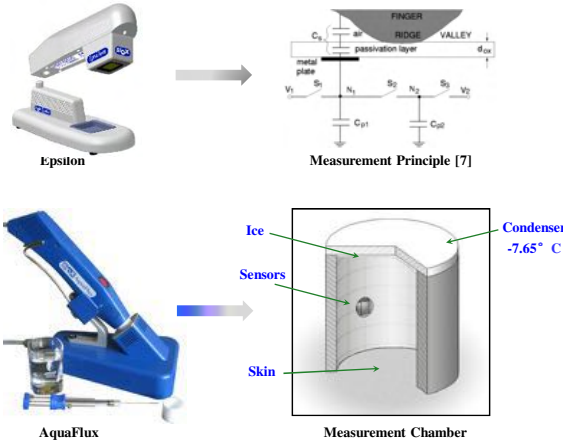


Figure 1. Epsilon permittivity imaging system and AquaFlux evaporimeter

Methods

All the measurements were performed under normal ambient laboratory conditions of 20-21°C and 40-50% RH. The volar forearm skin sites used were initially wiped clean with ETOH(H₂O) (95/5) solution. The volunteers were then acclimatized in the laboratory for 20 minutes prior to the experiments.

Three sunscreens of a well known brand with SPF (Sun Protection Factor) of 20, 30 and 50+ were used in the study. Four skin sites on the volar forearm of healthy volunteers were chosen: three skin sites as test sites for sunscreens of SPF 20, 30 and 50+; the fourth skin site was used as control, as illustrated in Figure 2. TEWL (trans-dermal water loss) and skin water content measurements were performed both before and after application of sunscreen. TEWL was measured using both AquaFlux and VapoMeter instruments, and skin water content was measured using the Epsilon permittivity imaging system.

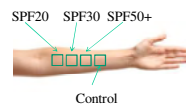


Figure 2. Four skin sites on the volar forearm. Three were test sites for sunscreen with SPF 20, 30 and 50+. The fourth skin site was chosen as control.

Results and Discussion

Figure 3 shows TEWL values of four volar forearm skin sites, before, 1 hour after, and 2 hours after the application of three different sunscreens. Figure 3 (A) shows the AquaFlux TEWL values, which were found to decrease consistently on all three sunscreen skin sites after the application of the sunscreens, while the control site remained more or less the same. Figure 3 (B) shows the VapoMeter TEWL values, which were found not consistent. This is likely due large instrumental coefficient of variation (CV) of the VapoMeter, as shown in Figure 3 (C). CV is calculated as the ratio of standard deviation over the mean measured TEWL value as a percentage.

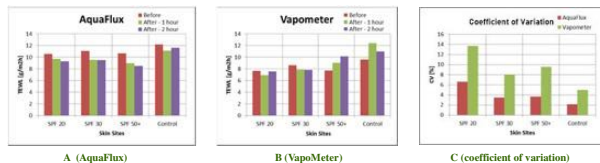


Figure 3. The TEWL values of four volar forearm skin sites before and after the sun tan lotion application, measured by AquaFlux (A), and VapoMeter (B), and their covariance (C).

Figure 4 shows the corresponding TEWL value changes before, 1 hour after, and 2 hours after the sunscreen application, measured with the AquaFlux and VapoMeter. The AquaFlux results show that the TEWL values decrease 1 hour after the sunscreen application, and continue to decrease 2 hours after. This is the same for sunscreens with SPF 20, SPF 30 and SPF 50+. Of interest is the proportional decrease in TEWL with SPF number; SPF 20 having the smallest TEWL decrease and SPF 50+ the largest. The control site has a small change with time. The VapoMeter results, however, do not show any consistent trend.

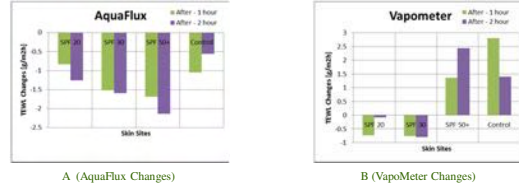


Figure 4. The TEWL value changes before and after sunscreen application, measured by AquaFlux (A) and VapoMeter.

Figure 5 below shows the corresponding Epsilon permittivity images before and after applying sunscreen. Before application, all four skin sites are relatively the dark, indicating low water content. After one hour, the three skin sites with the lotion applied became much brighter, indicating moisture content in the sunscreen. The sunscreen with SPF 20 has the highest brightness, hence the possible highest moisture content. Conversely, the sunscreen with SPF 50+ has the lowest brightness, hence the possible lowest moisture content. The control site remains more or less the same throughout.

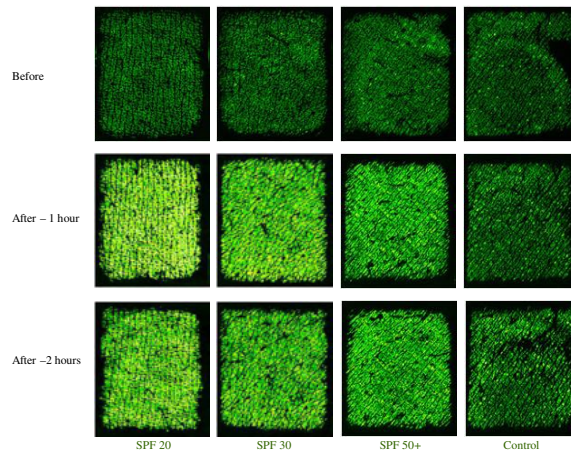


Figure 5. Epsilon permittivity images of four volar forearm test sites before, 1 hour after, and 2 hours after application of sunscreen. SPF 20, SPF 30, and SPF 50+ sunscreen was applied on three skin sites. The fourth skin site is used as control.

In order to improve the Epsilon measurement accuracy, a permittivity filter was applied to each image, eliminating pixel values below 2 and above 80. This built-in software feature filter removes the black regions, where there is poor skin contact with the sensor, as well as those with sweat gland activity. After filtering, the permittivity readouts are calculated as the mean of all remaining pixel values, correctly depicting hydration within the SC. Histograms of the analysed results corresponding to the images in Figure 5 are shown below in Figure 6, again indicating a proportional relationship, this time between hydration and SPF number.

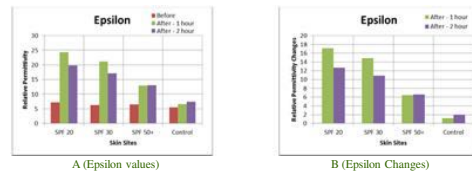


Figure 6. Epsilon mean permittivity readouts of the four skin sites before and after sunscreen application (A), and the corresponding change in permittivity at each site (B).

Conclusions

We present our latest study on precision skin condition measurement using AquaFlux and Epsilon research grade instrumentation. The overall results show that the AquaFlux and Epsilon are capable of detecting and quantifying subtle changes in skin condition after the application of different sunscreens. The AquaFlux results show a decrease in TEWL after the sunscreen application compared to the control site, with SPF 50+ having the most effect and SPF 20 the least. Using an alternative closed chamber evaporimeter, the VapoMeter, the results were inconclusive. Epsilon measurements show a significant increase in skin water content after sunscreen application, with SPF 20 increasing the most and SPF 50+ the least.

Acknowledgement

We thank London South Bank University and BioX Systems Ltd for the financial support.

References

- Lévesque, J.L. and Querleux, B. SkinChip, a new tool for investigating the skin surface in vivo. *Skin Research and Technology* 9, 343-347, (2003).
- Batiste, D., Giroin F. and Lévesque J.L. Capacitance imaging of the skin surface. *Skin Research and Technology* 12, pp99-104, (2006).
- Xiao, P., Singh, H., Zheng, X., Berg, E.P. and Imhof, R.E. In-vivo Skin Imaging For Hydration and Micro Relief Measurements. *Int J. Cos Sci.*, in process.
- Berg, E.P., Pascut, F.C., Ciortea, L.L., O'Driscoll, D., Xiao, P. and Imhof, R.R. AquaFlux - A New Instrument for Water Vapour Flux Density Measurement. *Proceedings of the 4th International Symposium on Humidity and Moisture, Center for Measurement Standards, ITRI, RoC, ISBN 957-774-423-0, 288-295, (2002).*
- Imhof, R.E., Berg, E.P., Chilcott, R.P., Ciortea, L.L., Pascut, F.C. and Xiao, P. New Instrument for the Measurement of Water Vapour Flux Density from Arbitrary Surfaces. *IFSCC Magazine*, Vol 5, No. 4, 297-301, (2002).
- Taylor, H. PhD Thesis, 2008.
- Fujitsu Fingerprint Sensor. <http://eldevic.fujitsu.com/fj/MARCOM/ind20-1e/pd/001.pdf>

ISBS 2022 DIGITAL CONGRESS ON BIOPHYSICS AND IMAGING OF THE SKIN

Traveling across Borders: Optical Skin Biopsies and Beyond

JUNE 2-3, 2022
BERLIN, GERMANY

CONGRESS PRESIDENT

Prof. Karsten König

ISBS PRESIDENT

Dr. Bernard Querleux

CONTACT

info@isbs-congress.com

www.isbs-congress.com

www.isbskin.org

ABOUT THE ISBS

The *International Society for Biophysics and Imaging of the Skin (ISBS)* focuses on the development, use and spread of knowledge on non-invasive investigation of human skin. Official journal of the ISBS is *SKIN RESEARCH AND TECHNOLOGY*.

CONGRESS VENUE

Langenbeck-Virchow-House

Luisenstrasse 58/59

10117 Berlin

